THE
PHYSICAL REVIEW
A Journal of Experimental and Theoretical Physics Established by E. L. Nichols in 1893
VOL. 53, NO. 10 MAY 15, 1938 SECOND SERIES

The Specific Ionization and Mass of Cosmic-Ray Particles

DALE R. CORSON AND ROBERT B. BRODE
Department of Physics, University of California, Berkeley, California
(Received March 25, 1938)

The specific ionization of 120 cosmic-ray tracks has been measured by counting droplets in photographs of delayed expansion cloud chamber tracks. For values of $H\rho$ between 10^3 and 2×10^5 the specific ionization as a function of $H\rho$ is found to be in good agreement with theory. The predicted minimum ionization for electrons of $H\rho\sim10^4$ ($\sim$2 Mev) is verified. These results are applied to the calculation of the mass of heavily ionizing cosmic-ray particles as observed by us and by others. The masses of all heavy cosmic-ray particles thus far reported, with one exception, do not seem to be in serious disagreement with a unique mass which lies in the limits $(200\pm50)m_0$.

TO obtain values for the specific ionization due to cosmic-ray particles several hundred cloud chamber photographs have been taken. The expansion was delayed to make possible the counting of the individual droplets in the tracks. The cloud chamber was 18 cm in diameter and was filled with nitrogen at about 1.5 atmospheres pressure. It was placed in a magnetic field of 800 gauss. The chamber was illuminated by a mercury arc lamp, operated with a fraction of an ohm series resistance and flashed on 220 volts d.c. for 0.1 second. The expansion was delayed for approximately 0.5 second by a cam mechanism set into operation by the tripping of a pair of Geiger counters.

The tracks were broadened by diffusion of the ions in the time between the passage of the ionizing particle and the expansion of the chamber (the clearing field was shorted out by the tripping of the Geiger counters). In spite of the breadth of the tracks it was possible to obtain quite accurate values for the curvature by measuring the coordinates of the estimated center of the band of droplets when observed with a measuring microscope.

The absence of turbulent distortions was checked by measuring tracks when the magnetic field was zero. These were found to be straight within the limits of experimental measurement except in the region less than two cm from the chamber walls. The droplets were easily counted as can be seen from the examples shown in Fig. 1. All results were reduced to 0°C and 760 mm of mercury pressure.

One hundred twenty tracks that were in sharp focus, so that the number of droplets per cm could be easily counted, were chosen for this preliminary survey. They were divided into seven $H\rho$ groups. In obtaining the mean number of droplets per cm in each group (plotted in Fig. 2) the mean number per cm in each track was weighted proportional to the total number of droplets in the track. The vertical lines represent the probable errors. In the lowest $H\rho$ group the radius of curvature is somewhat uncertain and the variation of ionization with

$H\rho$ is rapid. In this region large deviations from the mean are to be expected.

Discussion

The variation of the specific ionization in hydrogen is given theoretically by the formula[1]

$$I=\frac{A}{\beta^2}\left[\log k+\log\frac{\beta^2}{1-\beta^2}-\beta^2\right], \qquad (1)$$

where $k=1.6\times10^6$ for hydrogen. This is a function which varies nearly as $1/\beta^2$ for $\beta<0.9$, then passes through a minimum at $\beta\sim0.97$, and increases with increasing β. For electrons the value of $\beta=0.97$ corresponds to about 2 Mev. A smaller value of k must be used if this equation is to be applied to ionization in nitrogen. We have chosen $k=2\times10^4$ as an appropriate value. Since k enters only in the logarithmic term the choice of a value for k is not critical.

Our measurements do not give the primary ionization but the "probable" ionization,[2] i.e., the primary ionization plus the ionization produced by secondaries of energy lower than a certain critical energy. Secondaries of higher energies produce unresolvable clusters of ions. The manner in which the theoretical formula must be modified to be applicable to probable ionization is discussed by Oppenheimer.[3] Above the minimum point the probable ionization increases less rapidly than the primary ionization, but the changes in the shape of the curve below the minimum point are quite small.

The continuous curve in Fig. 2 is Eq. (1) with $k=2\times10^4$ and with the minimum ordinate arbitrarily adjusted to make the curve fit our observed points. The agreement of the theoretical curve with the experimental data is quite good. It is significant that our data differ from the classical $1/v^2$ variation of ionization with velocity, as shown by the dotted curve in Fig. 2. Our observations show the actual increase in ionization with $H\rho$, as predicted by theory.

A point of interest in connection with all our measurements is the ratio of probable to primary ionization. A number or observers[4–6] have measured the primary ionization of fast electrons by counting the number of distinct groups of droplets in sharp tracks, each group corresponding to one primary ion pair. For electrons with velocities comparable to those in the lower energy region of our observations all the observers report the number of primary ion pairs per cm (in air, nitrogen or oxygen at 0°C and 760 mm mercury pressure) to be about 20 or 25. By similar measurements on a few sharp tracks of energies in the minimum part of the curve we find between 14 and 18 primary ion pairs. Our total probable ionization is 50 ions or 25 ion pairs, which gives a ratio of probable to primary ionization of a little less than two. By counting the total number of droplets in diffuse tracks Wilson gives 1.8 for the same ratio. He says this value is low, however, because the larger groups of droplets were not resolved well enough to count. For lower energy electrons and more diffuse tracks he gives 3.5 for the ratio.

From the observed range of electrons, and the variation of range with $H\rho$ one can calculate the average energy loss per cm for an electron of given $H\rho$. If one takes the average energy per ion pair as 32 volts, this calculation indicates an average density of total ionization about twice that given by our droplet counts.

Calculation of Mass

In cloud chamber tracks of moving charged particles the observable quantities are ionization, range and radius of curvature (if in a magnetic field), and the rates of change of these quantities with distance. These quantities depend on the charge, mass and velocity of the particle. It is possible to represent very closely the relationships between these different quantities and their rates of change on a nomograph of straight parallel lines. Such a nomograph is shown in Fig. 3. m/m_0 is the ratio of rest mass to rest mass of the ordinary electron, D is the ratio of specific ionization to specific ionization at the minimum point, D' is the same ratio obtained by use of the $1/v^2$ law. R is the range in cm of

[1] Cf. Bethe, *Handbuch der Physik*, Vol. 24: 1.
[2] Williams, Proc. Roy. Soc. **A135**, 108 (1932).
[3] Oppenheimer, Phys. Rev. **47**, 44 (1935).
[4] C. T. R. Wilson, Proc. Roy. Soc. **A104**, 191 (1923).
[5] Williams and Terroux, Proc. Roy. Soc. **A126**, 289 (1930).
[6] Skramstad and Loughridge, Phys. Rev. **50**, 677 (1936).

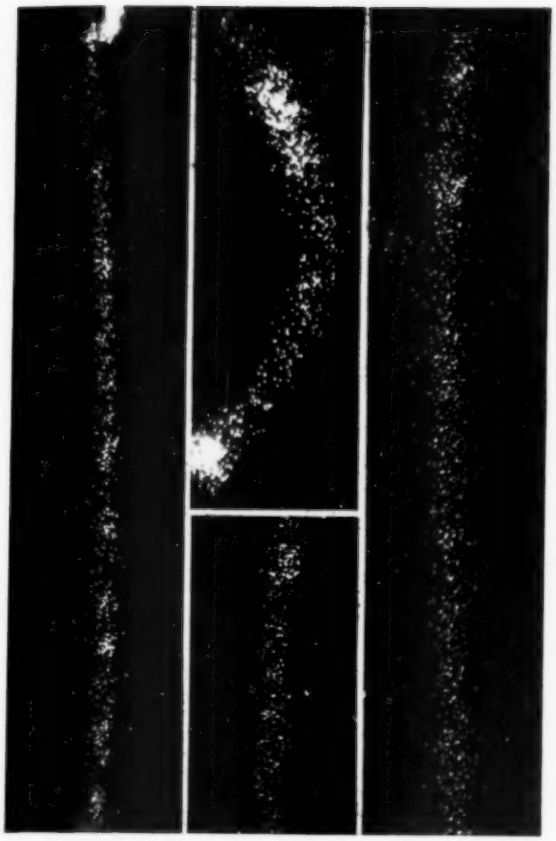

FIG. 1. Sections of electron tracks broadened by diffusion of the ions in delayed expansions.

air at 760 mm of mercury pressure and 15°C. $d(H\rho)/dR$ is the rate of change of $H\rho$ with distance. Any straight line drawn across the nomograph gives consistent values for all the quantities plotted. If the data include any two of the variables the mass of the particle in question is given at once.

From an inspection of the nomograph one sees that $H\rho$ and range afford the most accurate method of determining the mass, provided all the data are given with the same degree of precision. $H\rho$ and D also is a good way to determine the mass, for a relatively large change in D produces a relatively small change in m/m_0. D and range is a poor way to find m/m_0 for the value of D must be accurately given in order to determine m/m_0 within relatively small limits. This last method has the advantage that it does not involve a measurement of curvature, and so is free of distortions which may produce spurious curvatures. A significant fact is that a value of $H\rho$ and a minimum value for the range determine an upper limit on the mass.

The ionization is theoretically independent of the mass, is proportional to the square of the charge on the moving particle, and depends on the particle's velocity as given by Eq. (1). The fact that all particles with β near unity have approximately the same ionization indicates that all cosmic-ray particles carry the charge e. We have defined the relative specific ionization D as the ratio of the specific ionization at a given β to the ionization at the minimum, i.e. at $\beta \sim 0.97$. These values can be calculated from Eq. (1) when the specific ionization at the minimum is known. The experimental value of D is found by dividing the number of droplets per cm in the track by our observed minimum value of 50. In this way the value of β for any track can be found. Then the relationship between m, $H\rho$, and β for a charged particle moving in a magnetic field is given by the equation

$$m/m_0 = H\rho(e/m_0c)(1-\beta^2)^{\frac{1}{2}}/\beta,$$

where m_0 is the mass of the ordinary electron.

Since the loss of energy per cm of path of a charged particle depends only on its velocity one can write $R = kmf(v)$. R is the range in cm of air, m the particle's rest mass and $f(v)$ some function of velocity. This is true for relativistic as well as nonrelativistic energies. Then for all

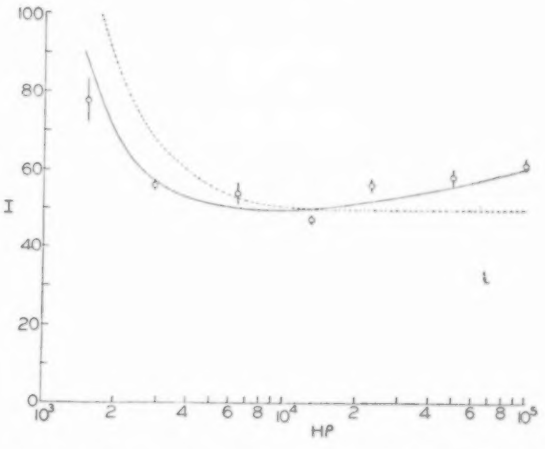

FIG. 2. Specific ionization *vs.* $H\rho$. I is the number of droplets per cm in nitrogen at 0°C and 760 mm pressure. The continuous curve is the theoretical equation (1). The dotted curve is the inverse square law. The vertical lines represent the probable errors of the measurements.

particles of the same velocity $R_1/R_2=m_1/m_2$. When the velocities are the same we also have $(H\rho)_1/(H\rho)_2=m_1/m_2$. Then we can use the known ranges of protons[7] to find the range R_1 of a particle of mass m_1 and $H\rho=(H\rho)_1$. Conversely, the range of a particle and its $H\rho$ determine its mass.

It is an experimental fact that the relation between range and velocity may be closely expressed as $R=kv^n$ or $R=k(H\rho)^n/m^{n-1}$. From this one gets

$$R=\rho/[n(d\rho/dR)].$$

Thus ρ and $d\rho/dR$ is sufficient information to determine the range and so the mass. The exponent "n" has a value varying from 3.45 to 3.70 for $10^4<H\rho<10^5$ and $80<m/m_0<300$.

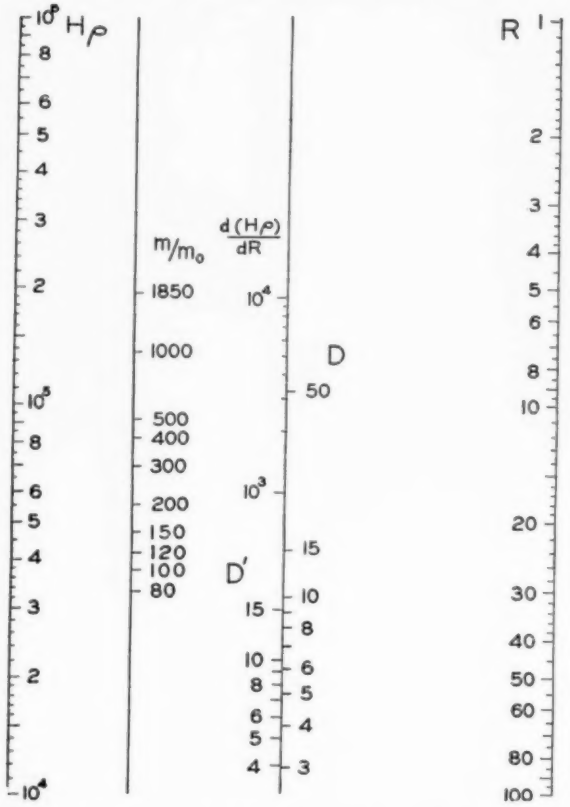

FIG. 3. Nomograph giving mass in terms of variables which can be determined from cloud chamber data. m/m_0 is the ratio of mass to the mass of the ordinary electron, D is the ratio of specific ionization to specific ionization at the minimum, D' is the same ratio from the $1/v^2$ law, R is the range in cm of air at 15°C and 750 mm pressure and $d(H\rho)dR$ is the rate of change of $H\rho$ with distance. Any straight line drawn across the nomograph gives consistent values for all the variables plotted.

[7] Cf. M. S. Livingston and H. A. Bethe, Rev. Mod. Phys. **9**, 269 (1937).

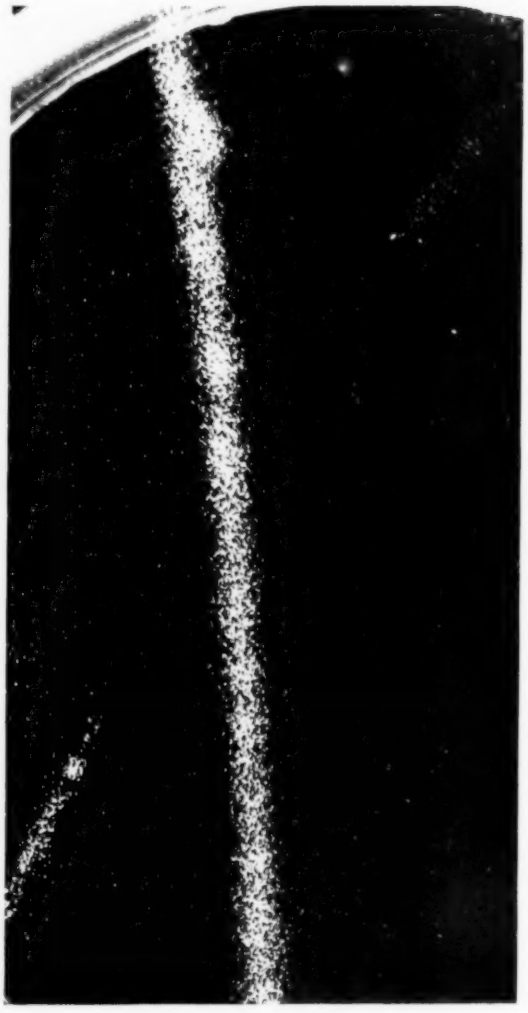

FIG. 4. A photograph of the heavy track previously reported by us. The density of ionization in this track is about 5.5 times that of an ordinary cosmic-ray track. The value of $H\rho=1.5\times10^5$ gives a mass of 250 times the mass of an electron.

It is also possible to find m/m_0 in terms of range and ionization (i.e., in terms of range and velocity), and thus eliminate the necessity of measuring curvature. But, as was pointed out in connection with the nomograph, this is usually not a good way to determine m/m_0.

APPLICATION TO HEAVY TRACKS

We have previously reported[8] a track of a heavily ionizing particle, reproduced here in Fig. 4. Because of an error in our calculations the $H\rho$ was incorrectly given. The correct value

[8] Corson and Brode, Phys. Rev. **53**, 215 (1938).

is $H\rho = 1.5 \times 10^5$. The number of droplets per cm is 265, which is about 5.5 times the minimum density of normal tracks. By the use of this as the value of D on the nomograph a value of $m/m_0 = 250$ is found.

Another track of interest is one already published.[9] This track has an $H\rho = 5.5 \times 10^4$ and an observable range of 18 cm (in nitrogen at 0°C and 760 mm of mercury pressure). These are sufficient data to place an upper limit of $200m_0$ on the mass. The track is out of focus slightly which makes a count of the specific ionization impossible. If the ion density were 10 times that of normal tracks the mass would be $125m_0$. The fact that undeflected tracks appear in the same region in the chamber makes it improbable that the curvature was produced by turbulence.

The track reported by Street and Stevenson[10] has an $H\rho = 9.6 \times 10^4$ and an ion density six times that of normal thin tracks. Using the $1/v^2$ law for ionization, D' in Fig. 3, Street and Stevenson gave a mass of $130m_0$. When one uses, instead of D', the column D in Fig. 3 the mass is found to be $160m_0$.

Two unusual tracks have been reported by Anderson and Neddermeyer.[11] One of these tracks has an apparent $H\rho = 5.5 \times 10^4$ and has a range of about four cm. This gives a mass of about $350m_0$. The other track has an apparent $H\rho = 1.4 \times 10^5$ and a range greater than five cm (the particle apparently passed out of the illuminated part of the chamber). This puts an upper limit of about $1000m_0$ on the mass of the particle.

Ruhlig and Crane[12] reported a track with a curvature of nine cm in a magnetic field of 2850 gauss, and a rate of change of ρ with distance of 0.6 ± 0.4. This gives a mass of $(120 \pm 30)m_0$. However, the track appears to have a range of at least five cm, which would place an upper limit of about $110m_0$ on the mass.

Nishina, Takeuchi and Ichimiya[13] reported a particle whose $H\rho$ changed from 7.4×10^5 to 4.9×10^5 in passing through 3.5 cm of Pb. If one assumes that this particle is losing energy only by ionization then the equivalent thickness of air[1] is about 1.8×10^5 cm, or a value of $d(H\rho)/dR = 1.4$. This gives a mass of about $200m_0$.

Discussion

Our measurements indicate that the variation of specific ionization with $H\rho$ (for $H\rho$'s between 10^3 and 2×10^5) is in good agreement with the theoretical equation (1). This agreement includes the verification of the minimum of ionization at $H\rho \sim 10^4$, as predicted by the theory. In determining the velocity (and so the mass) of heavily ionizing particles one should use, not the $1/v^2$ law, but Eq. (1). By use of Eq. (1), and consideration of the errors to which the experiments are subject, it seems that all the heavy tracks reported thus far, with the exception of Ruhlig's and Crane's, are not in serious disagreement with a unique mass lying within the limits $(200 \pm 50)m_0$. The disagreement between the different values given for the mass of the heavy particle may be due to errors in determining the radius of curvature in the magnetic field. When the curvature is small it may be influenced considerably by scattering and turbulence. The range can be determined with a relatively high degree of accuracy. In nearly every case one observes a minimum range, thus placing an upper limit on the mass.

We are indebted to Professor J. R. Oppenheimer for his helpful discussions and suggestions.

[9] Brode and Starr, Phys. Rev. **53**, 3 (1938), Fig. 4.
[10] Street and Stevenson, Phys. Rev. **52**, 1003 (1937).
[11] Anderson and Neddermeyer, Phys. Rev. **50**, 263 (1936), Figs. 12 and 13.
[12] Ruhlig and Crane, Phys. Rev. **53**, 266 (1938).
[13] Nishina, Takeuchi and Ichimiya, Phys. Rev. **52**, 1198 (1937).

On the Rotation of the Atomic Nucleus

E. TELLER, *George Washington University, Washington, D. C.*

AND

J. A. WHEELER, *University of North Carolina, Chapel Hill, N. C.*

(Received March 23, 1938)

The spacing of the levels in the fine structure of alpha- and beta-ray processes and the existence of metastable nuclear states (isomers, isobars) are in contradiction with the existence of low lying levels corresponding to the rotation of the nucleus as a whole. The exchange of the nuclear constituents effected through rotation, together with the fact that the particles are not rigidly bound to equilibrium positions in the nucleus, will in some cases forbid, in other cases perturb the lowest levels, and cause the first state of excitation to lie considerably higher. Simple models illustrating these effects are discussed in II. In III an estimate is made for the position of the lowest excited level for heavy nuclei. It is found to vary inversely with the mass.

I. INTRODUCTION

ACCORDING to Bohr and Kalckar[1] the lower levels of the heavier nuclei can be systematized if the nucleus is compared to a droplet. The low lying levels which are of importance in nuclear reactions will then be the vibrations of this droplet. Still lower levels are obtained, however, if the rotations of the droplet are taken into consideration. If we take as an example the nucleus Pb^{208}, assume a uniform distribution of mass throughout the nucleus and take its radius to be 12×10^{-13} cm, the moment of inertia 2.00×10^{-46} g cm^2 will be obtained. If we furthermore assume that the lowest rotational state of this nucleus corresponds to $J=0$, then the pure rotational energies corresponding to $J=1, 2, 3, \cdots$ will be 3.3, 10, 20, $\cdots$ kilovolts, approximately.

According to a proposition first put forward by Thibaud[2] the rotations of the nucleus might be used to explain fine structure observed in the emission of alpha-particles. The energy differences of rotation, however, are smaller than those observed in the fine structure. It is indeed reasonable to assume that, in general, nuclei will not have excited states which lie only a few thousand volts above the ground level.

Such extremely low levels would give rise to difficulties in the following ways:

(1) If in the process of alpha-particle emission the fundamental states of both the emitting and the resulting nuclei have $J=0$, it should be possible to observe not only the process $J=0$ to $J=0$ but also the processes $J=0$ to $J=1$, $J=0$ to $J=2$, $J=0$ to $J=3$. In the latter processes the alpha-particle would carry away the angular momentum $\hbar$, $2\hbar$, and $3\hbar$, respectively. According to Gamow's[3] formula the relative probabilities of these processes for a nuclear charge $Z=82$ would be approximately as given in Table I. Instead of finding such closely spaced levels as given in Table I no fine structure has been observed in transformations in which there is reason to assume that the fundamental states of initial and final nuclei have $J=0$.

(2) The explanation for the fine structure in the cases in which it is observed[4] is based on the idea that fine structure occurs if a transition to the fundamental state of the final nucleus would require the alpha-particle to carry away a very high angular momentum. Since such a process is improbable, the disintegration will lead in most cases to excited states which possess angular momenta differing from that of the original

TABLE I. *Relative probabilities of transitions calculated from Gamow's formula for a nuclear charge $Z=82$.*

TRANSITION	RELATIVE PROBABILITY	ENERGY CHANGE
$J=0 \quad J=0$	1.00	0
$J=0 \quad J=1$	0.84	3.3 Kev
$J=0 \quad J=2$	0.60	10 Kev
$J=0 \quad J=3$	0.36	20 Kev

[1] N. Bohr and F. Kalckar, Kgl. Danske Videnskab. Selskab. **14**, No. 10 (1937).

[2] J. Thibaud, Comptes rendus **191**, 656 (1930).

[3] G. Gamow, *Structure of Atomic Nuclei* (Clarendon Press, 1937), Eq. (56), p. 103.

[4] Reference 3, p. 108.

nucleus by fewer units. These excited states frequently lie several hundred thousand volts, or even more than a million volts, above the fundamental state of the final nucleus. If the final nucleus had rotational states lying close to its fundamental level there would be no reason why the alpha-process should not lead to these low lying levels rather than to those observed.

(3) The strong gamma-radiation accompanying some beta-disintegrations has been given an explanation similar to that of the fine structure of the alpha-rays.[5] Also in this case the hard gamma-rays would be difficult to understand if low lying energy levels were available.

(4) Metastable states of nuclei which do not emit gamma-rays but rather eject electrons from the atomic shell (coefficient of internal conversion equal to unity) are found to be lying more than a million volts over the fundamental state. If low lying rotational levels exist these strong, discrete beta-rays should always be accompanied by at least equally strong gamma-rays of only slightly smaller energy leading from the metastable state to the low lying rotational states.

(5) Metastable states of much longer life have been postulated by Weizsäcker[6] in order to explain isomeric nuclei. These long lives he explained by assuming that all transitions from the metastable state to states of lower energy would be connected with a great change of angular momentum. Evidently if Weizsäcker's hypothesis is to be upheld, one must assume the existence of a special level with a high angular momentum lying lower than all but a few of the rotational states of the droplet.

(6) The existence of the low lying levels of the droplet would not be consistent with the explanation given for the long periods of the potassium and rubidium radioactivities. According to Klemperer[7] a large change in the angular momentum should account for the small transition probability. Klemperer's suggestion has been confirmed for the case of rubidium by Kopfermann and Konopinski.[8] Low rotational levels of the product nucleus would make possible less strongly forbidden transitions. Still smaller transition probabilities have been assumed to account for the stability of the neighboring isobars. The low lying levels would invalidate this explanation too.

We conclude therefore that no such low lying levels are present in the nucleus.

It is our purpose to show that the application of the exclusion principle to the constituents of nuclei gives the possibility of reconciling the droplet model with the absence of low lying levels such as would follow from the rotation of the droplet. As the simplest model we consider N alpha-particles on a circle and spaced at equal distances. The rotation of the ring into itself (i.e., around an axis passing through the center of the circle and perpendicular to the plane of the circle) will interchange the alpha-particles. Since the first exchange takes place after a rotation by the angle $2\pi/N$, the Bose statistics of the alpha-particles will exclude all rotational states except those having the angular momentum $J=0$, $J=N$, $J=2N$, $\cdots$.

If we now permit rotations of a group of alpha-particles around any axis in space such simple exclusions of rotational states will be obtained only for nuclei for which particularly symmetrical configurations can be assumed. Thus, Wheeler[9] has found that for four alpha-particles arranged in a tetrahedron the first rotational excitation has $J=3$. If we arrange six alpha-particles on the vertices of an octahedron (this structure has been proposed by Wefelmeier[10] for Mg^{24}) the lowest excitation will lie at $J=4$. For twelve alpha-particles at the vertices of an icosahedron the lowest rotational excitation will be at $J=6$ (this icosahedron was assumed by Wefelmeier for Fe^{54} with the thirteenth alpha-particle in the center of the icosahedron and with two additional neutrons about the localization of which no definite statements are made). Apart from such symmetrical cases, $J=1$ or $J=2$ should be expected as the lowest allowed rotational state since, in most cases, there will be either no rotation which effects an interchange of the constituents of the nucleus, or else only a few rotations, mostly through the angle π, will effect such an interchange.

[5] Reference 3, p. 150.
[6] C. F. v. Weizsäcker, Naturwiss. **24**, 813 (1936).
[7] O. Klemperer, Proc. Roy. Soc. **A148**, 638 (1935).
[8] Kopfermann, Physik. Zeits. **38**, 960 (1937); Konopinski, N. Y. Meeting Am. Phys. Soc., Feb. 25, 1938.
[9] J. A. Wheeler, Phys. Rev. **52**, 1089 (1937).
[10] W. Wefelmeier, Naturwiss. **25**, 525 (1937).

We must remember, however, that the constituents of a nucleus cannot be represented as firmly bound to equilibrium positions. Indeed, the dimensions of the nucleus alone show that the kinetic energies of the nuclear constituents are larger than the nuclear binding energies, that is, the kinetic and potential energy in the nucleus are comparable and the binding energy is obtained as a relatively small difference between the two. Therefore it will be important to consider the following exchange between the constituents of the nucleus: we first perform a rotation which, although it does not actually produce an interchange of the particles, does bring them into positions which are close to positions obtainable by simple exchange; then we have to move the constituents of the nucleus only through comparatively short distances in order to complete the exchange. It will be necessary to investigate which of these two motions will correspond to a higher frequency: the rotation through a finite angle or the displacement through short distances. The first will be the case if the constituents are bound to equilibrium distances with potentials large compared with their kinetic energies and, if thus, no appreciable displacements can be obtained without passing over potential barriers. Then the nucleus may possess all rotational states which are allowed according to the symmetry of the equilibrium position. If, however, the rotation through a finite angle takes a longer time and corresponds to a smaller frequency than the subsequent displacements through short distances, then the process of rotation and the rotational levels will be strongly disturbed and we may expect the nucleus to act like a body of higher symmetry than would correspond to any "equilibrium position" of the constituent particles. The effect may be that the predicted low rotational levels are absent.

In the next section we shall consider the effect of exchanging the particles for simple models consisting of constituents satisfying Bose statistics (alpha-particles). In the last section we shall discuss the angular momentum and the excitation energy which we may expect for the lowest levels in heavy nuclei according to this modified droplet model.

II. Examples

In the following we select a few simple examples which illustrate how the possibility of small displacements from equilibrium increases the effective symmetry of a system and how this increase in symmetry reacts on the structure of the allowed rotational energy levels.

Two particles on a circle

Let us picture two identical particles, obeying Einstein-Bose statistics, free to rotate in a plane about the same fixed point to which both are coupled by inextensible rods of the same length. Between the two particles acts a potential which depends upon the angle θ between their two radii vectors. The potential has the same value for θ and $2\pi-\theta$. The minimum occurs for a value of $\theta=\theta_0$ close to, but definitely less than, 180°. In the extreme case where the potential valley is very deep and very narrow (rigid coupling) the energy levels of the system are simply those of a rotator with one degree of freedom and a moment of inertia I:

$$E=E_0+\hbar^2m^2/2I. \tag{1}$$

All values of m are allowed because the system has no symmetry with respect to its rotational axis. If, now, the rigidity of the binding is decreased, it must be remembered that the system actually possesses two equilibrium positions, at θ_0 and $2\pi-\theta_0$, and that the potential barrier between them, while high, allows the possibility of resonance between the two equilibrium positions. Thus each of the levels considered in the case of rigid coupling is really a double level with a separation $2\Delta E$ proportional to the frequency with which penetration through the barrier occurs. One easily finds from the W–K–B approximation that

$$\Delta E=\pm h\nu_{\text{class}}(n) \times \exp-\int\{2I[V(\theta)-E_{\text{vib}}(n)]\}^{\frac{1}{2}}d\theta/\hbar. \tag{2}$$

$\nu_{\text{class}}(n)$ represents the classical frequency of vibration in the nth vibrational level, and the integral in the exponent depends upon the area under the potential barrier. The positive or negative sign in the equation has to be applied

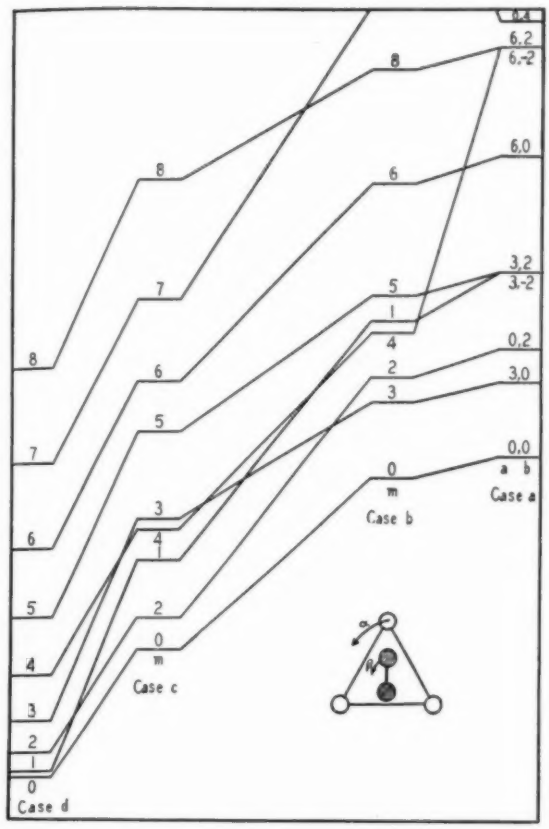

FIG. 1. The diagram in the lower right corner represents the triangle-dumbbell model. The curves represent the energy levels for different cases of coupling. In case (*d*) the coupling is rigid and the levels correspond to different values of the rotational quantum number m. In case (*c*) the coupling is loosened and we see the effect of the dumbbell penetrating the potential barrier to turn into another symmetrical position. In case (*a*) the dumbbell and triangle are allowed to rotate freely with the angular momenta $b\hbar$ and $a\hbar$. The total angular momentum $m\hbar=a\hbar+b\hbar$. In case (*b*) a small coupling is introduced causing repulsion between levels of the same m value. (See levels for $m=4$.)

according as the vibrational functions in the two minima are superposed with the opposite sign or with the same sign. If rotations of the system are taken into account, the symmetry of the wave function with regard to the exchange of two alpha-particles requires that it should remain unchanged if a rotation through 180° is performed and the oscillator is moved from one minimum to the other. Since a half-revolution multiplies by $(-1)^m$ (m is the rotational quantum number), only the energy shift which corresponds to superposition of the vibrational functions with the same sign is allowed for $m=0, 2, \cdots$, and with the opposite sign for $m=1, 3, \cdots$. Thus putting $|\Delta E|=Q$, we obtain for the total energy

$$E=E_{\text{vib}}(n)+\hbar^2m^2/2I-(-1)^mQ. \qquad (3)$$

As the rigidity of the binding is decreased, Q in general increases. When $2Q$ becomes as great as $(\hbar^2/2I)\{m_0^2-(m_0-1)^2\}$, already the odd level $m=m_0-1$ is raised higher than the even level $m=m_0$. This corresponds to the frequency of interchange $2Q/h$ becoming greater than the frequency of rotation $\hbar m_0/2\pi I$. Finally we shall find that a number of even m levels will lie below even the lowest odd level ($m=1$).

This approximates then the result we find for the case of equilibrium position of alpha-particles opposite each other (model for Be^8), where only even values of J occur.

Triangle-dumbbell model

A second instructive example is provided by what we may call the triangle-dumbbell model, illustrated in the lower right-hand portion of Fig. 1. The two rigidly coupled particles in the dumbbell are identical, obey Einstein-Bose statistics, and have only a single degree of freedom, that of rotation about their common center of gravity, which is also the center of rotation for the triangle. The latter is composed of three identical particles, again rigidly coupled and following the symmetric statistics. As extreme cases we may consider (*a*) no interaction between the two rotational degrees of freedom and (*d*) rigid coupling. In the first case the energy levels are determined by the sum of the quantum expressions for two free rotators of moments of inertia A and B:

$$E=\hbar^2a^2/2A+\hbar^2b^2/2B. \qquad (4)$$

Here the rotational quantum number b may take on only the values 0, ±2, ±4 $\cdots$ and a the values 0, ±3, ±6 $\cdots$, because of the symmetry of the system. In case (*d*) the coupling is so strong that we obtain effectively the problem of a single rotator having no symmetry against rotation, and possessing a moment of inertia equal to the sum $A+B$ of the two separate moments. The energy of the system is now

$$E=E_0+\hbar^2m^2/2(A+B), \qquad (5)$$

where m may take on *all* integral values.

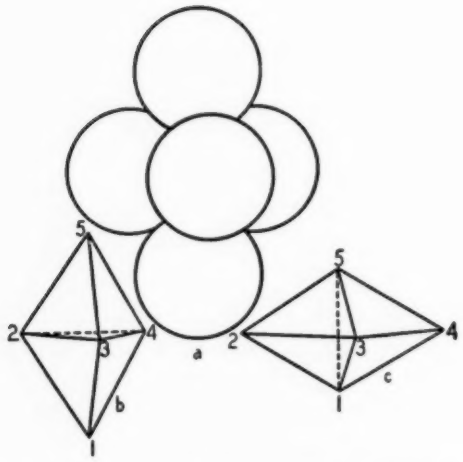

FIG. 2. (*a*) Bipyramid alpha-particle model for the nucleus Ne^{20}. (*b*, *c*), a distortion separating alpha-particles 2,4 and bringing particles 5,1 into contact. The result is an exchange plus rotation through 90 degrees.

The question as to how the transition occurs between the two preceding cases now presents itself in an interesting form, for it is clear that the order of the various rotational levels must go through some sort of mixing process.

First, let us commence with the case of a very weak field, say

$$V(\beta-\alpha)=-W\cos 6(\beta-\alpha),$$

which possesses a sixfold periodicity because of the symmetry of the two parts of the system. It is easy to calculate from the unperturbed wave functions

$$\Psi=(2\pi)^{-1}\exp i(a\alpha+b\beta), \tag{6}$$

that the first-order perturbation energy vanishes. In the second order we have

$$E=\hbar^2a^2/2A+\hbar^2b^2/2B - (W^2/36\hbar^2)(A^{-1}+B^{-1})^{-1}\left\{1-\left(\frac{Ba-Ab}{3A+3B}\right)^2\right\}^{-1}, \tag{7}$$

which represents a repulsion between energy levels possessing the same values of $m=a+b$. (See case (b) in Fig. 1.) On the other hand, proceeding from the side of strong interactions toward the intermediate case, we find it simplest to separate the wave equation

$$(\hbar^2/2A)d^2\psi/d\alpha^2+(\hbar^2/2B)d^2\psi/d\beta^2+\{E-V(\beta-\alpha)\}\psi=0 \tag{8}$$

by writing the wave function as the product

$$\psi=f(\varphi)\exp(im\theta) \tag{9}$$

of a part representing rotation of the system as a whole by the angle $\theta=(A\alpha+B\beta)/(A+B)$ times a part which depends only upon the relative orientation $\varphi=\beta-\alpha$ of the triangle and dumbbell. The wave function of the internal torsional vibration, $f(\varphi)$, must satisfy the equation

$$(\hbar^2/2)(A^{-1}+B^{-1})d^2f/d\varphi^2+\{E_\varphi-V(\varphi)\}f=0, \tag{10}$$

and it is also clear that it must obey a certain periodicity condition. From the picture in the lower right-hand portion of Fig. 1, one sees that a rigid rotation of the whole system by an angle $\theta=(2\pi A/3+2\pi B/2)/(A+B)$ followed by a rotation of the triangle relative to the dumbbell by an angle $\varphi=2\pi/6$ will carry the system from its original position to one where the rod has been given a half-turn, the triangle a third of a revolution. The requirement that the wave function have the same value for the two equivalent configurations tells us at once (see Eq. (9)) that

$$f(\varphi+2\pi/6)=f(\varphi)\exp -im(2\pi A/3+2\pi B/2)/(A+B). \tag{11}$$

The solutions of Eqs. (10) and (8), subject to this condition, may be obtained with the help of the W-K-B approximation and give us the energy values

$$E=E_{\text{vib}}(n)-(-1)^n2h\nu_{\text{class}}(n) \times\{\cos 2\pi m(A/3+B/2)/(A+B)\} \times\exp\{-\textstyle\int|p(\varphi)|d\varphi/\hbar\}+\hbar^2m^2/2(A+B), \tag{12}$$

where n is the quantum number of the torsional vibration.

The figure shows the influence of the possibility of displacements of the triangle and dumbbell with respect to each other. In the case (*d*) of the rigid coupling the low symmetry of our model caused the level of the total angular momentum $m=1$ to be the first excited state. In the intermediate cases (*c*) and (*b*) the level $m=1$ moves up strongly whereas the energy of the levels $m=2$ and $m=3$ are not raised to an

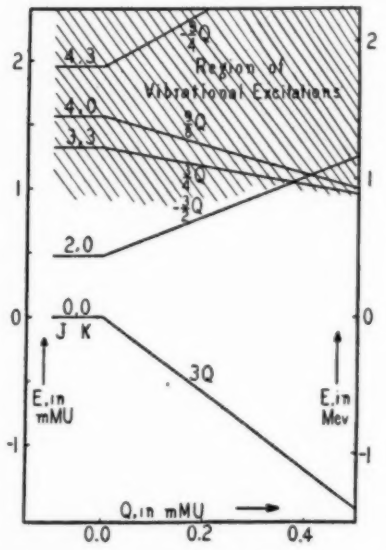

FIG. 3. The energy levels at the left represent the low rotational states allowed for the bipyramid neon model of Fig. 2. Jh stands for total angular momentum and Kh is the component of this along the axis of figure of the rigid model. The possibility of exchange between different configurations of the same energy (see Fig. 2) perturbs the levels. The shift is shown as a function of the value of the exchange integral Q for which a reasonable estimate is 0.17 mMU. Additional excited levels are found if the vibrations of the model are taken into consideration.

equal extent. Eventually, as we approach case (*a*), both the energy of the lowest excitation and also its angular momentum ($m=3$) become considerably greater than in the case of rigid coupling.

Bipyramid model

A further example of the qualitative considerations discussed above is furnished by a problem which can be considered as a model for the nucleus Ne^{20}. We may picture the stable state of the system as that in which five alpha-particles are situated at the vertices of a double pyramid (see Fig. 2). If we assume that the "bond distances" are the same between all pairs of alpha-particles, then this configuration gives the maximum possible number of bonds (9). Diagrams (*b*) and (*c*) show that a distortion of the nucleus in which the 2–4 bond is stretched and the distance between 1 and 5 is shortened will carry the system over into an equivalent position of the same energy but different orientation. For purposes of identification we may symbolize the original configuration by the expression 15 and the equivalent one by 42. By 15 we indicate that the alpha-particles 1 and 5 are located at the two opposite poles of the bipyramid and the three alpha-particles at the base are numbered clockwise when viewed from 1 towards 5. Thus 51 and 15 differ in the order of the alpha-particles in the base. Corresponding to the 20 ordered pairs, we have 20 different configurations of equal energy. Transitions similar to the change 15 to 42 pictured in the figure are 15 to 23, and 15 to 34. One can see qualitatively that other changes from 15, such as from 15 to 51, will encounter higher potential barriers.

A simple criterion for the most important "channels of intercommunication" is the value, r^2, of the sum of the squares of the displacements of the individual alpha-particles which occur during the distortion. In terms of the distance, c, between neighboring alpha-particles, r^2 is easily computed to be $0.74c^2$ for the change from 15 to 42, $2c^2$ for the change to 51, $1.75c^2$ for the change to 13, $2c^2$ for the change to 31, and $2.07c^2$ for the change to 24. As the penetration factor goes down exponentially with r^2, it is clear that the most important type of exchange is the one represented in the figure.

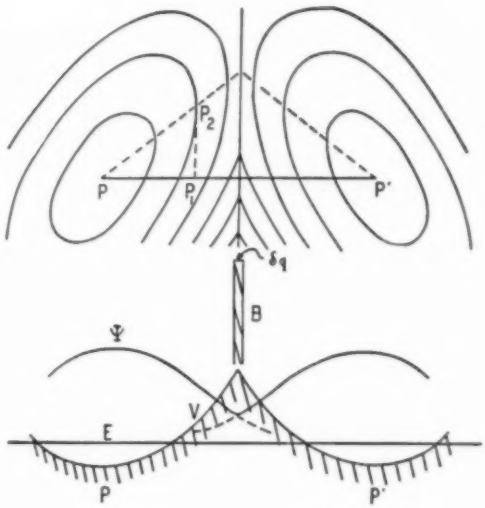

FIG. 4. The lower portion is a schematic diagram for the variation of potential energy which occurs when the system is subjected to a distortion carrying it from one equilibrium position P to an equivalent one P'. The order of magnitude of the potential barrier between P and P' is estimated to be 1.5 mMU for the change from 15 to 24. The fictitious potential barrier B has been introduced in such a way as to obtain a simple form for the zero-order wave function. The contour lines of this wave function are pictured above.

Neglecting at first these exchange phenomena, we may divide the energy of the nucleus into the kinetic energy of rotation of a symmetric top and the zero-point energy of the $3\times5-3-3=9$ vibrational degrees of freedom. In terms of the moments of inertia C and A along and at right angles to the figure axis, and the total angular momentum $J\hbar$ and its component $K\hbar$ along the figure axis, we have

$$E=E_0+J(J+1)\hbar^2/2A + (K^2\hbar^2/2)(C^{-1}-A^{-1}). \quad (13)$$

We shall not be interested in states of the system in which the vibrational degrees of freedom, q_1, q_2, $\cdots$, are excited, and shall therefore treat the system as a rigid rotator.

Only for certain values of J and K is it possible to obtain a rotational wave function whose value is unaltered by those rigid rotations of the model which effect an interchange of the alpha-particles, namely,

$$K=0\,;\ \text{even}\ J:\ \Psi\sim P_J(\cos\theta)f_{\text{vib}}(q)\,;$$

$$K=3n\neq0;\ \text{any}\ J:\ \Psi\sim P_J^{(K)}(\cos\theta) \times\{\exp(iK\chi)+(-1)^J\exp(-iK\chi)\}f_{\text{vib}}(q). \quad (14)$$

Here χ measures rotation about the axis of figure of the double pyramid, and θ is the angle between this axis and some fixed direction in space. The left-hand portion of Fig. 3 shows the position of the low rotational levels allowed according to our analysis. The absolute values of the rotational energies have been obtained by using $A=4.7\times10^{-48}$ g cm^2, $C=3.0\times10^{-48}$ g cm^2.

The occurrence of exchange processes by penetration through potential barriers means now that the total wave function will be a superposition of functions of the type (14):

$$\Psi=(20)^{-\frac{1}{2}}\sum_{c=1}^{20} f_K^{(J)}(\theta_c, \chi_c) f_{\text{vib}}(q_{1c}, q_{2c}, \cdots). \quad (15)$$

Here the summation goes over all 20 stable configurations of the five alpha-particles. The Eulerian angles θ_c and χ_c and the vibrational coordinates q_c are defined in the same way for the various configurations, so that Ψ is symmetric with respect to all interchanges of the alpha-particles. If we write V_c for the potential for which the cth term in Ψ would represent an accurate solution of the wave equation, and V for the actual potential, then by making a first-order perturbation calculation for the change in energy due to leakage through the barriers, we obtain

$$E=E_0+E_{\text{rot}}(J, K)$$
$$+3\int f_K^{(J)*}(\theta_{42}, \chi_{42}) f_{\text{vib}}{}^*(q_{42})(V-V_{15})$$
$$\times f_K^{(J)}(\theta_{15}, \chi_{15}) f_{\text{vib}}(q_{15}) d\tau. \quad (16)$$

In the derivation we have made use of the symmetry of Ψ and the fact that from a given configuration, 15, the most important exchange processes lead only to the three equivalent equilibrium positions 42, 23, and 34.

To carry out the integration over angles, we note from Fig. 2 that the orientation of the configuration 15 differs from that of 42 by a rotation, R, of 90°. Hence according to group theory, the integral of $f_K^{(J)*}(\theta_{42}, \chi_{42}) f_K^{(J)}(\theta_{15}, \chi_{15})$ over all space orientations may be expressed in a simple manner in terms of the elements $D^{(J)}{}_{K,K}(R)$ and $D^{(J)}{}_{-K,K}(R)$ of the standard rotational transformation matrix[11] for $R=90°$, whose values are given by

$$D^{(J)}{}_{KK}(0, 90°, 0)$$
$$=(-1)^{J-K} D^{(J)}{}_{-K,K}(0, 90°, 0)=c_{JK};$$
$$c_{JK}=2^{-J}\sum_{f=0}^{J-K}(-1)^f \frac{(J+K)!}{f!(J+K-f)!}$$
$$\times\frac{(J-K)!}{f!(J-K-f)!}. \quad (17)$$

After the integration over angles, we have left the vibrational part of the exchange integral, defined by

$$Q=\int f^*_{\text{vib}}(q_{12})(V-V_{15}) f_{\text{vib}}(q_{15}) dq. \quad (18)$$

Our result for the position of the low rotational levels, taking account of exchange, is expressed in the equation

$$E=E_0+E_{\text{rot}}(J, K)$$
$$+3\begin{Bmatrix} c_{JK} \\ 2c_{JK} \end{Bmatrix} Q\cdot\begin{Bmatrix} K=0\,;\ \text{even } J \\ K=3n\neq0\,;\ \text{any } J \end{Bmatrix}. \quad (19)$$

The energy values are shown in Fig. 3 as a function of the magnitude of the vibrational exchange integral, Q. A reasonable estimate gives $Q=-0.17$ mMU, so that the first excited rotational level, $J=2$, is raised up 0.75 mMU with respect to the ground state. However, already if Q be as great as -0.38 mMU, the effect is so pronounced that the levels $J=3$ and $J=2$ become interchanged, with the level of greater angular momentum lying lower. The example shows in a striking manner the disturbance of the normal order of rotational levels caused by the existence of resonance between geometrically similar configurations of a system of five identical particles.

To obtain the estimate we have just used for the value of the vibrational exchange integral Q, we express the potential and kinetic energies for small oscillations from equilibrium in terms of suitable normal coordinates $q_1, q_2, \cdots, q_s$:

$$V=(m_a/2)\Sigma\omega_i^2 q_i^2, \quad (20)$$
$$T=(m_a/2)\Sigma\dot{q}_i^2. \quad (21)$$

[11] E. Wigner, *Gruppentheorie und Quantenmechanik* (Braunschweig, 1931), p. 180.

Here $\omega_i/2\pi$ is the classical frequency of vibration of the corresponding normal coordinate. The wave function for the normal state (zero-point vibration) has the value

$$\Psi=(m_\alpha/\pi\hbar)^{n/4}(\omega_1\omega_2\cdots\omega_n)^{\frac{1}{4}}\exp\{-\Sigma m_\alpha\omega_i q_i/2\hbar\}, \quad (22)$$

if we suppose the vibration to occur in the neighborhood of one equilibrium position P. Actually the representative point of the system can penetrate through the potential barrier represented schematically in the lower portion of Fig. 4 and vibrate about the second minimum P'. If, as shown in the figure, we join together in the center of the barrier the unperturbed wave functions for the two minima, we obtain a solution of the wave equation

$$(\hbar^2/2m_\alpha)\Sigma\partial^2\Psi/\partial q_i^2+(E-V_1)\Psi=0 \quad (23)$$

for the unperturbed value of E. Here the potential V_1 is not the same as the actual potential V, however, but has been obtained from it by superposing a fictitious potential wall, very narrow and extremely high, in such a way as to bring about continuity in the normal derivatives of the wave functions on the two sides. Using q_{norm} to denote the coordinate measured parallel to the direction PP', and calling the height and width of the barrier B and δq, we easily obtain in fact the relation

$$-(\hbar^2/m_\alpha)(\partial\Psi_{\text{left}}/\partial q_{\text{norm}})=B\delta q\Psi \quad (24)$$

by integrating (23).

To obtain the correct energy value, we must remove the above-mentioned fictitious potential. Treating this alteration as a small change, we obtain by a first-order perturbation calculation

$$\Delta E=Q=\int\Psi^2(V-V_1)d\tau=-\int B\delta q\Psi^2 dS$$
$$=(\hbar^2/m_\alpha)\int\Psi_{\text{left}}(\partial\Psi_{\text{left}}/\partial q_{\text{norm}})dS, \quad (25)$$

where the integration goes over the $n-1$ dimensional surface normal to PP'. It would appear at first sight that the result should be divided by 2 because both parts of the total wave function are normalized to 1; but in the one-dimensional case one can readily prove that a compensating factor of 2 enters, just because of the fact that the perturbation is not small. It seems reasonable to expect this result in general, so we use (25) as it stands, without rigorous analysis. The integration may be carried out directly, from (22), and gives

$$Q=-\hbar\omega(m_\alpha\omega/\pi\hbar)^{\frac{1}{2}}(r/2)\exp\{-(m_\alpha\omega/\hbar)(r/2)^2\}. \quad (26)$$

Here r is the distance from P to P' and $\omega/2\pi$ is that frequency with which the system would oscillate if constrained to move along the straight line PP' with a potential energy which at every point P_1 on its path (see upper part of Fig. 4) is given by the value of V, not at P_1, but at that point P_2, equally distant from the surface of join, where the wave function has its maximum value. The contour representation of the wave function in the figure is drawn in such a way as to emphasize that in general no normal mode of vibration will lie in the direction PP'.

Following the methods used in reference 9, we find for the normal vibrations of neon characteristic energies ranging from $\hbar\omega_1=0.8$ mMU to $\hbar\omega_9=2.2$ mMU. An estimate for the value of the vibrational exchange integral is obtained from Eq. (26) by substituting for ω a harmonic mean of the 9 characteristic frequencies, and for r^2 the value $0.74c^2$ mentioned earlier. With $\hbar\omega=1.2$ mMU and $r=7.8\times10^{-13}$ cm we find $Q=-0.17$ mMU, which is the value used above in discussing the energy level perturbations shown in Fig. 3. It is of interest to note that the value of the vibrational exchange integral given by (26) will for no value of ω ever exceed in magnitude the limit $Q=-0.925\hbar^2/m_\alpha r^2$.

III. First Excited States of Heavy Nuclei

The actual behavior of nuclei cannot be represented in any mathematically rigorous form; we must be content to estimate the order of magnitude of the excitation energies as they would follow from the simplest possible assumptions. We must investigate in particular in what way the excitation energies will change if the number of the nuclear constituents increases.

The reason why the first excited rotational levels will be strongly disturbed is that the phase of the wave function will be changed by a rotation. If a further small displacement of the alpha-particles suffices to complete an exchange of the constituents (and restore the sign of the wave function) then it follows that the phase of the wave function must change on a comparatively short path. Such change of phase, however, requires an increase of kinetic energy unless a potential barrier forces the amplitude of the wave function to approach zero irrespective of its phase.

Alpha-particle model

We shall first assume that no potential barriers are present. Let a nucleus composed of N_α alpha-particles[12] be pictured in the $3N_\alpha$-dimensional configuration space. A phase change φ over a distance r will cause the momentum to increase by the amount $\hbar\varphi/r$, where r^2 is the sum of the squares of the displacements of the alpha-particles. If originally the momentum and kinetic energy were zero, the result would be to increase the energy by $\hbar^2\varphi^2/2mr^2$. Even if in the original case a considerable zero-point energy and corresponding momenta p_0 are present, the

[12] The nucleus is assumed to be composed of alpha-particles rather than of protons and neutrons in order to simplify the argument. A detailed consideration of particles which possess spin and obey the Fermi statistics would lead in a more complicated way to results similar to those obtained in the text.

average increase of the kinetic energy is still

$$\{p_0+\hbar\varphi/r\}_{Av}^2/2m-p_0^2/2m=\hbar^2\varphi^2/2mr^2, \quad (27)$$

since the expression $\{p_0\hbar\varphi/r\}_{Av}$ vanishes, because of the random direction of p_0 in the unperturbed state.

In order to obtain the perturbation of the rotational levels, the expression $\hbar^2\varphi^2/2mr^2$ should be averaged over all orientations. For an order of magnitude estimate, it will be sufficient to substitute both for φ and for r their maximum possible values. Thus, we set

$$\varphi\sim\pi$$
$$r^2\sim N_\alpha(\delta/2)^2, \quad (28)$$

where N_α again is the number of alpha-particles and δ is their average distance. We thus obtain for the probable increase in excitation energy[13]

$$\Delta E\sim 4\pi^2\hbar^2/2N_\alpha m_\alpha\delta^2, \quad (29)$$

It will be seen that this quantity decreases with the -1 power of the mass and reaches for heavy nuclei a value of about 100 kilovolts. Thus, according to this picture, we shall not expect in general an excitation energy of less than this order of magnitude for nuclei of any atomic number. Exceptions may occur if the nucleus has a spin due to the spin of protons or neutrons; then the lowest excitation energies might be determined by spin-orbit interaction rather than by the factors considered above.

In the model just described, no definite statement can be made about the angular momenta of the levels. Of course, if the nucleus is composed of alpha-particles obeying Bose statistics, the wave function for the lowest level must not have any nodes and must thus belong to the quantum number $J=0$. The first excited level, then, may have any J value for which the rotational energy does not considerably exceed the ΔE given in (29). Therefore we have for the probable upper value for the rotational quantum number J_{exc} of the first excited state the relation

$$\hbar^2 J_{exc}(J_{exc}+1)/2I\sim 4\pi^2\hbar^2/2N_\alpha m_\alpha\delta^2. \quad (30)$$

Here I is the moment of inertia of the nucleus, given by

$$I=10^{-1}(18/\pi^2)^{\frac{1}{3}}N_\alpha^{5/3}m_\alpha\delta^2. \quad (31)$$

Thus we obtain

$$J_{exc}\sim 2.2N_\alpha^{\frac{1}{3}}, \quad (32)$$

which for heavy nuclei gives an angular quantum number $J_{exc}=8$.

Another characteristic J value is the one above which the order of rotational levels will become normal. We shall call this J value the quantum number of collective rotation, J_{col}, since for higher angular momenta the rotational energies approach those of a rigid body. We obtain for J_{col} the relation

$$(\hbar^2/2I)\{(J_{col}+1)(J_{col}+2)-J_{col}(J_{col}+1)\}$$
$$\sim 4\pi^2\hbar^2/2N_\alpha m_\alpha\delta^2, \quad (33)$$

which leads to

$$J_{col}\sim 2.4N_\alpha^{\frac{1}{3}}. \quad (34)$$

For heavy nuclei J_{col} is about 36, and the corresponding energy of rotation is $E_{rot}\sim 2$ Mev. Therefore one cannot expect to determine the moment of inertia of a nucleus described by our present model from a study of energy levels and their angular momenta, since in the region where the rotational levels assume their proper order there will be present a great number of vibrational excitations.

Another interpretation for J_{col} is obtained by comparing the classical frequency of rotation with the frequency of the small displacements which complete the rotational exchange of alpha-particles. This comparison gives

$$\hbar J_{col}/2\pi I\sim\Delta E/2\pi\hbar, \quad (35)$$

which is equivalent to Eq. (33).

To obtain an interpretation of J_{exc}, we shall compare the time necessary to rotate an alpha-particle on the surface of the nucleus through half the distance between two alpha-particles, with the time $\hbar/\Delta E$ required for an essential disturbance of the phase of the wave function by the displacement of the alpha-particles. We then have

$$\{r/(\delta/2)\}\hbar J_{exc}/I\sim\Delta E/\hbar, \quad (36)$$

which leads to a value for J_{exc} differing from

[13] This estimate of the first excitation assumes that of all the low lying levels that for $J=0$ is the only one which, due to the favorable phase relations, is not raised.

that given in (32) only by the factor $(\pi^2/10)^{\frac{1}{2}}$. For J values smaller than J_{exc} it is impossible to follow the rotation of the nucleus, even if we restrict ourselves to an angle $\delta/2r$ and if we use the best possible method of following the rotation, that is, a coordinate system fixed by a statistical study of all alpha-particles.

Thomas-Fermi model

In the above estimates, we used a model in which alpha-particles could exchange without crossing potential barriers. It is of interest to see how these results compare with estimates which one can obtain from the Thomas-Fermi model of the nucleus.[14] We consider a nucleus which consists of N particles (protons and neutrons). The number of protons and neutrons shall be even and equal, so that each cell in phase space will be occupied by four particles. If the radius of the nucleus is r and the maximum momentum P_m, we have for the volume in phase space

$$(4\pi/3)P_m^3(4\pi/3)r^3=(N/4)(2\pi\hbar)^3. \quad (37)$$

For the maximum angular momentum of a particle we obtain

$$P_m r/\hbar=2.4(N/4)^{\frac{1}{3}}=2.4N_\alpha^{\frac{1}{3}}. \quad (38)$$

The close resemblance between this value and J_{exc} may be explained in the following way: if the neutrons and protons are supposed to move in spherically symmetrical fields and if their angular moments are composed according to the rules of vector addition, the lowest state will become an S level in consequence of the attraction between constituent particles. If, then, one neutron or proton is lifted to a level of the same or a neighboring shell a group of excited levels will result the average angular momenta of which will be comparable with the value given in (38). Thus the J values for the lowest excited states will be similar for the α-particle picture and the Thomas-Fermi model.

An estimate of the energy of the first excited state in the Thomas-Fermi model reveals no immediate agreement with the alpha-particle picture. If the excitation energy ΔE is due to the transition from one shell into the next one we may write

$$\Delta E=P_m\Delta P_m/m_H, \quad (39)$$

where ΔP_m, the change of momentum of the excited neutron or proton, is given by

$$(4\pi/3)3P_m^2\Delta P_m(4\pi/3)r^3=g(2\pi\hbar)^3. \quad (40)$$

g is the degree of degeneracy in the shell into which the neutron or proton is lifted. Dividing (40) by (37) we obtain

$$3\Delta P_m/P_m=4g/N. \quad (41)$$

Since the density of nuclei is roughly constant P_m will not vary with N in a systematic way. However, $g\sim 2P_m r/\hbar$ will be proportional (according to (38)) to $N^{\frac{1}{3}}$. Thus we get

$$\Delta E\sim\frac{8P_m^3 r}{3m_H N\hbar}=\frac{8\cdot 10^7\text{ ev}}{N^{\frac{1}{3}}}. \quad (42)$$

This equation differs from (29) both in its dependence on N and in the high values of $\Delta E\sim 2\cdot 10^6$ ev which are obtained from it for heavy nuclei.

The Thomas-Fermi model leads, however, to closer agreement with the alpha-particle picture if one carries out the discussion in greater detail. We shall discuss two such improved pictures.

First we shall assume that we deal with an incomplete shell and that the first excited state corresponds to the transition of a neutron or proton from one degenerate state of this shell to another. Then the excitation energy will correspond to the diminished coupling of the particles in the incomplete shell. Its order of magnitude will be given by the change of interaction between two particles in the same orbit. For short range exchange forces this interaction will be proportional to N^{-1}.[15] Since for the lightest nuclei the interaction is[16] of the order of 10^7 ev to $4\cdot 10^7$ ev for the heaviest nuclei excitation energies of 10^5 ev are obtained. This, as well as the dependence on N is in agreement with (29).

The above estimate was based on a model in which the nuclear proper function is not simply

[14] Similarity of results may be expected in view of the comparison carried out by Euler, Zeits. f. Physik **105**, 553 (1937).

[15] Wigner has found this dependence from the application of the symmetry properties of nuclear wave functions to the kinks in the mass defect curve. See Phys. Rev. **51**, 954 (1937).

[16] Breit, Condon and Present, Phys. Rev. **50**, 825 (1936).

a product function of the individual particles but rather a linear combination of those products which would have the same energy if each particle is assumed to move in a spherically symmetrical field. A second kind of improvement on the individual particle approximation would be to retain the product form of the proper function but to drop the assumption that the particles move in a field of spherical symmetry. Then in estimating the excitation energy ΔE the equations (39), (40) and (41) remain valid. Only g must be set equal to one since the absence of symmetry in the field will remove the degeneracy of the individual particle proper function. Thus we obtain

$$3\Delta P_m/P_m = 4/N \tag{41a}$$

and $$\Delta E = 4P_m^2/3m_H N = (2.7\cdot 10^7/N) \text{ ev}, \tag{43}$$

which has the same dependence on N and the same order of magnitude as (29).

Comparison with experience

Unfortunately there is no direct experimental procedure to determine the position of the first excited level of a heavy nucleus. The arguments adduced in the introduction against low lying rotational levels might be used however to test the orders of magnitude we have obtained in Eqs. (29) and (43) for the excitation energy. We shall discuss here only our last argument (6) concerning the stability of isobars and the radioactivity of potassium and rubidium.

The upper limits of the beta-ray spectra of potassium and rubidium are $7\cdot 10^5$ ev and $2.5\cdot 10^5$ ev, respectively. The explanation of the long periods require that there should be no levels in the product nuclei lying much lower than the beta-limit (unless beta-transitions into these levels are strongly forbidden). Thus we see that the lowest excitation energy of suitable angular momentum must be a few hundred thousand volts in both cases; the limit is more strict for the heavier element, rubidium.

The number of neighboring pairs of isobars can be explained statistically if one postulates a mechanism whereby such a pair will be stable whenever the energy difference between initial and final atoms is less than 50,000 ev.[17] Now with a neutrino of zero mass a beta-disintegration of this energy will yield too short a period of decay if the transition is an allowed one. A satisfactory explanation of the isobars can be obtained, however, by assuming that the angular momenta of the two isobars differ by three or more units. If the difference in angular momenta is great enough the energy difference might be 10^5 ev or even more. This explanation will only hold, however, if in general there exist in the product nucleus no excited levels below 10^5 ev with suitable angular momenta to which transitions may occur. We see therefore that general experience points towards a value of $\sim 10^5$ ev for the lowest excitation energy. The calculations on the "thermal properties" of nuclei indicate[18] that the lowest excited states cannot be much higher than this quantity.

The effect of potential barriers

In conclusion we shall discuss on the basis of the alpha-particle model how the dependence of the lowest nuclear excitation on N_α will change if potential barriers must be crossed when the alpha-particles are displaced. For the lightest nuclei the transition from freely moving alpha-particles to strongly bound alpha-particles is a gradual one. As has been shown in the examples discussed in the second section the low lying energy levels approximate gradually the levels of a rigid top as the potential barriers become higher.

For heavy nuclei, however, even low potential barriers which for light nuclei had no strong effect will become important. The reason is that in heavy nuclei many alpha-particles have to cross the barriers which causes an increase both in the effective width and height of the barrier. Thus for heavy nuclei low lying rotational levels can be avoided only if the displacement of the alpha-particles can be performed on such a path in configuration space on which the "kinetic energy" of the system never becomes negative. It is sufficient to have low potential barriers to effect a sudden change to the rotational spectrum of a rigid body. This change may be called a change of phase (or state) since it occurs suddenly for a system of many particles.

[17] Bethe and Bacher, Rev. Mod. Phys. **8**, 199 (1936).

[18] Weisskopf, Phys. Rev. **52**, 295 (1937); Landau, Physik. Zeits. Sowjetunion **11**, 556 (1937).

It is interesting to note in this connection that the low temperature modification of liquid helium[19] has an unmeasurably small viscosity.[20] Since helium does not solidify unless it is compressed it is reasonable to assume that it is kept in the liquid state because of the zero-point vibrations of the atoms[21] which, for helium, are comparable with the heat of evaporation. The experiments on the viscosity of helium indicate that in a "quantum liquid" the particles may rearrange without crossing potential barriers.

The absence of low lying rotational levels in heavy nuclei definitely indicates therefore that if nuclei are to be compared with a phase of matter in macroscopic experiments the correct analog to use is not a crystallite but a droplet of a "quantum liquid" such as the low temperature modification of liquid helium.

[19] W. H. Keesom and M. Wolfke, "Comm. Phys. Lab. Leyden," No. 190b.
[20] P. Kapitza, Nature **141**, 74 (1938); J. F. Allen and A. D. Misener, Nature **141**, 75 (1938).
[21] Simon, Nature **133**, 460 and 529 (1934); F. London, Proc. Roy. Soc. **153**, 576 (1935).

MAY 15, 1938 PHYSICAL REVIEW VOLUME 53

New Experimental Evidence for the Existence of a Neutrino

H. R. Crane and J. Halpern
University of Michigan, Ann Arbor, Michigan
(Received March 24, 1938)

A new method is used for determining the energy of recoil of the nucleus in the individual beta-disintegration process. A gaseous compound of radiochlorine is placed in a cloud chamber. The clearing field is removed long enough before the expansion to allow the ions to spread out so that the resulting droplets can be seen individually. A cluster of droplets appears at the beginning of the track, and this is believed to be produced by the recoil nucleus. From the number of droplets an estimate is made of the kinetic energy of the nucleus, and this is compared with that calculated from the observed curvature of the beta-ray track. It is found that the laws of momentum as well as those of energy indicate that a third particle participates in the disintegration.

Introduction

In the experiment to be described[1] the momenta of both the electron and the recoil nucleus have been simultaneously measured for the elementary beta-disintegration process. This is the first experiment which has given any information at all regarding the momentum relations in the *individual* disintegration event. Although the results are of limited accuracy, they strongly indicate that momentum is not conserved between the electron and the nucleus alone. Hence the laws of momentum, as well as those of energy, indicate that a third particle participates in the disintegration.

The idea of observing the disintegration of a substance in the form of a gas in a cloud chamber has been suggested many times as a possible way of measuring the momentum or energy of recoil and the direction of recoil of the nucleus emitting the beta-ray. The difficulty with such a scheme is that the length of track made by the nucleus is far too short for observation, even in a cloud chamber operated at the lowest possible pressure. The nucleus will, however, produce a number of ion pairs concentrated in a very small region of space, and the number of ion pairs will be a function of the kinetic energy of the nucleus. It occurred to the authors that if these ions could be allowed to diffuse into a cluster several millimeters in diameter before the condensation were brought about, the individual droplets could be counted, and hence the kinetic energy of the nucleus could be estimated. It was found that this could be accomplished, and by applying a magnetic field to the chamber it was possible to know the momentum of the electron in each case, so that the estimated momentum of the nucleus could be compared with that of the electron.

[1] Halpern and Crane, Abstract 5, New York Meeting of the American Physical Society, Feb. 25–26, 1938.

Apparatus and Experimental Method

An automatic Wilson cloud chamber[2] 15 cm in diameter and 4 cm deep was used, which was filled with air at atmospheric pressure, ethyl alcohol vapor, and a trace of a gaseous compound of the radioactive material. In order to allow the ions to diffuse before the alcohol vapor was made to condense upon them, the clearing field was removed a fraction of a second before the expansion. This was accomplished by means of an adjustable contact in the automatic timing system. Two Sept 35 mm cameras, having f:3.5 lenses were placed 25 cm above the chamber and at a 30 degree angle to each other. This gave close-up views from two directions of only a part of the chamber. The tracks were illuminated by means of a carbon arc, flashed at about 200 amperes, and were photographed at 1/15 second exposure. A rectangular coordinate system of lines 3 cm apart was scratched on the lower surface of the glass top plate of the chamber. By measuring the apparent position of the beginning point of a track with respect to the lines on the plate in each of the views, an accurate determination of the distance of the point below the plate was possible. The two stereoscopic views were projected at the same time, but were not superimposed on the same screen. The position of a given point on a track relative to the coordinate system was simply recorded for each of the two views. Only those tracks which were found to begin at a point well within the illuminated portion of the chamber were included in the final data.

The radioactive material used in the first part of the experiment was radiochlorine, Cl^{38}, produced by bombardment of NaCl by 6 Mev deuterons in the University of Michigan cyclotron. This emits negative electrons with a half-life of approximately 37 minutes, and with an upper energy limit of about 5 Mev.[3] The combination of high energy, long half-life and fairly low atomic weight make this element suitable for our purpose. A gaseous compound of the chlorine suitable for introduction into the cloud chamber was made by the following procedure. The bombarded NaCl (a fraction of a gram) was put into a test tube containing about 5 cc of sulphuric acid, diluted 1 to 3, and a few grams of manganese dioxide. This produced free chlorine in solution. A few cc of ethylene dichloride were introduced into the test tube. This formed a layer above the sulphuric acid. Ethylene gas (generated by dropping ethylene dibromide upon zinc metal) was then bubbled through the liquid in the test tube. The ethylene combined with the chlorine in the lower layer, forming ethylene dichloride, which dissolved in the ethylene dichloride of the upper layer. After bubbling for about 15 minutes the upper layer was drawn off and was shaken vigorously with a large quantity of water in order to remove traces of sodium (which was also radioactive) and also traces of free chlorine and of sulphuric acid. The amount of radioactive ethylene dichloride introduced into the cloud chamber was just that which could exist in the vapor state at room temperature, which was several drops. Into the otherwise dry chamber just slightly more ethyl alcohol than necessary to saturate the volume was added, and the chamber was sealed up with air in it at atmospheric pressure. The presence of an excess of either of the liquids was avoided in order to insure that as large a fraction as possible of the radioactive compound would remain in the vapor state. The time taken for the chemical procedure and for clearing the cloud chamber was 30 to 40 minutes. Needless to say, only a minute fraction of the original activity of the NaCl appeared in the cloud chamber at the end of the procedure, but sufficient activity was always obtained if the NaCl was bombarded for about 5 minutes with 6 microamperes of deu-

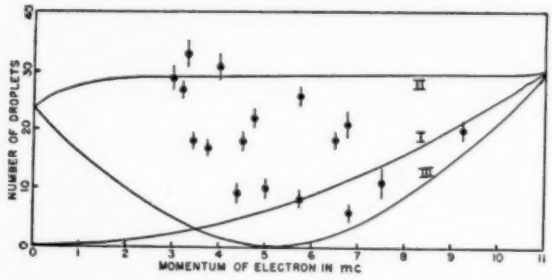

Fig. 1. Numbers of droplets produced by the recoil nuclei (corrected), shown in relation to theoretical predictions made on three different assumptions, as follows: curve I, no neutrino; curve II, neutrino and electron escape in the same direction; curve III, neutrino and electron escape in opposite directions.

[2] Crane, Rev. Sci. Inst. **8**, 440 (1937).

[3] Kurie, Richardson and Paxton, Phys. Rev. **49**, 368 (1936).

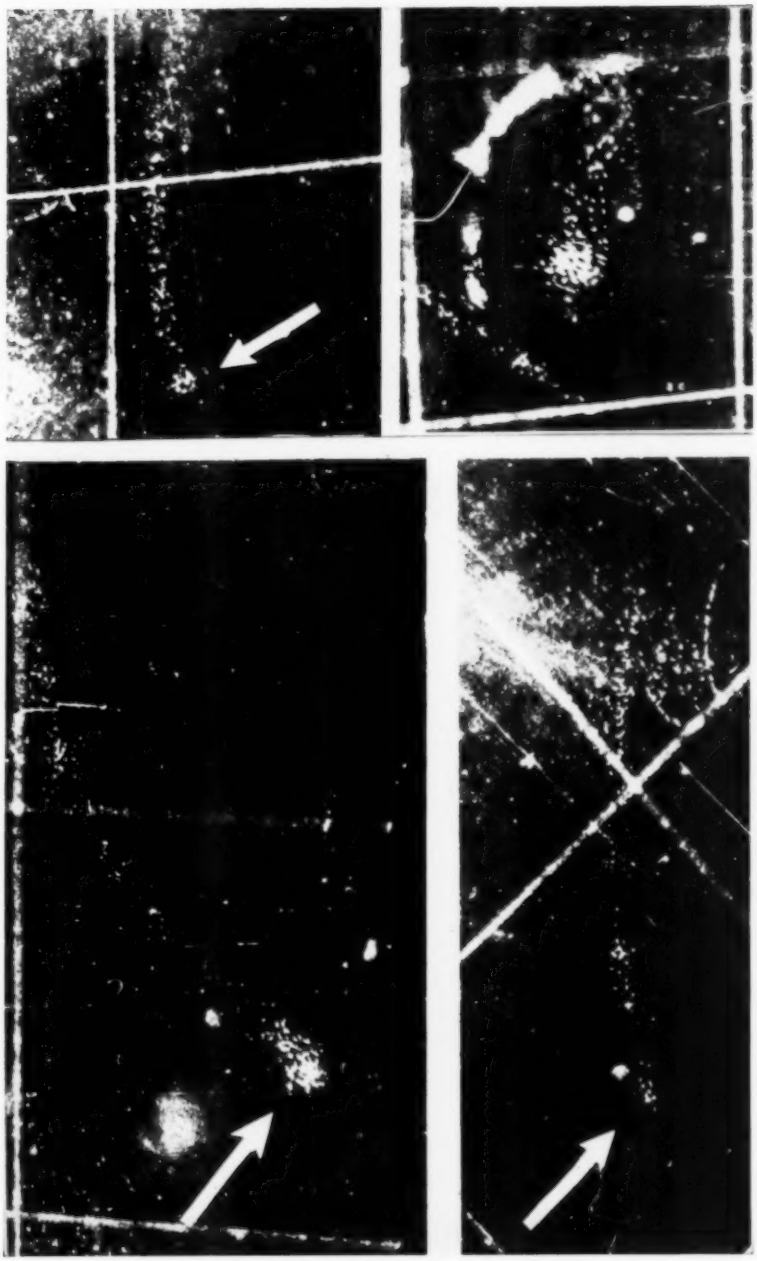

FIG. 2. Four different beta-ray tracks of intermediate energy, showing clusters of droplets at their beginning points.

terons at 6 Mev. The time of bombardment affords a convenient control on the final activity in the chamber, if the chemical procedure is standardized. From 200 to 300 photographs were taken with each loading of the chamber.

The gaseous compound of radiophosphorus[3] (P^{32}), which was used as the control in the second part of the experiment, was prepared as follows. Calcium phosphide (Ca_3P_2) was bombarded by 6 Mev deuterons in the cyclotron. This was decomposed by dropping water onto the solid Ca_3P_2 in an atmosphere of nitrogen. The resulting mixture of PH_3 and nitrogen was passed into the cloud chamber, which had already been flushed with nitrogen. The necessary amount of absolute ethyl alcohol was added,

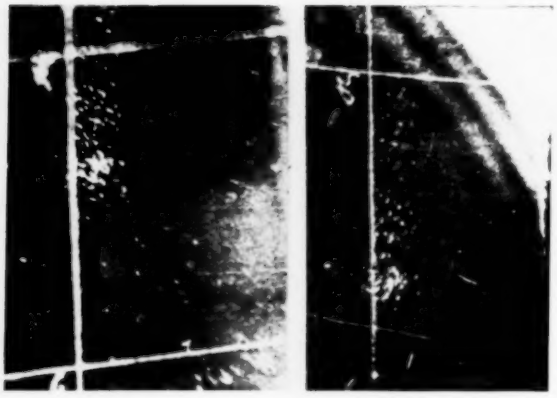

FIG. 3. An electron of high energy, in which the momentum of the electron is sufficient to account for the observed recoil of the nucleus. A stereoscopic pair of photographs is shown.

and additional nitrogen flushed through the chamber to reduce the activity to the optimum value. It was necessary to take precautions against having traces of oxygen present, because of its action on PH_3.

In determining the number of droplets to be assigned to the recoil nucleus, we made the simplifying assumption that the ions originating at a given point on a track diffuse in such a way as to fill with uniform density a sphere whose center is at the source and whose radius depends upon the time and speed of diffusion. On this assumption, the ions for which the recoil nucleus is responsible will fill a sphere of diameter equal to the width of the electron track. In the two-dimensional photograph a circle of this diameter is drawn around the nuclear cluster, the center of which is supposedly at the point of disintegration. The number of droplets inside the circle which are not due to the nucleus but to the electron can easily be calculated on the above assumptions to be nearly ρR, where ρ is the linear density of droplets along the electron track, and R is the radius of the circle. Accordingly we have subtracted ρR from the observed number of droplets in each cluster. ρ was determined by counting the droplets along several centimeters of the particular track. It is obvious that this correction, as it is here determined, is not dependent upon the track lying in a plane perpendicular to the direction of the camera: it is correct for any projection, provided ρ is determined in the same projection.

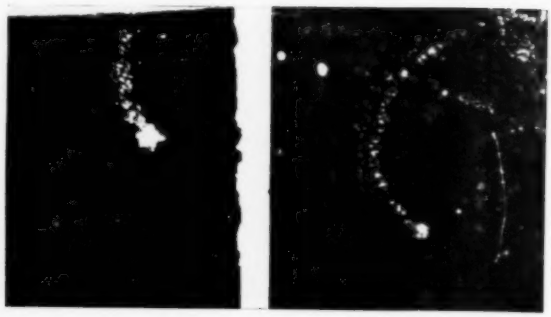

FIG. 4. Two separate tracks of low energy which are clear cases in which the nuclear recoil is larger than that expected from the electron momentum alone.

RESULTS

The results of the droplet counts on the 17 cases obtained with radiochlorine are shown as the dots in Fig. 1. No cases of electrons having less than 1 Mev energy are included, for a reason which will be given later in the discussion. The number of droplets produced by the electron within the region over which the droplets due to the nucleus extend, is subject to statistical fluctuation. To give an idea as to the amount of uncertainty due to this cause, a vertical line of length equal to $(\rho R)^{\frac{1}{2}}$ is drawn through each point. It is more difficult to estimate the uncertainty in the actual counting of the droplets, because this depends largely upon the quality of a given track. We estimate that this error ranges from 2 to 5 droplets.

In Figs. 2 to 4 are shown a number of the tracks obtained. Although all tracks were analyzed stereoscopically, both views are reproduced in only two of the examples. The ruled lines on the chamber top are visible, and are 3 cm apart.

The theoretical expectations for the number of ions produced by the nucleus were derived on three different assumptions. 1. That the momentum of the nucleus is equal to that of the electron (equivalent to assuming that there is no neutrino). 2. That a neutrino of zero or very small rest mass escapes in the same direction as the direction of flight of the electron, and that its momentum is $(W-E)/c$, where W is the upper limit energy of the beta-ray spectrum of Cl^{38} (taken as 5 Mev) and where E is the energy of the electron, calculated from its curvature in the magnetic field. 3. The same as 2 except that the electron and neutrino escape in opposite

directions. In all the above calculations the kinetic energy of the nucleus was calculated from the momentum (its mass is known) and it was assumed that one ion pair (or two droplets) would be produced for each 30 electron volts of kinetic energy. The three possibilities are plotted in Fig. 1. It is clear that if all possible directions of emission of the neutrino with respect to that of the electron are considered, curves 2 and 3 will represent upper and lower limits for the number of droplets, and all the area between them will be permitted.

It is well known that a moving ion is able to produce other ions when its kinetic energy (in the moving coordinates of the collision) is only slightly above the ionization potential of the gas through which it is passing. But the question of the total number of ion pairs a heavy ion of a few hundred electron volts energy will produce before it comes to rest is difficult to answer. It would not be expected to produce more than the usual one ion pair per 30 ev, and could not under any circumstance produce more than one per 16.7 ev, which is the average ionization potential of air. On the other hand it could lose rather large fractions of its energy by thermal collisions without ionization. The numbers of droplets indicated by the points in Fig. 1 may therefore in some cases give too low values for the recoil momentum of the nucleus, but are less likely to give values which are too high.

Possibilities other than ionization by the recoil nucleus exist for producing ions in the neighborhood of the disintegrating atom. The escaping beta-ray may disturb the outer electronic structure of the atom, which may in its readjustment emit an electron of a few hundred volts energy, or may emit a soft x-ray quantum which will be absorbed in the immediate vicinity. To test this we carried out a control experiment, with radiophosphorus, P^{32}, instead of Cl^{38}. P^{32} is a good control because it has about the same atomic weight as Cl^{38}, emits negative electrons, but has a much lower upper energy limit. The greatest possible recoil energy for the P^{32} is 85 electrons volts, which should produce less than 6 droplets. Out of $25P^{32}$ disintegrations in the gas obtained, only two had detectable clusters of droplets at their beginning points. This negative result makes us feel certain that the clusters of droplets observed in the experiment with Cl^{38} were actually caused by the recoil of the nucleus.

Discussion

Meaning of the results obtained

It can be seen from the data presented that in the cases in which beta-rays of small momentum are emitted from radiochlorine the momentum received by the nucleus is usually much greater than that which it could have received from the beta-ray alone. This statement is not subject to any assumption about the efficiency of ionization by the nucleus: it is true even if we assume that the entire kinetic energy of the nucleus is utilized in ionization. This result has a bearing upon certain of the hypotheses which can be made as to the mechanism of beta-disintegration.

1. Suppose that the nucleus retains the excess energy temporarily, emitting it later by any means we may care to postulate. Momentum would then be conserved between the beta-ray and the nucleus, and the data would have to fall on curve 1, Fig. 1.

2. Suppose that the beta-ray carries off all the energy of disintegration, partly as kinetic energy and partly as extra mass, as has been suggested by the group in this laboratory,[4] by Jauncey,[5] and undoubtedly by others. Since the curvature of the beta-ray track in the magnetic field gives the momentum directly (assuming constant charge) the data in this case also would have to fall on curve 1, Fig. 1.

3. If the beta-ray spectrum owes its continuous distribution to a failure of the law of the conservation of energy, there is no reason to believe that the law of the conservation of momentum does not fail also. The present data are not able to eliminate this possibility. However, the experiment is inherently capable of throwing light upon the question if carried far enough, because if the above were true we should expect to find some cases in which the recoil momentum of the nucleus would be less than

[4] Breit, Rev. Sci. Inst. **8**, 141 (1937); Zahn and Spees, Phys. Rev. **53**, 524 (1937).

[5] Jauncey, Phys. Rev. **52**, 1256 (1937); Phys. Rev. **53**, 106 (1938); Phys. Rev. **53**, 197 (1938); Phys. Rev. **53**, 319 (1938).

the minimum which could be given to it by any combination of electron and neutrino energies or angles. Such cases would fall in the area below curve 3 on the right-hand side of the diagram in Fig. 1.

Of all the possibilities mentioned, the hypothesis that a neutrino is emitted simultaneously with the electron seems to fit the data best.

Lower energy component in the Cl^{38} beta-ray spectrum

Kurie, Richardson and Paxton[3] investigated the beta-ray spectrum of chlorine after bombardment with deuterons and found that it could be resolved into two components of about equal intensity and of K. U. upper limits 6.1 and 1.5 Mev. The actual observed upper limits, which we prefer to use in connection with our experiment, are about 5 and 1.2 Mev. They also found that gamma-rays of 2.4 and 1.9 Mev were emitted. The most reasonable assumption seems to be that the 1.2 Mev beta-ray spectrum and the gamma-rays are associated, since the sum of the energies, $1.2+2.4+1.9=5.5$ Mev, is about the same as the energy of the other beta-ray component. It is therefore reasonable to say that no gamma-rays are associated with the 5 Mev beta-ray component.

In our experiment we must be careful to include only those disintegrations which belong to the 5 Mev component, if we are to compare the results with the predicted recoil momenta. An electron which belongs to the 1.2 Mev spectrum, emitted practically simultaneously with the two gamma-ray quanta might give considerable recoil to the nucleus, but would tell nothing about the neutrino. We have therefore included in our data only those cases in which the electron has more than 1 Mev energy; it is fairly certain that these belong to the 5 Mev spectrum.

Use of other gases and radioactive substances

The use of hydrogen in the cloud chamber instead of air would decrease the linear density of ionization of the electron track, which would be an advantage, in that it would decrease the number of droplets to be subtracted from the nuclear cluster. On the other hand the droplets would fall faster, make sharp photography more difficult, and, most important of all, the number of ions produced in hydrogen by the nucleus would probably be much smaller than in air. In the collision of the recoil nucleus (A^{38} after the disintegration) with H_2, the kinetic energy of the A^{38} in the moving coordinates of the center of gravity of the system would be very small indeed, and ionization might not result. It is therefore better to use a gas of atomic weight comparable to that of the Cl^{38}.

The use of He^6 as the radioactive material would give a much greater recoil energy, because the upper limit of its spectrum is about the same as that of Cl^{38} and its mass is much smaller. He^6 has a half-life of 1 second, which means that it would have to be introduced into the chamber before each expansion. It would be difficult to maintain ideal conditions in the chamber under these circumstances, but perhaps not impossible.

Direction of emission of neutrino

The present experiment is inherently capable of giving the distribution in angle of emission of the neutrino with respect to the direction of emission of the electron. An accurate knowledge of the recoil momentum and the electron momentum would make it possible to solve for the angle in each case. Before the results can be interpreted in this way we must obtain exact information as to the efficiency of ionization by slow ions. The higher recoil energy of He^6 would lessen this difficulty.

Acknowledgments

The authors wish to extend their thanks to Professor J. M. Cork, Dr. R. L. Thornton and the other members of the University of Michigan cyclotron group for their generosity in supplying the many samples of radioactive chlorine and phosphorus, to Mr. D. W. Stewart for advice and assistance regarding the chemical procedures used, and to the Rackham Endowment Fund for the financial support of this work.

Elastic and Inelastic Scattering of Fast Neutrons

D. C. GRAHAME AND G. T. SEABORG
Department of Chemistry, University of California, Berkeley, California

(Received January 24, 1938)

Cross sections for the combined processes of absorption+inelastic scattering of fast neutrons ($E \geq 4.5$ Mev and $E \geq 7$ Mev) have been measured for a number of elements by the use of absorbing cylinders and aluminum or iron detectors. A smooth increase with increasing atomic number is found. For neutrons of energies ≥ 7 Mev the ratio of these cross sections to the cross sections for absorption+total scattering (Dunning) is nearly constant at a value of about 0.4. The existence of a scattering of fast neutrons in which little or no energy is lost has been demonstrated experimentally and approximate cross sections for the process have been obtained. Cross sections for an "effective absorption" of medium fast neutrons have also been determined. These cross sections, which are smaller than those obtained for the faster neutrons mentioned above, show a maximum at about $Z=50$ and a marked decrease for the heaviest elements. The cross sections obtained by Aoki and Lea from experiments on the yield of gamma-rays from the action of fast neutrons on matter are in agreement with the present results.

INTRODUCTION

THE absorption scattering cross sections of atomic nuclei for fast neutrons have been measured for a considerable number of elements by Dunning.[1] These cross sections are the sum of the cross sections for three types of interaction of fast neutrons with nuclei: (a) absorption (transmutations due to simple capture, proton emission, double neutron emission, or alpha-emission), (b) elastic scattering, and (c) inelastic scattering. Experiment has not yet shown decisively what fraction of the total cross section is due to each of the three named processes. In the present investigation two series of experiments have been performed which yield cross sections of atomic nuclei for the combined processes of absorption and inelastic scattering for fast neutrons having energies greater than 4 and 7 Mev, respectively. As Weisskopf has pointed out,[2] the results of experiments on the inelastic scattering of such fast neutrons are especially suitable for theoretical investigation because the number of excited states in which the nucleus may be left when the neutron is reemitted will be large enough to make statistical considerations valid. Effective absorption cross sections for medium fast neutrons (so called in order to distinguish them from the faster neutrons used in the first-mentioned experiments) were reported in a previous paper.[3] These measurements have been repeated and extended to include a greater number of elements. Interesting comparisons can now be made between the results obtained with neutrons of different energies, and the conclusions thus reached are of assistance in interpreting the measurements of Aoki[4] and Lea[5] on the intensities of the gamma-rays excited by fast neutrons in various substances.

SCATTERING OF FAST NEUTRONS

The considerations of Bohr[6, 7] have shown that the phenomena which occur upon the impact of a neutron (or other heavy particle) with an atomic nucleus must be treated as two independent processes, namely the formation and eventual breaking up of an intermediate metastable compound nucleus. Frenkel made the suggestion that the compound system formed by the impact of a fast neutron with a nucleus may reemit a neutron with an energy corresponding to the "temperature" of the residual nucleus, in a manner analogous to an ordinary evaporation process.[8] This process of inelastic scattering was treated in a quantitative manner by Weisskopf[2] who applied statistical methods to the case

[1] Dunning, Phys. Rev. **45**, 586 (1934).
[2] Weisskopf, Phys. Rev. **52**, 295 (1937).
[3] Seaborg, Gibson, Grahame, Phys. Rev. **52**, 408 (1937).
[4] Aoki, Proc. Phys.-Math. Soc. Japan **19**, 369 (1935).
[5] Lea, Proc. Roy. Soc. (London) **A150**, 637 (1935).
[6] Bohr, Science **86**, 161 (1937).
[7] Bohr and Kalckar, Vidensk. Selsk. Math.-fys. Medd. **14**, 10 (1937).
[8] Frenkel, Physik. Zeits. Sowjetunion **9**, 533 (1936).

of collisions of fast neutrons ($E>3$ Mev) with heavy nuclei ($A>100$). He found that the reemitted neutrons should have, on the average, energies much less than the energies of the incident neutrons. For example, neutrons with an energy of 10 Mev will be reemitted with a Maxwellian distribution having a mean energy of about 2 Mev. The nucleus is left in an excited state as a result of this energy loss by the neutrons and subsequently returns to the ground state by the emission of one or more gamma-rays.

A study of the cross sections for absorption and inelastic scattering of this kind for fast neutrons may be made by using the radioactivity induced in aluminum or iron. These substances become radioactive under the action of fast neutrons through the reactions:[9, 10]

$Al^{27}+n\rightarrow Mg^{27}+p$ $\quad Mg^{27}\rightarrow Al^{27}+e^-$ (10.3 min.)
$Fe^{56}+n\rightarrow Mn^{56}+p$ $\quad Mn^{56}\rightarrow Fe^{56}+e^-$ (2.6 hr.)

In each case the final stable nucleus is identical with the initial nucleus. From the upper energy limits of the emitted electrons[11–14] and the heights of the potential barriers for protons of the nuclei formed,[15] one may estimate the least energy required for the neutron to produce an observable radioactivity. From such considerations one estimates that neutron energies of about 4.5 and 7.0 Mev are required to activate aluminum (10.3-min. period) and iron, respectively.

The effective absorption of such fast neutrons was measured by observing the decrease in activity of an aluminum or iron detector caused by surrounding a source of neutrons (200 mg Ra+Be) with a cylinder of any one of a number of elements. If the inelastically scattered neutrons have a Maxwellian distribution of energies, the fraction having energies greater than 7.0 Mev probably will not exceed a few percent. Hence we may state that fast neutrons which have been inelastically scattered by the Bohr process will not, in general, retain enough energy to induce radioactivity in an iron detector. That this is also approximately true for an aluminum detector may be inferred from the fact that the results obtained with iron and aluminum detectors were found to be nearly the same. The success of the method probably also depends, in part, upon the fact that even those neutrons which retain sufficient energy to induce radioactivity in the detector after an inelastic scattering process must be expected to have a reduced probability for doing so as a result of their diminished energy.

The quantity measured in these experiments is the total cross section for all processes by which the neutron loses a large fraction of its energy or is absorbed. The values called absorption+inelastic scattering cross sections in the text are therefore more strictly cross sections for absorption+inelastic scattering with large energy losses. If a form of inelastic scattering occurs in which only a small fraction of the energy is lost, the experiments will not detect the process to any marked extent.

The cylindrical absorbers used in these experiments were 17.8 cm long and approximately 10 cm in diameter. The source of neutrons (13 cm long and 1.78 cm in diameter) was placed centrally in a 1.78 cm hole through the axis of the cylinder. Flexible targets of iron or aluminum (made of small strips held together with Cellophane tape) fitted around the curved surface of the cylinders. The radioactivity induced in these targets was measured with a thin-walled steel Geiger-Müller counter. In the measurements made without the absorbers, the geometrical conditions were accurately preserved by the use of identical blanks. When aluminum targets were used, measurements were made alternately with and without the absorbing cylinders in order to eliminate the effects of any changes in the sensitivity of the counter. When the longer (2.6-hr.) period induced in iron was used, the sensitivity of the counter was checked regularly during the measurements.

The results of these measurements are presented in Table I and plotted in Fig. 1 together

[9] Fermi, Amaldi, d'Agostino, Rasetti, Segrè, Proc. Roy. Soc. (London) **A146**, 483 (1934).
[10] The small amounts of Na^{24} and Al^{28} produced in aluminum under the experimental conditions adopted have been taken into consideration. Iron detectors have the advantage that Mn^{56} is the only radioactive element known to be formed by the action of neutrons on iron.
[11] Henderson, Phys. Rev. **48**, 855 (1935).
[12] Brown and Mitchell, Phys. Rev. **50**, 593 (1936).
[13] Gaerttner, Turin, Crane, Phys. Rev. **49**, 793 (1936).
[14] Alichanow, Alichanian, Dzelepow, Nature **136**, 257 (1935).
[15] Bethe, Rev. Mod. Phys. **9**, 172 (1937). See Table XXXIII.

with Dunning's cross sections[1] for the total scattering+absorption of fast neutrons.

The cross sections σ in Table I have been calculated from the fraction transmitted T by use of the relation $T=e^{-N\sigma t}$, where N is the number of nuclei per cm³ and t is the average path length of the neutrons in the absorbers. The probable errors given refer to the errors in the measurements only and are not intended to include systematic errors inherent in the method. Under the experimental conditions here used the average length of path of a neutron originating on the axis of the cylinder and passing in a straight line through the absorber and detector is 24 percent greater than the wall thickness stated in column 2 of Table I. (This 24 percent is a weighted average which takes account of the obliquity of the path of the neutron in both the absorber and the detector.)

Two corrections to the cross sections in Table I must be considered. Neutrons which are scattered in the absorber with negligible energy losses will have, on the average, longer paths through the absorber than the calculations take into account. An approximate calculation of this correction may be made by assuming isotropic scattering and neglecting scattering processes after the first. Dunning's scattering cross sections have been used for Al, Zn, Sn and Pb, and interpolated values have been taken for Sb and Bi. It is assumed from Table II that 40 percent of the collisions are inelastic with large energy losses. (The calculation is not very sensitive to this quantity.) The result of such a calculation indicates that the cross sections in Table I should be reduced by about 13 percent (15 percent for Zn) to account for the effect of single scattering in the absorber. For scattering processes after the first the calculation becomes very complex, but a careful consideration of the problem suggests that a complete correction for single and multiple scattering would reduce the calculated cross sections by about 20 percent (23 percent for Zn).

TABLE I. *Measurements of absorption+inelastic scattering cross sections for fast neutrons.*

Element	Wall Thickness cm	Fraction Transmitted: $Fe^{56}(n,p)Mn^{56}$ Detection $E\geq 7$ Mev	Fraction Transmitted: $Al^{27}(n,p)Mg^{27}$ Detection $E\geq 4.5$ Mev	Cross Section $\times 10^{25}$ cm²
Al	4.2	0.75±0.03		9.3±1.3
Zn	4.2	0.59±0.03		15.4±1.5
Sb	4.2	0.73±0.03		17.9±2.3
Pb	4.2	0.69±0.03		21.3±2.4
Bi	4.2	0.71±0.02		23.2±2.0
C	4.3		0.83±0.02	4.2±0.5
Al	4.2		0.78±0.02	7.8±0.8
Zn	4.2		0.58±0.02	15.9±1.0
Sn	4.1		0.72±0.02	17.1±1.5
Sb	4.2		0.74±0.02	17.6±1.5
Pb	4.2		0.71±0.02	19.7±1.6
Bi	4.2		0.74±0.01	19.8±0.9

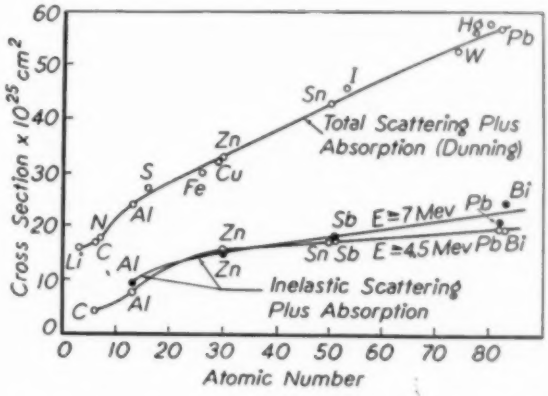
Cross Section × 10²⁵ cm²
Atomic Number
Total Scattering Plus Absorption (Dunning)
Inelastic Scattering Plus Absorption
Sb E≥7Mev Pb Bi
Sn Sb E≥4.5Mev Pb Bi
Li C N Al S Fe Cu Zn Sn I W Hg Pb Bi

FIG. 1. Upper curve, total scattering+absorption cross sections for fast neutrons (Dunning). Lower curves, inelastic scattering+absorption cross sections for fast neutrons as measured with iron detectors ● or with aluminum detectors ○.

The second correction to be considered is that which arises from the increased obliquity in the detector of those neutrons which have been scattered in the absorber with negligible energy losses. The magnitude of this correction may be estimated from a calculation similar to the first by which it is found that the average path through the detector is 6 percent greater than it would be in the absence of the absorber. On account of the exponential nature of the calculation of the cross sections, this correction will amount to 16 percent of the total cross section (13 percent for Zn) and acts to increase the cross sections over the values given in Table I. Since these corrections act in opposite directions, the net result of both corrections is a correction smaller than the probable error of the measurements themselves, except possibly in the case of zinc.[15a]

[15a] A corrected value for the cross section of zinc with iron detection gives $\sigma=14.1\times10^{-25}$ cm². This value corresponds to a sticking probability of 0.43 for Table II instead of the value 0.47 there reported.

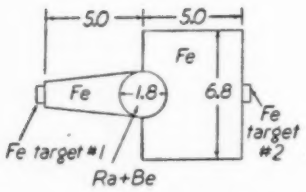

FIG. 2. Experimental arrangement for demonstrating scattering of fast neutrons with small energy losses (elastic or inelastic).

Collie and Griffiths[16] made measurements of the effective absorption of fast neutrons in spherical absorbers of several elements, and their results are in fair agreement with comparable values in Table I. Ehrenberg[17] measured the effective absorption of fast neutrons in a silver cylinder using aluminum and silicon detectors. His results yielded a cross section for silver somewhat larger than that expected from the curves in Fig. 1. However, Ehrenberg used the wall thickness of his silver cylinder for the path length of the neutrons in the silver. Since the average path length of the neutrons was presumably greater than the wall thickness, it is reasonable that his result should have been too large. The magnitude of the correction involved cannot be estimated from his published data.

Figure 1 shows a gradual increase in the cross sections for absorption+inelastic scattering from the lightest to the heaviest elements. No large differences were observed between the results obtained with aluminum and with iron detectors, although the results do suggest slightly larger cross sections for the neutrons detected by iron ($E \geq 7$ Mev) than for the neutrons detected by aluminum ($E \geq 4.5$ Mev), at least in the case of the heavier elements. The cross section given for carbon is doubtless too large because here elastic scattering may cause a neutron to lose nearly one-third of its energy in a single collision.

The cross sections listed in Table I give the sum of the cross sections for absorption and for inelastic scattering with large energy losses. Theoretical considerations lead one to expect that for any but the lightest elements the true absorption cross sections for fast neutrons will be small compared to the cross sections for inelastic scattering.[18] Thus one may say to a good approximation that the cross sections given in Table I refer to the single process of inelastic scattering with large energy losses.

One infers that the differences between the cross sections for inelastic scattering+absorption as given in Table I and Dunning's cross sections for total scattering+absorption give at once the cross sections for elastic scattering or for inelastic scattering with *small* energy losses. This procedure assumes that the absolute magnitudes of both sets of cross sections are correct. Dunning's cross sections were determined under good geometrical conditions, and none of the disturbing factors would tend to make his cross sections too large in any event. The values in Table I cannot be sufficiently in error to alter the conclusion that a large difference exists between the two sets of values. Thus it appears that the difference between these results and those of Dunning is real and attributable to elastic scattering or to inelastic scattering with small energy losses.

It is to be noted that a form of inelastic scattering of fast neutrons may occur in which there is a less complete amalgamation of the incident neutron with the nucleus and which might be designated by the term surface scattering. Such a process might often give rise to small energy losses.

Since no direct evidence for scattering with small energy losses (either elastic or inelastic) has been reported, experiments were carried out to give qualitative proof that such scattering does occur. A view of the apparatus used is given in Fig. 2. Two iron targets (composed of thin strips stacked together) were activated simultaneously in the positions shown, and the intensity of their activities compared. If a neutron may be scattered and still retain sufficient energy to induce radioactivity in iron, then target No. 1 (Fig. 2) will be less active than target No. 2 because in the latter case the mass of iron not directly between the source and the target may scatter into the target neutrons that would otherwise be lost. The activity observed in target No. 2 was 25 ± 5 percent greater than that observed in target No. 1. This result is in qualitative agreement with the supposition that

[16] Collie and Griffiths, Proc. Roy. Soc. (London) **A155**, 434 (1936).
[17] Ehrenberg, Nature **136**, 870 (1935).
[18] Bethe, Rev. Mod. Phys. **9**, §65 (1937).

the difference between Dunning's curve and the lower curves in Fig. 1 gives the cross section for scattering of fast neutrons with small energy losses (elastic or inelastic).

Additional evidence for such scattering was obtained as follows: An aluminum detector in the form of a cylinder surrounded the source of neutrons, and measurements were made with and without a large iron block (back-scatterer) entirely surrounding this assembly. When the iron back-scatterer was in place, the 10.3-min. activity in aluminum was increased 4.5 ± 1.0 percent by the action of neutrons scattered from the iron block into the detector.

Table II shows, in column 2, cross sections for scattering of fast neutrons with small energy losses (elastic or inelastic) obtained by difference from Dunning's values for absorption+total scattering and the values in Table I for absorption+inelastic scattering as measured with iron targets. Column 3 gives the ratio of the absorption+inelastic scattering cross section to Dunning's cross section for the same elements. This ratio, which is nearly constant at a value of about 0.4, represents the fraction of the neutron-nucleus collisions which are inelastic with large energy losses. This ratio is the sticking probability, ξ, as defined by Bethe[18] in the equation $\xi=\sigma/\pi R^2$, where σ is the absorption+inelastic scattering cross section and where, in this case, Dunning's cross sections are used for πR^2.

Scattering of Medium Fast Neutrons

In a previous paper[3] cross sections for the combined processes of absorption and inelastic scattering were reported for medium fast neutrons; these measurements have now been repeated under improved experimental conditions and have been extended to include a greater number of elements. In these experiments a source of fast neutrons was enclosed within a lead block of such dimensions that the neutrons to be studied passed through 30 centimeters of lead before reaching the detector. The detector used was a Geiger-Müller counter surrounded by copper. Neutrons which impinge upon the copper nuclei may undergo inelastic scattering, and the gamma-rays resulting from this process are detected by the counter. In order to be detected in this manner, the neutron must have an energy not less than the energy of the first excited state of the copper nucleus. Since this method of detection certainly detects neutrons with energies less than a million volts, the average energy of the neutrons to which it responds will be much less than that of the aluminum and iron detectors used in the previous section. Such neutrons will be called medium fast neutrons in order to distinguish them from the faster neutrons employed in the experiments described above.

Table II. *Cross sections for scattering with small energy losses and sticking probabilities for fast neutrons ($E\geq7$ Mev).*

Element	Cross Section $\times10^{25}$ cm²	Sticking Probability (see text)
Al	15	0.39
Zn	18	0.47
Sb	26	0.41
Pb	37	0.37
Bi	39	0.39

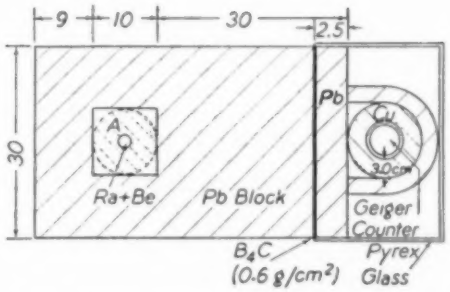

Fig. 3. Experimental arrangement for measuring effective absorption of medium fast neutrons.

The exact experimental arrangement used was a modification of that described in the previous paper and is shown in Fig. 3. The source of fast neutrons (200 mg Ra+Be) was mounted at the center of the cavity A within the lead block, which was large enough to absorb nearly all of the gamma-rays emitted by the radium source in the direction of the counter. The counter used was made from a steel tube (12.5 cm×3.8 cm, 0.13 mm wall thickness) and was filled with a mixture of argon and ethyl alcohol vapor (10 cm A+0.3 cm C_2H_5OH).[19] Boron carbide and Pyrex glass surrounded the copper detector, as shown, to prevent slow neutrons from the source, or neutrons slowed in the floor and walls of the room from acting on the detector system. The entire assembly was mounted on a steel table well

[19] Trost, Zeits. f. Physik **105**, 399 (1937).

removed from neighboring walls or other hydrogenous material.

When the radium-beryllium source was introduced at the cavity A (Fig. 3), the counting rate increased from the natural background of 35 per minute to 160 per minute. This increase in counting rate was due chiefly to the gamma-rays produced by fast neutrons in the detector.[3] A small fraction of the increase caused by the radium-beryllium source will, of course, be due to the incomplete absorption in the large lead block of the primary gamma-rays from radium and its decay products. The magnitude of this effect was determined by methods previously described,[3] but another and more accurate determination has been made by replacing the radium-beryllium source by 150 millicuries of pure radon.[20] With the arrangement shown in Fig. 3, the effects due to primary gamma-rays were found to be very small; however, in the work which follows, the appropriate corrections have been made in every case.

TABLE III. *Measurements of effective absorption cross sections for medium fast neutrons.*

Element	Wall Thickness cm	Fraction Transmitted		Cross Section $\times 10^{25}$ cm^2
		Cu$(n, n\gamma)$Cu Detection	Pb$(n, n\gamma)$Pb Detection	
C($\rho=1.7$)	4.3	0.959±0.015		1.1±0.4
Al	4.2	0.933±0.015		2.7±0.6
S($\rho=2.0$)	4.0	0.918±0.015		5.7±1.1
Cl(CCl_4)	4.3	0.944±0.015		5.1±1.5
Fe	4.1	0.817±0.015		5.7±0.5
Cu	3.5	0.823±0.015		6.5±0.6
Zn	4.2	0.833±0.015		6.7±0.6
Cd($\rho=7.7$)	4.1	0.855±0.015		9.2±1.0
Sn	4.1	0.886±0.015		7.8±1.1
Sb	4.2	0.864±0.015		10.5±1.2
I($\rho=4.5$)	4.1	0.922±0.015		9.2±1.7
Hg	3.9	0.851±0.015		10.0±1.1
Pb	4.2	0.881±0.010		9.1±0.8
Bi	4.2	0.927±0.010		6.3±0.9
C($\rho=1.3$)	4.1		0.98±0.02	0.6±0.6
Al	4.2		0.92±0.02	3.4±0.8
S($\rho=2.0$)	4.0		0.93±0.02	5.0±1.4
Cl(CCl_4)	4.0		0.92±0.02	8.3±2.1
Fe	4.0		0.80±0.02	6.2±0.7
Cu	3.5		0.77±0.02	8.9±0.9
Cd($\rho=7.3$)	4.3		0.82±0.02	12.1±1.4
Hg	3.9		0.86±0.02	9.4±1.5
Pb	4.2		0.90±0.02	7.3±1.6

[20] The radon was enclosed in soft glass. Such a gamma-ray source gives a small intensity of neutrons from the action of alpha-particles on the constituents of glass. Their presence was easily demonstrated by the use of a BF_3-filled proportional counter and their effect was allowed for in this determination.

The effective absorption cross sections for medium fast neutrons were measured by surrounding the source at A with cylindrical absorbers and observing the decrease in counting rate of the Geiger-Müller counter. Those neutrons which have been inelastically scattered in the absorber with large energy losses will have a greatly diminished probability of exciting gamma-rays in the detector by a second inelastic collision. Experimentally, this will manifest itself as an effective absorption of the neutrons. The results of such measurements are presented in Table III together with results obtained in a similar manner by using lead instead of copper as the detector. Figs. 4a and 4b show both sets of data graphically. The cross sections given have been calculated from the mean free paths determined by the transmissions observed. The suitability of this method of calculation has been checked by showing that the absorption is approximately exponential with thickness of absorber. The values given are somewhat smaller than those reported in the previous paper because of a more accurate determination of the intensity of primary gamma-rays reaching the counter from the radium source.

The curves in Figs. 4a and 4b show a gradual rise with atomic number up to about $Z=50$ and a small decrease in cross section for the heaviest elements studied. In particular, the cross section for bismuth (Fig. 4a) is certainly much smaller than those for lead and mercury. A marked decrease for lead and bismuth has been observed by Aoki in experiments on the intensity of the gamma-rays excited in various elements by 2.4 Mev $(D+D)$ neutrons.[4] The values obtained by Aoki give a direct measure of the relative cross sections for inelastic scattering, provided that the number of gamma-rays emitted by the participating nuclei and the efficiency of their detection remain the same from element to element. Aoki's results for the elements here studied are presented for comparison in Fig. 4c. The general agreement between the three sets of values shows that the small cross sections observed in the heavy elements must be real. These low cross sections for heavy nuclei indicate that medium fast neutrons either lack the energy necessary to undergo inelastic scattering with a high probability or, more likely, undergo

inelastic scattering with much smaller energy losses. The experiments already described with more energetic neutrons (Table I) do not show this decrease in the cross sections for the heavy elements.

The absolute values of the cross sections in Table III are very much smaller than those obtained in Table I for more energetic neutrons. This result is undoubtedly due in large part to the fact that neutrons which are inelastically scattered in the absorbers may still retain enough energy to be detected by the copper or lead detector. It may also indicate that medium fast neutrons which are inelastically scattered lose on the average a smaller fraction of their energy than the faster neutrons employed in the first experiments, in agreement with the calculations of Weisskopf who showed that the energy of the inelastically scattered neutrons should be approximately proportional to the square root of the energy of the incident neutrons.[2] In addition it is not improbable that the sticking probability of fast neutrons increases with increasing energy of the neutrons as a result of the more closely spaced levels associated with higher energies of excitation in the compound nucleus.

Measurements on the intensity of gamma-rays produced by the action of fast neutrons on matter have been made by Lea[5] as well as by Aoki. The results of the two workers differed markedly for the heavier elements. Lea found a continual increase in the cross sections with atomic number, even up to lead and bismuth, whereas Aoki found a falling off for these elements as already shown (Fig. 4*c*). Moreover the yield of gamma-rays seemed to be larger in the experiments of Lea than in those by Aoki. These differences are evidently attributable to the higher energies of the neutrons used by Lea. He used fast neutrons from the interaction of polonium alpha-particles with beryllium (without the interposition of lead or other substances which would have slowed down the neutrons by inelastic scattering), whereas Aoki used the less energetic (2.4 Mev) neutrons from the action of deuterons on deuterium.

Several investigations have dealt with the intensity of gamma-rays produced by radium-beryllium neutrons acting on lead.[3, 21–23] In such experiments it has always been necessary to pass

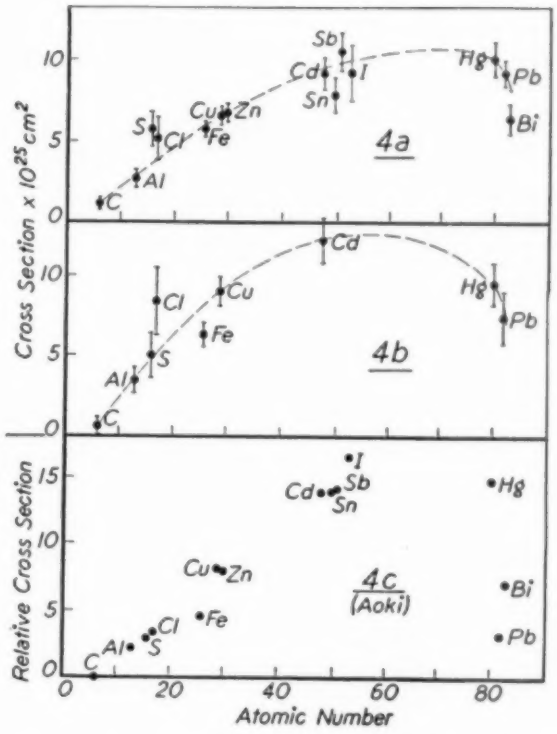

FIG. 4. *a*, Effective absorption cross sections for medium fast neutrons as measured with a Cu detector; *b*, same, measured with a Pb detector; *c*, relative cross sections for the production of gamma-rays by 2.4 Mev neutrons (Aoki).

the neutrons through large thicknesses of some dense substance in order to absorb the primary gamma-rays, and hence the neutrons emerge with reduced energies, as already pointed out. This fact is adequate to explain fully the fact that Lea, with his more energetic neutrons, observed large yields of gamma-rays from lead whereas Kikuchi and co-workers failed in their earlier experiments to find any gamma-rays whatsoever from the process.

We take this opportunity to express our gratitude to Professor G. E. Gibson and Dr. W. F. Libby of the department of chemistry and to Professor J. R. Oppenheimer of the department of physics for valuable advice and suggestions. Thanks are due also to Dr. L. R. Taussig of the University of California Medical School for a gift of radon used in the gamma-ray control experiments.

[21] Kikuchi, Aoki, Husimi, Proc. Phys.-Math. Soc. Japan **18**, 297 (1936).
[22] Gibson, Seaborg, Grahame, Phys. Rev. **51**, 370 (1937).
[23] Takeda, Proc. Phys.-Math. Soc. Japan **19**, 835 (1937).

The Experimental Verification of the Quantum-Mechanical Dispersion Theory by Reflection and Diffuse Scattering of X-Rays from Zinc

W. A. BRUCE
Wayman Crow Hall of Physics, Washington University, St. Louis, Missouri
(Received March 12, 1938)

Hönl used his dispersion theory to develop a formula for the x-ray scattering power of an atom for wave-lengths near the absorption edge. He expressed his formula as the difference Δf between his value and f calculated by some method such as that of Hartree. In this paper it is shown that the F values obtained in the powder crystal experiments of Brindley, Wollan and Harvey, and Miller may be used to verify this formula when they are corrected by the proper temperature factor given by recent experiments in diffuse scattering. The diffuse scattering experiment also gives f values which may be used to verify the Hönl theory. It is shown that all existing data on the f values of zinc are in good agreement when they have been corrected by the Jauncey and Bruce temperature factor and the Hönl Δf. A working formula for Hönl's Δf for any element and for any wave-length is given together with a table of theoretical values of Δf for zinc. From a consideration of all experimental results for zinc a set of f values has been constructed and these are given in a table. This table shows that there is electron distortion and reasons are advanced for believing that the distortion of the electron atmosphere extends deeper into the atom than the valence electrons.

1. INTRODUCTION

THE study of the scattering of x-rays by matter has been considerably delayed by the difficulty of separating the contributing factors in the intensity measurements of the scattered x-rays. In the ideal case of the Thomson scattering from a group of free electrons, the scattered intensity at an angle ϕ with the primary beam is independent of the variable $(\sin \frac{1}{2}\phi)/\lambda$. The grouping of these same electrons into the tightly bound formation of the atom introduces a function of $(\sin \frac{1}{2}\phi)/\lambda$ by virtue of the fact that there are definite space relations among the electrons. However, the complications due to these relations are not nearly so troublesome as the difficulties caused by the natural vibrations of the electrons, for the phase angle of a scattered wave from an electron is a function of the difference between the frequency ν of the primary radiation and the natural frequency ν_e of the electron in the atom. On the classical picture, if ν is much greater than ν_e, the scattered radiation is practically in phase with the primary radiation. If ν is slightly less than ν_e, the scattered ray is approximately 180° out of phase with the primary ray. Between these limits any value of the phase angle is possible. Thus all scattering experiments which will be free from the influence of this phase change must be made with a primary radiation whose frequency is much larger than any of the natural frequencies of the electrons. Practically, this means $\nu \gg \nu_K$, where ν_K is the natural frequency of the K electrons.

Hartree[1] and other wave mechanists have calculated the scattering factor of an atom for $\nu \gg \nu_K$. They have obtained values which give better agreement with experiment than the simple classical theories. Hönl[2] has developed a very complete quantum-mechanical treatment of the phase angle problem for ν near ν_K. He has made use of his theory to predict the structure factors of Fe, Mo, and W. Hönl shows that his numerical values agree fairly well with certain experimental results.

In addition to the above-mentioned scattering problems from free atoms, we encounter other factors when we go to the crystalline state. As the atoms forming crystals are crowded together. the form of the potential barrier[3] of the atom is changed. The outermost conduction electrons are free to move in a periodic field. The effect of the conduction electrons has been discussed by Zener[4] and Scharwächter,[5] but both theory and experiment indicate that any effect on the f values is negligible at values of $(\sin \frac{1}{2}\phi)/\lambda$ greater than about 0.2. The motions of the next layer of electrons are less profoundly affected by the interatomic spacing, but they do move in orbits which are probably affected by the anisotropy of

[1] D. R. Hartree, Proc. Camb. Phil. Soc. **24**, 89 (1928).
[2] H. Hönl, Ann. d. Physik **18**, 625 (1933).
[3] J. C. Slater, Rev. Mod. Phys. **6**, 209 (1934).
[4] C. Zener, Phys. Rev. **48**, 573 (1935).
[5] W. Scharwächter, Physik. Zeits. **38**, 165 (1937).

the crystal. We now have a picture of the crystal composed of a relatively few conduction electrons wandering to and fro in a rather free manner and of atoms whose scattering power has been made anisotropic.

We must now modify the whole picture by considering the thermal vibrations of the atoms. The effect of temperature on the scattering power of the atoms in a crystal has had several theoretical treatments[6] for the case of isotropic crystals. Zener[7] has made a theoretical study of the thermal vibrations in anisotropic crystals. For the cases of both isotropic and anisotropic crystals, it is assumed that each atom vibrates as a whole in the crystal lattice. A truer picture may be that the amplitude of vibration is different for the inner electrons than for the outer electrons—some distortion of the outer electron atmosphere being perhaps due to the thermal vibrations. However, in this paper we shall separate the thermal vibrations from the distortion of the outer electron atmosphere.

2. The Atomic Structure Factor

Hönl's method of attacking the problem of the scattering power of an atom in the region of anamolous dispersion was first suggested by Waller,[8] who used a formula involving induced dipoles, quadrupoles, and octopoles in an atom which was under the influence of an electromagnetic wave. Hönl succeeded in developing the solution into a rapidly converging series by the use of spherical harmonics. The fact that Hönl did not include in his calculations the effect of spin or relativity is of no consequence in this paper since $h\nu_K$ for zinc is less than mc^2 by a factor of 50. The structure factor obtained by Hönl differs from the Hartree f by

$$\Delta f = -\xi_1^{(0)} - \frac{1}{2}\frac{\eta_1^{(0)}}{f+\xi_1^{(0)}} + \text{quadrupole terms}, \quad (1)$$

where, according to Hönl's notation,

$$\xi_1^{(0)} = (2^7 e^{-4}/9)(4Q_2' - Q_3'), \quad (2)$$

$$Q_n' = -\frac{x^2}{(1-\delta)^2}\int_x^\infty \left(\frac{1}{\zeta-1}+\frac{1}{\zeta+1}\right)d\zeta, \quad (3)$$

[6] See C. Zener and G. E. M. Jauncey, Phys. Rev. **49**, 17 (1936).
[7] C. Zener, Phys. Rev. **49**, 122 (1936).
[8] I. Waller, Zeits. f. Physik **51**, 213 (1928).

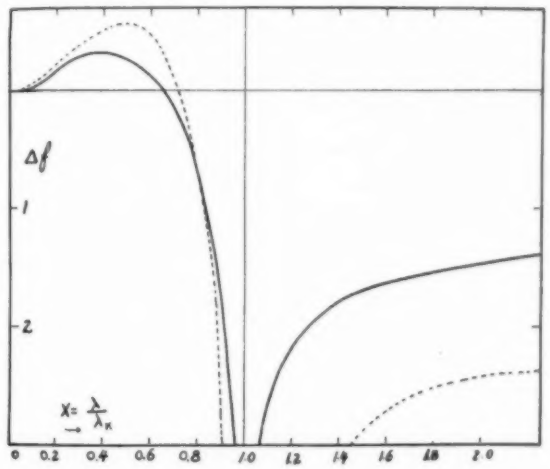

FIG. 1. The solid curve is the approximate Δf for zinc. It is assumed that other terms in (1) than the first are insignificant. The dotted curve is the classical theory.

$$\delta = \frac{(z-s)^2 - h\nu_K/Rhc}{(z-s)^2}, \quad (4)$$

$$x = \lambda/\lambda_K, \quad (5)$$

and s is the screening constant for the K shell. A table of values of δ is given elsewhere.[9] These values indicate a slowly varying function of the atomic number with the value of δ for zinc being 0.205.

On integration, (3) gives

$$Q_2' = \frac{x^2}{(1-\delta)^2}\log\left|1-\frac{1}{x^2}\right| \quad (3a)$$

and $$Q_3' = \left(2x^2 + x^3\log\left|\frac{1-x}{1+x}\right|\right)\Big/(1-\delta)^3. \quad (3b)$$

If only the $\xi_1^{(0)}$ term is considered, (1) becomes

$$\Delta f = 0.26\left\{\frac{4x^2}{(1-\delta)^2}\log\left|1-\frac{1}{x^2}\right| - \frac{2x^2}{(1-\delta)^3} - \frac{x^3}{(1-\delta)^3}\log\left|\frac{1-x}{1+x}\right|\right\}. \quad (1a)$$

This formula can be used for calculating Δf for any atom and any wave-length and should be of use to other physicists when they are comparing experimental results with theory.

The solid curve of Fig. 1 is the graph of $\xi_1^{(0)}$ *vs.* x for zinc. In this simplification of Δf the wave mechanical picture differs from the clas-

[9] H. Hönl, Zeits. f. Physik **84**, 1 (1933).

sical picture principally because of the fact that wave mechanics considers the scattering power of the K electrons to be a function of the atomic number. For instance, in zinc the effective strength of the K shell is 1.31[9] rather than the classical value of 2. The broken curve shows the relation between $\xi_1^{(0)}$ and x for zinc on the Kramers-Kallmann-Mark theory.[10]

The second and third terms in (1) involve functions of $(\sin \frac{1}{2}\phi)/\lambda$. In the second term

$$\eta_1^{(0)} = -\pi \frac{2^7 e^{-4}}{9} \left(\frac{4x^2}{(1-\delta)^2} - \frac{x^3}{(1-\delta)^3} \right) \qquad (6)$$

and in reality depends upon the absorption coefficient of the scattering material. This means that while it may have an appreciable value on the short wave-length side of the absorption edge, its magnitude on the long wave-length side is insignificant. This explains why the second term has been omitted in comparison with experimental data. In the experiments on zinc the value of the second term is two percent of the first term.

The third term is a quadrupole term which would normally be significant in the L absorption edge problem. Its effect is very small in the case of the K region and for the element zinc.

Table I gives the values of $\xi_1^{(0)}$ and of $\eta_1^{(0)}$ for various values of x in the case of zinc.

There seems to be little data to test the angle-dependence part of Hönl's theory. Rusterholtz[11] gives an empirical formula which he obtained by using primary rays of Zn $K\alpha$ and a scatterer of copper. This made $x=\lambda/\lambda_K=1.038$. His formula came out to be

$$\Delta f = 3.68 - 0.03(\sin \tfrac{1}{2}\phi)/\lambda.$$

The Hönl formula for these conditions is

$$\Delta f = 3.50 - \frac{0.025}{f-3.50} + 0.016 \frac{2\cos^2\phi}{1+\cos^2\phi}.$$

Numerically these two formulas agree pretty well over the experimental range. It is noted that the quadrupole term is included. In this case the quadrupole term is of some importance because of the closeness of x to unity.

3. Powdered Crystal Structure Factors

Structure factors for powdered zinc have been obtained for Cu $K\alpha$-rays ($\lambda=1.54$A) by Brindley[12] and by Wollan and Harvey[13] and for Mo $K\alpha$-rays ($\lambda=0.71$A) by Miller.[14] These experiments give F values rather than f values. The true atomic structure factors, f, are obtained from the experimental F values by means of

$$f = Fe^M. \qquad (7)$$

In each experiment the front face method was used and the powder was obtained by sublimation.[12, 15]

If we call $f_{0.71}$ the structure factor of zinc for $\lambda=0.71$A and $f_{1.54}$ the structure factor for $\lambda=1.54$A and if we define $\Delta f'$ by

$$\Delta f' = f_{0.71} - f_{1.54}, \qquad (8)$$

then

$$\Delta f' = \Delta f_{0.71} - \Delta f_{1.54}, \qquad (9)$$

where Δf_λ is obtained from (1) or (1a) for $x=\lambda/\lambda_K$. For a given reflection e^M is the same regardless of the wave-length and hence by (7) and (9)

$$\Delta f' = (F_{0.71} - F_{1.54})e^M. \qquad (10)$$

Values of F are listed in Table II. The values shown in column 4 are the averages of Brindley's and of Wollan and Harvey's values for $\lambda=1.54$. Column 5 shows Miller's values for $\lambda=0.71$.

[10] See A. H. Compton and S. K. Allison, *X-Rays in Theory and Experiment*, p. 292.
[11] A. A. Rusterholtz, Zeits. f. Physik **82**, 538 (1933).
[12] G. W. Brindley, Phil. Mag. **21**, 790 (1936).
[13] E. O. Wollan and G. G. Harvey, Phys. Rev. **51**, 1054 (1937).
[14] R. D. Miller, Phys. Rev. **51**, 959 (1937).
[15] W. A. Bruce, Rev. Sci. Inst. **8**, 451 (1937).

Table I. *Values of $\xi_1^{(0)}$ and $\eta_1^{(0)}$ for various values of x in the case of zinc.*

x	0.2	0.4	0.6	0.8	0.9	1.1	1.2	1.4	1.6	1.8	2.0
$\xi_1^{(0)}$	0.164	0.301	0.125	−0.692	−1.72	−2.66	−2.17	−1.78	−1.61	−1.53	−1.46
$\eta_1^{(0)}$	−0.206	−0.726	−1.52	−2.49	−3.01						

TABLE II. *Values of F.*

1 LINE	2 ψ	3 e^M	4 $F_{1.54}$	5 $F_{0.71}$	6 $f_{0.44}$	7 $F_{1.54}e^M$	8 $\Delta f'$ $(\lambda=1.54)$ $(\lambda=0.44)$	9 $\Delta f'$ $(\lambda=1.54)$ $(\lambda=0.71)$	10 $\Delta f_{II'}$
0002	0	1.10	19.7	22.3	23.7	21.7	2.0	2.86	2.43
$10\bar{1}0$	90	1.03	22.7	24.2	25.2	23.4	1.8	1.55	2.44
$10\bar{1}1$	65.0	1.06	19.3	22.0	23.9	20.4	3.5	2.86	2.44
$10\bar{1}2$	47.0	1.14	16.7	18.7	21.2	19.0	2.2	2.28	2.44
$10\bar{1}3$	35.6	1.20	13.7	15.9	18.7	16.4	2.3	2.64	2.45
$10\bar{2}0$	90.0								
$11\bar{2}2$	61.7	1.21	12.0	13.9	17.1	14.5	2.6	2.30	2.45
$20\bar{2}1$	76.9	1.17	12.4	13.9	16.7	14.5	2.2	2.75	2.45
$20\bar{2}3$	55.0	1.42	8.1	10.2	14.7	11.5	3.2	2.98	2.45
$10\bar{1}5$	23.2	1.69	6.7	8.2	13.7	11.3	2.4	2.54	2.46
$11\bar{2}4$	42.8								
$21\bar{3}1$	80	1.29	7.7	9.7	13.2	9.94	3.2	2.58	2.47
0006	0	1.49	6.3	7.8	12.3	9.4	2.9	2.24	2.47
$21\bar{3}2$	70.6								

4. Temperature Factor and Structure Factor from Diffuse Scattering

From the theory of diffuse scattering from single crystals of zinc[16, 17] we have

$$S=S_{\text{coh}}+S_{\text{inc}}/(1+\alpha \text{ vers } \phi)^3, \tag{11}$$

where
$$S_{\text{coh}}=f^2(1-e^{-2M})/Z \tag{12}$$

and
$$S_{\text{inc}}=1-\Sigma E_r^2/Z. \tag{13}$$

In diffuse scattering experiments the intensities involved are so small that it has been found advantageous to use the continuous spectrum, and so the equation[17]

$$\left(\frac{S\rho}{\mu}\right)_{\text{exp}}=\int(S_{\text{coh}}+S_{\text{inc}})\frac{\rho}{\mu}Id\lambda \tag{14}$$

has been developed. In this, $I(\lambda)$ is the distribution of the energy in the continuous spectrum. The integral involving S_{inc} can be calculated and (14) then is reducible to the form

$$\bar{G}(t)=\int G(t/\lambda)I(\lambda)d\lambda, \tag{15}$$

where $t=(\sin\frac{1}{2}\phi)$, and $G(t)$ and $I(\lambda)$ are experimental quantities. By a transformation of variables, this takes the form

$$h(t)=\int g(s)I(t,s)ds, \tag{16}$$

where $h(t)$ is a known function of t (an experimental curve) and $I(\lambda)$ is a known function of λ (also an experimental curve). Eq. (16) is an integral equation of the first kind.[18] This equation possesses a unique solution for our experimental conditions but there is no standard procedure for obtaining the solution. However, a graphic solution has been obtained and is explained in detail elsewhere.[17] By means of this graphic solution values of f and M have been obtained. These values of f are shown in column 6 of Table II. These f values are assigned to an average wave-length of 0.44A.

At a given temperature the temperature factor depends only upon the angle of orientation ψ and the scattering angle ϕ, and the formula for M at $T=295°$K is given by the empirical relation

$$M=(2.34\cos^2\psi+0.68\sin^2\psi)(\sin^2\tfrac{1}{2}\phi)/\lambda^2, \tag{17}$$

in which the constants of the equation are those found by Jauncey and Bruce.[17] The trigonometrical functions of the orientation angle are those given by Zener's theory.[7] The temperature factors obtained by use of (7) and the orientation angles in column 2 are listed in column 3.

There are several advantages in the diffuse scattering method, despite the low intensity and the tedious mathematics. In a soft metal like zinc where it is possible for small particles to be strained by van der Waals forces, it is very good to be able to use large single crystals that can be annealed, after they are grown and polished, and thus made entirely strain free.

[16] G. E. M. Jauncey and W. A. Bruce, Phys. Rev. **50**, 408 (1936).

[17] G. E. M. Jauncey and W. A. Bruce, Phys. Rev. **51**, 1068 (1937).

[18] See R. Courant and D. Hilbert, *Methoden der Mathematischen Physik*, p. 97.

5. Results and Comparison with Theory

The f values for $\lambda = 1.54$A are shown in column 7 of Table II. These are obtained from the F values by multiplying the corresponding values shown in columns 3 and 4. Column 8 shows experimental values of $f_{0.44} - f_{1.54}$. Experimental values of $f_{0.71} - f_{1.54}$ are shown in column 9. The theoretical values of $f_{0.71} - f_{1.54}$ are shown in column 10. For these it is necessary to include the $\eta_1^{(0)}$ term and there is a slight dependence on angle. However, the variation is smaller than the experimental error and so the average of the values shown in column 9 is compared with that of column 10 thus

$$\left.\begin{aligned}\Delta f'_{\text{exp}} &= 2.40\\ \Delta f'_{\text{theo}} &= 2.45\end{aligned}\right] 0.71\text{A to } 1.54\text{A}.$$

The theoretical value of $f_{0.44} - f_{1.54}$ is 2.45 and is practically constant with the angle. A comparison with the experiment is shown thus

$$\left.\begin{aligned}\Delta f'_{\text{exp}} &= 2.57\\ \Delta f'_{\text{theo}} &= 2.49\end{aligned}\right] 0.44\text{A to } 1.54\text{A}.$$

This is a clear verification of the validity of Hönl's theory. It also gives one considerable faith in the f values of zinc as given by these four experiments and in the M values as given by Jauncey and Bruce. Table III lists the average of the experimental f values of the four experiments corrected for the change in structure factor due to the nearness of the K absorption edge.

Table III. *Structure factors for zinc.*

$(\sin\frac{1}{2}\phi)/\lambda$	0.1	0.2	0.3	0.4	0.5	0.6	0.8	1.0
f for $\psi = 0°$	27.0	23.5	20.2	17.0	14.4	12.5	9.5	7.3
f for $\psi = 90°$	28.4	25.9	21.5	18.2	14.9			

It is interesting to note that the f values for $(\sin\frac{1}{2}\phi)/\lambda = 0.2$ for $\psi = 0°$ and 90° differ by 2.4 electrons which is greater than 2. By reference to James and Brindley's paper[19] on the calculation of quantum-mechanical f values, it is seen that at this value of $(\sin\frac{1}{2}\phi)/\lambda$ the scattering for the two valence electrons is negligibly small, and so this variation of 2.4 electrons cannot be due to the valence electrons as stated in a previous paper.[17] The electron asymmetry thus extends deeper into the atom than the valence electrons.

The author wishes to thank Professor G. E. M. Jauncey for his encouragement and guidance in this work.

[19] James and Brindley, Phil. Mag. **7**, 81 (1931).

MAY 15, 1938 PHYSICAL REVIEW VOLUME 53

The Band Spectra of SrCl and SrH

Kenneth R. More* and S. D. Cornell
Sloane Physics Laboratory, Yale University, New Haven, Connecticut

(Received March 30, 1938)

The spectra of SrCl and SrH are observed in absorption. The SrCl analysis given by Parker is confirmed. Measurement of the relative intensities of corresponding bands of the electronic doublet $^2\Pi \rightarrow {}^2\Sigma$ indicates that $^2\Sigma$ is the ground state. Rotational analyses of several bands of the C and D systems of SrH lead to values of B_e of 4.008 and 1.925 for the C and D states, respectively. Vibrational analyses of the two systems give $\omega_e = 1206.2$, $x_e\omega_e = 17.0$ for the $X\,^2\Sigma$ state; $\omega_e = 1347$, $x_e\omega_e = 23.5$ for the $C\,^2\Sigma$ state and $\omega_e = 1014.1$ and $x_e\omega_e = 15.4$ for the $D\,^2\Sigma$ state. The perturbations in the C and D states are discussed in terms of the interactions of the C, D, and E states.

Introduction

A TOTAL of five band systems of the SrH molecule have been reported in a series of papers by Watson and Fredrickson[1–4] and their co-workers. All but one of these systems have a strong (0,0) band, together with a weak (0,1)

* Sterling Fellow.

[1] W. W. Watson and W. R. Fredrickson, Phys. Rev. **39**, 765 (1932).

[2] W. R. Fredrickson, M. E. Hogan, Jr. and W. W. Watson, Phys. Rev. **48**, 602 (1935).

[3] W. W. Watson, W. R. Fredrickson and M. E. Hogan, Jr., Phys. Rev. **49**, 150 (1936).

[4] R. F. Humphreys and W. R. Fredrickson, Phys. Rev. **50**, 542 (1936).

band, and very weak (1,1) and (2,2) bands. The exception to this is the D system, $D^2\Sigma \rightarrow X\,^2\Sigma$. Watson, Fredrickson and Hogan[3] report two bands of this system, corresponding to transitions from a common state of unknown v' value to the ground state vibrational levels for which v'' equals 2 and 3. No other bands of this system have been reported. The D state differs from the other states of the SrH molecule in that the B constant has a value of about 1.9, while the B constants for the other states vary from 3.3 to 3.9. This same difference is found in the case of the corresponding states of CaH as reported by Grundström.[5] It is interesting to note that in the D system of CaH the bands of the $v'=0$ and $v''=0$ progressions are more prominent than are the corresponding bands of the other systems, and that the (0,0) band is absent. It is also observed that the vibrational frequency for the D state is appreciably less than that in the ground state.

The present investigation was undertaken primarily for the purpose of extending the analysis of the D system of SrH. Since the work on SrH just discussed was done in emission it was felt that it would be profitable to attempt the problem in absorption. During the course of the experimental work it became evident that some interesting information was being obtained about the C system of SrH, and about the band systems of the SrCl molecule. These latter bands were observed because of the presence of some chloride as an impurity in the material used for the core of the furnace in the earlier part of the work. Indeed the red bands were extremely strong and were well developed at relatively low furnace temperatures.

A high temperature vacuum furnace which was constructed for such spectroscopic investigations was used for the study of the absorption spectra to be considered. The furnace will be described in another article.

In order to obtain the spectrograms, light from a tungsten filament lamp operated considerably over its rated voltage was passed through the core tube of the furnace and focused on the slit of the spectrograph by means of a suitable optical system. For the study of the SrH and SrCl bands, strontium metal was distributed along the core tube and the furnace filled with hydrogen to a pressure of about 70 cm of mercury. In the case of the SrCl bands, zirconium oxide cores were used and the furnace heated to a temperature of 800° to 1000°C. The chlorine came mainly from the core because the chloride bands were much weaker when graphite cores were used. Temperatures of the order of 1600° to 2000°C were found necessary for the observation of the D system of SrH. Graphite cores were used in this case.

The spectra were photographed in the second order of a 21-foot grating in a stigmatic mounting. The dispersion was about 2.5A per mm. Eastman II-O and I-F plates were used in the regions below and above 5000A, respectively. Exposure times of the order of 2 to 5 minutes were ample. It was thus possible to obtain an exposure before the strontium metal all diffused out of the core.

Strontium Chloride

Two band systems of strontium chloride have been observed in emission by Hedfeld[6] and by Parker,[7] and in absorption by Walters and Barratt.[8] The latter apparently used rather low dispersion. According to the analyses of Hedfeld and of Parker the red system is due to a transition of the type $^2\Pi \rightarrow {}^2\Sigma$. It was not possible to tell from the emission data which of the two states involved was the ground state.

Both band systems previously reported are present on our spectrograms. Our data confirm the analyses already published, and extend some of the sequences to higher members. It is of interest that sequences extending as far as the (12,12) band are observed in absorption at temperatures of about 1500°C. Since the vibrational frequency for the ground state of SrCl is 300 cm^{-1}, an appreciable number of molecules are excited to levels up to about 3500 cm^{-1} above the level $v''=0$.

If the ground state of SrCl is $^2\Pi$, with the electronic interval of 607 cm^{-1} which is observed, the relative intensities of corresponding bands of the two members of the doublet observed in

[5] B. Grundström, Zeits. f. Physik **75**, 302 (1932).

[6] K. Hedfeld, Zeits. f. Physik **68**, 610 (1931)

[7] A. E. Parker, Phys. Rev. **47**, 349 (1935).

[8] O. H. Walters and S. Barratt, Proc. Roy. Soc. **A118**, 120 (1928).

absorption can be calculated from the Boltzmann factor for the temperature used. For a temperature of 800°C the ratio of intensities is about 0.5 to 1. A spectrogram taken at a temperature which was certainly not greater than 800°C has been photometered in order to determine the relative intensities of the two members of the electronic doublet. The Q heads of the $\Delta v=0$ sequences were compared. Within the limits of accuracy the intensities were equal. This indicates that the ground state is $^2\Sigma$. It should be pointed out that even though the plate used for this comparison was not calibrated the result should be reasonably accurate. The galvanometer deflections produced by the background and by the absorption band heads, when compared with the clear plate and total blackness deflections, indicated that the blackenings involved fell on the straight line portion of the plate calibration curve. At any rate conditions were such that a true intensity ratio of 0.5 to 1 could hardly give equal blackenings. The result that the ground state is $^2\Sigma$ is in agreement with the work of Jenkins and Harvey[9] who report the ground states of CaF and SrF and BaF to be $^2\Sigma$.

Strontium Hydride

A. The *C* system

The (0,0) and (0,1) bands of the $C\,^2\Sigma \leftrightarrows X\,^2\Sigma$ band system which have been reported by Fredrickson, Hogan and Watson[2] and by Humphreys and Fredrickson[4] are present on the absorption spectrograms taken with the furnace at a temperature of about 1500°C. These bands do not show the predissociation cut off at $K'=19$ which was reported for the emission bands excited at low hydrogen pressures. This is in agreement with the work of Humphreys and Fredrickson,[4] who extended the R branch of the (0,0) band to members as high as $K''=49$ by operating a strontium arc in hydrogen at pressures above 400 mm of mercury. It is of interest that the band lines obtained in absorption are relatively sharp from the origin to $K''=18$, beyond which point they are somewhat diffuse.

In addition to the (0,0) and (0,1) bands, the (1,0), (1,1) and (2,2) bands are present on the absorption spectrograms. The (0,0) band is much more intense than the others. The (1,0) band was not observed in emission by the authors mentioned. It, of course, lies far beyond the predissociation limit at $K'=19$ in the (0,0) band. Like the high K value lines of the (0,0) band, the lines of the (1,0) band are diffuse. The assignment of frequencies in the (1,0) band is given in Table I. This analysis was made with the help of the lower state combination differences given by Watson and Fredrickson.[1] The weakness of this band and the presence of perturbations make the assignments somewhat doubtful in some cases. The (1,1) and (2,2) bands are very weak but the positions of the heads are reasonably certain.

The rotational and vibrational constants of the C state are given in Tables V and VI, respectively. The B_1' value was obtained from an analysis of the (1,0) band, and the B_0' value is that given by Humphreys and Fredrickson.[4] The vibrational constants are obtained from the vibrational array for the C system which is given in Table II. This array was constructed from head data. The lower state frequencies found from this array are in good agreement with those found from the D system which is discussed in the following.

Table I. *Assignment of frequencies in the* $C\,^2\Sigma \leftarrow X\,^2\Sigma$ *(1,0) band of* SrH.

K''	R	P	K''	R	P
0	27619.5		12	45.0	49.9
1	27.2	27604.3	13	58.0	49.9
2	35.4	597.7	14	70.8	49.9
3	43.7	91.0	15	85.1	49.9
4	54.1	84.7	16	96.8 99.4	49.9
5	60.6	78.5		801.5	
6	67.2	73.3	17	19.9	49.9
7	74.8	66.1	18	31.1	49.9
8	85.5	59.5	19	44.2	57.8
9	96.1 708.5	49.9	20	59.4 61.5	
10	08.5 20.6	49.9	21		
			22	91.2	57.8
11	28.0 32.7	49.9 57.8			59.5

[9] F. A. Jenkins and A. Harvey, Phys. Rev. **39**, 922 (1931).

TABLE II. *Wave numbers of the band-heads of the* $C\,^2\Sigma \leftarrow X\,^2\Sigma$ *system of* SrH.

v' \ v''	0	1	2
0	26251	25080	
1	27550	26380	
2			26495

B. The *D* system

Bands attributed to the *D* system were found throughout the region from 4000 to 5600A, with the strongest ones between 4080 and 4480A. No bands were observed between 4480 and 4720A because of the extreme breadth of the strontium resonance line at 4607A. The band lines from 4720 to 5000A were all weak. The band (v',2) reported by Watson, Fredrickson and Hogan[3] was present. The region of the (v',3) band was not photographed.

With the aid of the known lower state combination differences, and the combination differences for the level of unknown v', six bands have been analyzed.

The bands at 19580 and 20752 have upper state combination differences equal to those reported for the (v',2) and (v',3) bands, and lower state combination differences which correspond to values of 1 and 0 respectively for v''. The band at 20561 cm^{-1} gives a value of 1 for v'' and upper state combination differences slightly lower than those of the two already discussed. The bands at 22686, 23611, and 24500 cm^{-1}, which incidentally are the strongest observed, all indicate that $v''=0$, and that the upper state combination differences decrease uniformly in going from one band to the next. The wave numbers 20752, 22686, 23611, 24500 and the change in B' indicate that these bands for which $v''=0$ belong to the $v''=0$ progression with one member missing. The missing member falls in the region of the strontium resonance line. It is also evident that the bands 20752, 19580, 18442 (v',2), and 17338 (v',3) form a v' progression. It is probable that this is the $v'=0$ progression.

The rotational quantum assignments of the six bands discussed are given in Table III. The vibrational array for the *D* system, using origin

TABLE III. *Assignment of frequencies in the* $D\,^2\Sigma \leftarrow N\,^2\Sigma$ *band system of* SrH.

(0,0) Band			(3,0) Band			(4,0) Band		
K''	R	P	K''	R	P	K''	R	P
0			0	23614.6		0	24504.8	
1			1	14.6	23604.0	1	04.8	24493.6
2	20754.0		2	11.0	593.1	2	00.7	82.4
3			3	04.0	79.1	3	493.6	67.8
4	37.4		4	593.1	60.1	4	82.4	49.3
5	24.6	20681.1	5	79.1	38.6	5	67.8	27.2
6	06.4	56.1	6	61.5	13.5	6	49.3	02.3
7	685.0	30.3	7	40.3	485.0	7	27.2	373.1
8	63.0	597.4	8	15.5	52.8	8	02.3	40.6
9	34.1	62.2	9	488.5	18.1	9	373.1	04.1
	31.9			87.0	17.1			
10	05.1	25.9	10	57.5	379.0	10	40.6	265.1
				55.7	77.4			
11	572.1	482.1				11	04.1	22.2
	70.3	79.4	11	24.0	37.1			21.1
				21.3	35.5			
12	44.3	42.7				12	268.3	176.1
	38.4	38.9	12	388.1	292.5		65.1	74.3
				84.4	90.1			
13	506.3	394.0				13	28.2	26.7
	496.6	86.9	13	49.9	44.8		23.9	24.5
				45.6	41.7			
14	69.7	49.8				14	181.0	074.9
		44.5	14	10.6	194.6		76.1	71.6
				08.2	90.6			
15	31.1	298.9				15	44.4	20.9
	27.8	88.3	15	271.1	42.7		41.3	16.1
					38.0			
						16	08.9	23959.7
			16	32.6	089.7		04.8	57.1
					87.5			
			17	03.0	36.2	17	082.4	09.3
							78.8	06.2
			18	181.4	22983.9			
				73.5		18	62.0	859.5
							52.1	57.1
			19	61.2	40.8			
				57.4		19	20.9	19.1
							11.6	17.4
			20		906.2			
					898.1	20	23993.0	786.0
			21		73.0		80.1	76.6
					68.1			

(2,0) Band			(0,1) Band			(1,1) Band		
K''	R	P	K''	R	P	K''	R	P
0			0			0	20565.6	
1	22689.7		1			1	65.6	20554.6
2	86.5		2	19581.7		2	62.6	44.3
3	80.0	22653.6	3	75.3	19551.1	3	56.9	30.2
4		36.3	4	66.2	31.7	4	47.4	13.3
5	55.9	14.8	5	53.8	11.1	5	33.5	493.7
6	38.7	589.9	6	38.0	488.0	6	17.6	69.7
7	18.4	61.6	7	19.8	62.5	7	01.5	42.7
	17.6			18.7				
						8	479.4	13.3
8	595.1	30.2	8	497.1			77.3	
	93.7	29.1						
			9	71.6		9	54.2	380.9
9	68.3	496.1		68.9			52.5	78.3
	66.0	94.6						
			10			10	27.8	44.5
10	38.8	58.1					24.3	42.3
	35.9	56.5	11	17.7	322.5			
				14.0	20.2	11	398.0	07.1
11	06.5	17.1					94.0	04.0
	03.0	15.0						
						12		266.3
12	467.5	373.6					63.8	62.5
	63.1	70.4						
						13	34.2	23.1
13	36.4	27.4					18.8	18.5
	32.5	23.4						
						14	301.4	178.6
14	03.5							73.2
	02.5							
						15	262.5	31.8
15	373.6						57.2	16.8
	70.4							
						16	37.8	085.3
							35.7	84.5
						17	06.7	
							06.2	

TABLE IV. *Wave numbers of the band-origins of the* $D\,^2\Sigma \leftarrow X\,^2\Sigma$ *system of* SrH.

v' \ v''	0	1	2	3
0	20751.4	19580.0	18441.8	17337.5
1		20561.8		
2	22686.4			
3	23611.0			
4	24500.5			

data, is shown in Table IV. The rotational and vibrational constants of the $D\,^2\Sigma$ and $X\,^2\Sigma$ states are given in Tables V and VI.

The origins of the bands of the D system are given by the following formula:

$$\nu = 20847.6 + \{1014.1(v'+\tfrac{1}{2}) - 15.4(v'+\tfrac{1}{2})^2\} - \{1206.2(v''+\tfrac{1}{2}) - 17.0(v''+\tfrac{1}{2})^2\}.$$

A comparison of the intensity distributions in the case of emission and absorption is of interest. The strongest bands observed in emission by Watson, Fredrickson and Hogan[3] were those analyzed and now called the (0,2) and (0,3) bands. The strongest bands observed in absorption are the (3,0) and (4,0), followed in the order of decreasing intensity by (2,0), (1,1), (0,1), (0,0) and (0,2), the latter three being about equal. This indicates that the distribution may be represented by a broad Condon parabola. In the case of the absorption bands the (0,2) and (0,3) bands are weakened by the Boltzmann factor, since the vibrational energies of states for $v''=2$ and 3 are 2310 and 3404 cm^{-1} above the $v''=0$ state. This effect is not present in emission. This intensity distribution is similar to that found by Grundström[5] for the D system of CaH.

The Mecke rule, which states that B_e/ω_e is constant for all states of a molecule, is violated by the D state of SrH, as it is for the D state of CaH. The ratio B_e/ω_e equals 1.9×10^{-3} for the D state, 3.1×10^{-3} for the ground state and 2.9×10^{-3} for the C state.

Most of the bands of the C and D systems show perturbations after the first few members of a band. The (1,0) band of the C system shows perturbations similar to those reported for the (0,0) band by Humphreys and Fredrickson.[4] It was not possible to trace these perturbations in detail because the band was not extended to high enough values of K. The (0,0), (1,1), (2,0), (3,0), and (4,0) bands of the D system all show perturbations of the type illustrated by Watson, Fredrickson and Hogan[3] in the case of the (0,3) band (called $(v',3)$ in their paper). At a K' value of 10 to 15 the observed frequencies suddenly deviate by a marked amount from the frequencies calculated from a fourth power equation which fits the observed values up to the K' in question. The deviations in some cases reach values of 50 to 100 cm^{-1}. The values of K' at which the perturbations begin are different in the different bands, but all fall in the range 10 to 15. The states which interact with the C and D states to cause these perturbations, and the predissociation in the C state will be discussed after the dissociation products and the heats of dissociation are considered.

DISCUSSION

In order to obtain some idea of the probable products of dissociation to be associated with each molecular state, approximate values of the heats of dissociation for the X, C, and D states were determined by the method of Rydberg. The values of the vibrational constants found for these states were used in this determination. Since the vibrational constants for the $A\,^2\Pi$, $B\,^2\Sigma$, and $E\,^2\Pi$ states of SrH are not known it was not possible to calculate the heats of

TABLE V. *Rotational constants of the* $C\,^2\Sigma$ *and* $D\,^2\Sigma$ *states of* SrH.

$C\,^2\Sigma$	$D\,^2\Sigma$	$D\,^2\Sigma$
$B_0=3.942$	$B_0=1.914$	$B_4=1.816$
$B_1=3.810$	$B_1=1.890$	$\alpha=0.024$
$\alpha=0.132$	$B_2=1.865$	$B_e=1.925$
$B_e=4.008$	$B_3=1.841$	$D=-0.3\times10^{-4}$
$D=-1.4\times10^{-4}$		

TABLE VI. *Vibrational constants of the* $X\,^2\Sigma$, $C\,^2\Sigma$, *and* $D\,^2\Sigma$ *states of* SrH.

$X\,^2\Sigma$ (FROM ORIGIN DATA)	$C\,^2\Sigma$ (FROM HEAD DATA)	$D\,^2\Sigma$ (FROM ORIGIN DATA)
$\omega_e=1206.2$	$\omega_e=1347$	$\omega_e=1014.1$
$x_e\omega_e=17.0$	$x_e\omega_e=23.5$	$x_e\omega_e=15.4$

dissociation for those states. However, some idea of the values was obtained from the probable dissociation products, once the results for the X, C, and D states were used to make a correlation with the known atomic states. The heats of dissociation are given in Table VII.

The potential energy curves for the X, C, and D states, obtained by using the Morse function, are shown in Fig. 1. The states of the Sr atom into which the molecules dissociate from the various molecular states are shown at the right of the figure. Potential curves for the A, B, and E states are also shown. They were obtained from the known positions of the minima and the probable dissociation limits.

It is seen that the D state is the only known state which can cause the predissociation in the C state. This determines the heat of dissociation of the D state, because the dissociation limit must be lower than the predissociation cut off in the C state. The value of the dissociation energy thus found for the D state is lower than that found from the vibrational constants by the Rydberg method. It thus seems reasonable to assume that the values given by the Rydberg method are high rather than low for the X and C states. By taking a value of the dissociation energy of the ground state somewhat lower than that calculated, it is possible to correlate the dissociation limits with the atomic terms as shown in Fig. 1. The probable configurations and dissociation products are given in Table VII. It should be pointed out in this connection that if the dissociation energy of the ground state is higher rather than lower than the value calculated from the molecular constants, the ^3P state of the atom could be the dissociation limit of the D state. In this case the A, B, D, and perhaps the E states would all approach the ^3P term as a dissociation limit. It seems reasonable however to take the correlation given because the dissociation energy in the D state is considerably lower than that calculated by the Rydberg method.

TABLE VII. *Probable configurations and dissociation products of the* SrH *molecule.*

STATE	PROBABLE CONFIGURATION	DISSOCIATION PRODUCTS	DISSOCIATION ENERGY, (cm^{-1})
$X\,^2\Sigma$	$5s\sigma^2 4d\sigma$	Sr, ^1S+H, ^2S	10,000
$A\,^2\Pi$	$5s\sigma^2 5p\pi$	Sr, ^3P+H, ^2S	11,000
$B\,^2\Sigma$	$5s\sigma^2 5p\sigma$	Sr, ^3P+H, ^2S	10,000
$E\,^2\Pi$	$5s\sigma^2 4d\pi$?	Sr, ^3D+H, ^2S	9,500?
$D\,^2\Sigma$	$5s\sigma 5p\sigma 4d\sigma$	Sr, ^3D+H, ^2S	7,500
$C\,^2\Sigma$	$5s\sigma^2 6s\sigma$	Sr, ^3S+H, ^2S	12,500

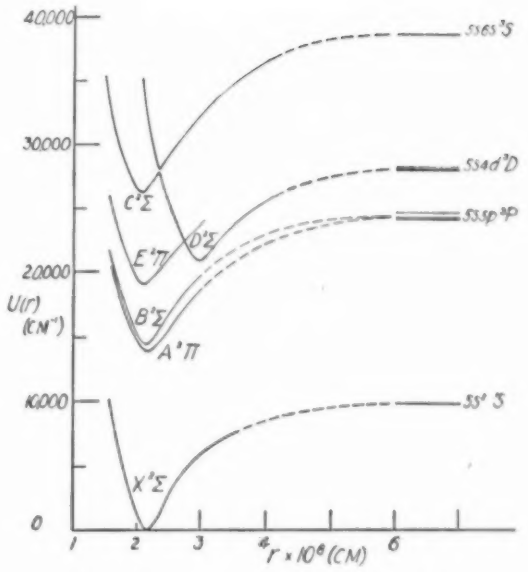

FIG. 1. Potential energy curves for SrH.

From the relative positions of the potential energy curves shown it is seen that the levels of the D state are perturbed probably by levels of the E state. The curves of the C and D states do not actually cross, because levels of the same Λ value cannot do so. In view of the indicated shapes of the C and D curves, they merge in the manner shown. This merging of the curves occurs in the region of predissociation of the C state. The predissociation is to be accounted for by this interaction of the C and D states, together with the relative positions of the point of merging and the dissociation limit of the D state.

In conclusion the authors wish to express their appreciation to Professor W. W. Watson for many stimulating discussions of this work.

On the Saturation of Nuclear Forces

C. CRITCHFIELD AND E. TELLER
George Washington University, Washington, D. C.

(Received March 12, 1938)

The forces between heavy elementary particles, i.e., neutrons and protons, are investigated on the hypothesis that they emit electron-positron pairs. It is also assumed that the interaction of the heavy particles with the field of light particles is large compared with the kinetic energy of the light particles. It is shown that potentials result which are of the same order of magnitude as the kinetic energy of the light particles. When many heavy particles interact the total potential energy is found to be proportional to the number of heavy particles.

INTRODUCTION

THE mass defect of most atomic nuclei is roughly proportional to the number of heavy elementary particles contained in the nucleus. This shows that the binding energy per elementary particle is, in first approximation, independent of the number of particles constituting the nucleus.

Since the heavy particles obey the Fermi-Dirac statistics the average kinetic energy of a heavy particle will vary with the two-thirds power of the density whenever the density is sufficiently high and the velocities of the heavy particles are small compared with the velocity of light. Thus, under these conditions, the kinetic energy in a given volume element of a heavy nucleus will be proportional to the five-thirds power of the density. If, on the other hand, the total potential energy is a sum of potential energies acting between pairs of heavy particles and if the range of the potential energy is small compared with the nuclear radius the total potential energy in a given volume within the nucleus will be proportional to the square of the density. If attraction is assumed between all heavy particles, the binding energy would then increase with increasing density and stability could not be reached before the nuclear radius becomes as small as the range of the attractive forces. In this case, however, the mass defect for heavy nuclei would increase more rapidly than the number of heavy particles contained in the nucleus.[1]

In order to escape this difficulty Heisenberg[2] and Majorana have assumed an interaction between heavy particles which is of the exchange type. For such interactions it follows that a neutron or proton can only interact with a limited number of other neutrons or protons. The following mechanism for this exchange interaction has been proposed:[3] a neutron emits an electron and a neutrino and turns into a proton; a proton absorbs the emitted pair and becomes a neutron. Thus an exchange of charge between a neutron and proton takes place.

This picture, however, cannot explain in a simple way why the forces between two protons (between which no such simple exchange of charge can take place) is of the same order of magnitude as the force between a neutron and proton.[4, 5] Moreover, the probability of electron-neutrino pair emission can be estimated by extrapolating the probabilities of beta-decay processes. Performing this extrapolation either in accordance with the theory proposed by Fermi[6] or with that proposed by Uhlenbeck and Konopinski[7] one obtains a too small value for the interaction between heavy particles.

Gamow and Teller[8] and Wentzel[9] have therefore suggested that an emission and reabsorption of electron-positron pairs should be responsible for the nuclear forces. The equality of proton-proton and proton-neutron forces is then more easily understood and also sufficient freedom is obtained to explain the magnitude of the nuclear

[1] These arguments were first put forward by Heisenberg at the Solvay Congress, 1933.
[2] W. Heisenberg, "Rapports de Congres Solvay, 1933."
[3] D. Iwanenko and I. Tamm, Nature **133**, 981 (1934).
[4] M. A. Tuve, L. R. Hafstad and N. P. Heydenburg, Phys. Rev. **50**, 806 (1936).
[5] G. Breit, E. Condon and R. Present, Phys. Rev. **50**, 825 (1936).
[6] E. Fermi, Zeits. f. Physik **88**, 161 (1934).
[7] K. Konopinski and G. Uhlenbeck, Phys. Rev. **48**, 7 (1935).
[8] G. Gamow and E. Teller, Phys. Rev. **51**, 289 (1937).
[9] G. Wentzel, Helv. Phys. Acta **10**, 107 (1936).

forces. Since, however, according to this hypothesis the charge is not exchanged and since a study of the neutron-proton interaction forces has eliminated the possibility that the major part of the neutron-proton interaction[10] is due to spin exchange we must conclude that if nuclear forces are due to electron-positron pair emission the main part of the forces between heavy elementary particles is not of the exchange type.[11] The purpose of the present paper is to show that the interaction between heavy particles resulting from the pair-emission hypothesis is compatible with the proportionality between mass defect and number of heavy particles.

In order to do this it will be necessary to drop the assumption that the total potential energy within the nucleus can be represented as a sum of interactions between pairs of heavy particles and that the potential energy is proportional to the square of their number. Indeed, this is correct only if the virtual states into which the light particles may be emitted are occupied only with a very small probability. If, however, the term in the Hamiltonian, H', which gives rise to the creation and annihilation of the light particles is large compared with the kinetic energy, E_{kin}, of the light particles in the virtual state a saturation phenomenon may result and the potential energy may increase less strongly than with the square of the number of particles. It then follows from the argument given in the beginning of the introduction that if the potential energy increase less strongly than the five-thirds power of the density the density of heavy nuclei will not depend strongly on the number of particles within the nucleus, and the mass defect divided by the number of particles in the nucleus will remain roughly constant.

We shall assume therefore, in the following discussion, that $H' \gg E_{\text{kin}}$. This assumption is just the opposite of the one usually made, namely $H' \ll E_{\text{kin}}$, which served to justify the treatment of the emission and absorption of light particles by a perturbation method.

In order to simplify the treatment we assume that not only the charge but also the spin of a heavy particle remains unchanged if light particles are emitted. Furthermore, the Coulomb interactions will be neglected. Thus, finer features such as spin dependence of nuclear potentials and the difference between proton and neutron mass will not be obtained from the present development.

Part I. One Heavy Particle

We consider at first one heavy particle and discuss the effect of the operator H' giving rise to emission and absorption of electron-positron pairs. The kinetic energy of the light particles, E_{kin}, will be neglected in accordance with the hypothesis $E_{\text{kin}} \ll H'$. The effect of E_{kin} will be taken into consideration as a perturbation in Part III.

It is convenient to adopt the "hole theory" of positrons in developing the formalism for the emission and absorption of pairs. Thus, emission of a pair will correspond to the transition from a state of negative to a state of positive energy, and an annihilation of a pair, a transition from a positive to a negative state.

Since we assume that a heavy particle after emission is in the same state in which it was before emission of a pair there is a possibility that a second pair be emitted before the first is reabsorbed. In general, a single heavy particle might emit successively in this way any number of pairs without reabsorbing them. If, however, pairs can be emitted only into a limited number of states, the exclusion principle will limit the number of pairs which can be emitted.

In particular we shall suppose the interaction H' to be such that emission (or absorption) can take place only into four states $A\uparrow$, $A\downarrow$, $B\uparrow$, $B\downarrow$. $A\uparrow$ and $A\downarrow$ are two spherically symmetrical electron states with positive kinetic energy, differing only in spin direction. $B\uparrow$ and $B\downarrow$ on the other hand, are states of negative kinetic energy. The absence of an electron from $B\uparrow$ is equivalent

[10] If the neutron-proton interaction be due to pure spin exchange there could not be an attraction between a neutron and a proton for both parallel and anti-parallel spins.

[11] If the probabilities of electron-positron, electron-neutrino and positron-neutrino emissions are of the same order of magnitude, an exchange of charge would remain possible and there would be no necessity for abandoning exchange forces. This suggestion is implied in Feenberg's discussion (Phys. Rev. **51**, 777 (1937)) of heavy particle interactions. The order of magnitude of nuclear forces would then still require an explanation (see Kemmer, Phys. Rev. **52**, 906 (1937)) which can, perhaps, be given in terms of heavy electrons and neutrinos (see Bhabha, Nature **141**, 117 (1938) and Kemmer, Nature **141**, 116 (1938)).

to the existence of a positron in a corresponding state with its spin pointing downward. We shall assume that the dependence on space coordinates of the A's and B's is the same. In general all negative states orthogonal to the B's shall be assumed as filled. $B\uparrow$ or $B\downarrow$, however, shall be filled only if the factor $B\uparrow$ or $B\downarrow$ explicitly appears in the proper function.

The formalism used in quantizing the wave equation will be adopted. Associated with the electron wave function $A\uparrow$ is the operator $a\uparrow$ which acts on the functional ψ, i.e., on the wave function of all electrons. $a\uparrow\psi$ is zero if the state $A\uparrow$ is represented in ψ as filled and $a\uparrow\psi=(\psi, A\uparrow)$ if $A\uparrow$ is empty. $(\psi, A\uparrow)$ is the properly antisymmetrized product wave function of ψ and $A\uparrow$. This means that $a\uparrow$ gives rise to the appearance of an electron in the state $A\uparrow$ if $A\uparrow$ be empty and is equivalent to zero if $A\uparrow$ be full. In accordance with the formalism, $a\uparrow^*$ acting on $(\psi, A\uparrow)$ gives ψ and acting on ψ gives zero, so that $a\uparrow^*$ causes the disappearance of an electron from $A\uparrow$ if $A\uparrow$ be full and is equivalent to zero if $A\uparrow$ be empty. In the same way $a\downarrow$, $a\downarrow^*$ are connected with $A\downarrow$; $b\uparrow$, $b\uparrow^*$ with $B\uparrow$; and $b\downarrow$, $b\downarrow^*$ with $B\downarrow$. For normalized functions the commutation laws hold:

$$\begin{aligned} &xx^*+x^*x=1, && xy+yx=0,\\ &xy^*+y^*x=0\ (x\neq y), && x^*y^*+y^*x^*=0, \qquad (1)\\ &\qquad x,\ y=a\uparrow,\ a\downarrow,\ b\uparrow,\ b\downarrow. \end{aligned}$$

The term giving rise to pair emission and absorption in the Hamiltonian will then be

$$H'=\sigma O, \qquad (2)$$

where σ is a positive constant and the operator O may be written[12]

$$O\equiv a\uparrow b\uparrow^*+b\uparrow a\uparrow^*+a\downarrow b\downarrow^*+b\downarrow a\downarrow^*. \qquad (3)$$

The first and third terms represent the production, the second and fourth terms the absorption of an electron-positron pair.

If we write the pair emission operator, O, as the sum of two commuting operators, $O\uparrow$ and $O\downarrow$:

$$\begin{aligned} &O\uparrow\equiv a\uparrow b\uparrow^*+b\uparrow a\uparrow^*, && O=O\uparrow+O\downarrow,\\ &O\downarrow\equiv a\downarrow b\downarrow^*+b\downarrow a\downarrow^*, && O\uparrow O\downarrow-O\downarrow O\uparrow=\text{zero}, \qquad (4) \end{aligned}$$

iteration of $O\uparrow$ gives, because of (1),

$$\begin{aligned} &O\uparrow O\uparrow=a\uparrow b\uparrow^* b\uparrow a\uparrow^*+b\uparrow a\uparrow^* a\uparrow b\uparrow^*,\\ &(O\uparrow)^3=O\uparrow \text{ and similarly}\\ &(O\downarrow)^3=O\downarrow. \end{aligned}$$

The proper values of $O\uparrow$ and $O\downarrow$ are therefore ±1 and zero.

It is readily seen that the proper functionals of $O\uparrow$ belonging to the proper value -1 will be those for which the state $(A\uparrow-B\uparrow)/\sqrt{2}$ is full and the state $(A\uparrow+B\uparrow)/\sqrt{2}$ is empty. For the functionals belonging to the proper value $+1$ the state $(A\uparrow-B\uparrow)/\sqrt{2}$ is empty and $(A\uparrow+B\uparrow)/\sqrt{2}$ is full; for the proper value zero both states $(A\uparrow-B\uparrow)/\sqrt{2}$ and $(A\uparrow+B\uparrow)/\sqrt{2}$ have to be full (i.e. there is an electron in $A\uparrow$ but there is no corresponding positron present) or both have to be empty (i.e., we have a positron but no electron). All these proper functionals are degenerate since the presence of electrons in any state orthogonal to $A\uparrow$ and $B\uparrow$ will have no effect on the proper value. Similar statements are obtained for $O\downarrow$ if $A\downarrow$ and $B\downarrow$ are used instead of $A\uparrow$ and $B\uparrow$.

Since $O\uparrow$ and $O\downarrow$ commute the proper values of $O=O\uparrow+O\downarrow$ will be the sums of the proper values of $O\uparrow$ and $O\downarrow$. Thus we obtain ±2, ±1, and zero. The corresponding proper functionals will be products of the proper functionals of $O\uparrow$ and $O\downarrow$. The proper functionals for the lowest proper value, -2, will be characterized by the states' $(A\uparrow-B\uparrow)/\sqrt{2}$ and $(A\downarrow-B\downarrow)/\sqrt{2}$ being filled and the states' $(A\uparrow+B\uparrow)/\sqrt{2}$ and $(A\downarrow+B\downarrow)/\sqrt{2}$ being empty. We again have degeneracy since any state orthogonal to $A\uparrow$, $A\downarrow$, $B\uparrow$, $B\downarrow$ may be filled or empty. This degeneracy means merely that the state of the nucleus will not depend upon extranuclear electrons or positrons. The lowest proper value of H' is therefore -2σ. Since σ is assumed to be large all other states lie high and therefore will not be excited. We shall be concerned only with the lowest state.[13]

We propose to consider the energy -2σ as part of the proper energy (or mass) of the proton or neutron. Because of its negative value it cannot represent, of course, the complete proper energy.

[12] A somewhat more general form for H' may be obtained by adding $\lambda(a\uparrow a\uparrow^*+a\downarrow a\downarrow^*+b\uparrow b\uparrow^*+b\downarrow b\downarrow^*)$ where λ is a new constant. However, as long as $\sigma-\lambda\gg E_{\text{kin}}$ our main argument remains unchanged.

[13] The exclusion of the proper value zero means that the wave functions of atomic electrons must be orthogonal to $[A\uparrow]$ and $[A\downarrow]$. This amounts to a boundary condition which all atomic wave functions must satisfy near the nucleus. If the spatial extension of $[A\uparrow]$ and $[A\downarrow]$ is very small compared with that of an atom the influence of this boundary condition will be small. It might account for an essential part of the isotope effects in atomic spectra.

This energy, -2σ, can be, however, incorporated into the proper energy only if it can be shown that the corresponding part of the energy for N particles (neutrons or protons) will be $-2N\sigma$ independently of their configuration. This proof is given in the next section.

Part II. Several Heavy Particles

The operator $H'(N)$ corresponding to the emission and absorption of pairs by N heavy particles will be the sum of operators H_k'

$$H'(N)=\sum_{k=1}^{N}H_k'=\sigma\sum_{k=1}^{N}O_k, \tag{5}$$

where H_k' corresponds to the emission and absorption of pairs by the kth particle. We may thus write:

$$O_k\equiv a_k\uparrow b_k\uparrow^*+b_k\uparrow a_k\uparrow^*+a_k\downarrow b_k\downarrow^*+b_k\downarrow a_k\downarrow^*, \tag{3k}$$

where $a_k\uparrow$ and $a_k\uparrow^*$ are operators associated with the electron state $A_k\uparrow$ which is the same spherical function as $A\uparrow$ with its center being located at the kth particle. Similar statements hold for $a_k\downarrow$, $a_k\downarrow^*$, $b_k\uparrow$, $b_k\uparrow^*$ and $b_k\downarrow$, $b_k\downarrow^*$. The proper functions of (5) are not, in general, simple because $A_k\uparrow$ is not orthogonal to $A_m\uparrow$, and so on for $A\downarrow$ and the B's.

However, two particular cases can be investigated at once: the first is that in which the N particles are far enough apart so that all A's and all B's can be considered orthogonal. Then the lowest proper value of $H'(N)$ is the sum of the lowest values of H_k' or just $-2N\sigma$. The proper functionals belonging to this value are those functionals in which all $(A_k\uparrow-B_k\uparrow)/\sqrt{2}$ and $(A_k\downarrow-B_k\downarrow)/\sqrt{2}$ are filled and all $(A_k\uparrow+B_k\uparrow)/\sqrt{2}$ and $(A_k\downarrow+B_k\downarrow)/\sqrt{2}$ are empty.

The second simple case is obtained when the positions of all heavy particles coincide[14] and all O_k's become identical with O_1. Then (5) becomes

$$H'(N)=N\sigma O_1$$

and the lowest proper value is again $-2N\sigma$. In the corresponding proper functionals $(A_1\uparrow-B_1\uparrow)/\sqrt{2}$ and $(A_1\downarrow-B_1\downarrow)/\sqrt{2}$ are filled and $(A_1\uparrow+B_1\uparrow)/\sqrt{2}$ and $(A_1\downarrow+B_1\downarrow)$ are empty.

[14] The fact that the Pauli principle would prohibit more than four heavy particles' occupying the same point is important in the determination of the behavior of particles in nuclei but not of essential interest in this consideration of the potential in which they move.

To show that the lowest proper value of $H'(N)$ is always $-2N\sigma$ we define the quantities

$$\epsilon_{km}=\int A_k\uparrow^*A_m\uparrow dv=\int A_k\downarrow^*A_m\downarrow dv$$
$$=\int B_k\uparrow^*B_m\uparrow dv=\int B_k\downarrow^*B_m\downarrow dv \tag{6}$$

with $\epsilon_{kk}=1$.

The commutation relations may be written:

$$x_kx_m^*+x_m^*x_k=\epsilon_{mk},$$
$$x_k,\ y_k=a_k\uparrow,\ a_k\downarrow,\ b_k\uparrow,\text{ or }b_k\downarrow, \tag{7}$$
$$x_ky_m^*+y_m^*x_k=\text{zero},\quad x\neq y\text{ etc.}$$

It is possible to choose a set of $4N$ orthogonal states $A_\lambda\uparrow$, $A_\lambda\downarrow$, $B_\lambda\uparrow$ and $B_\lambda\downarrow$ related to $A_k\uparrow$, $A_k\downarrow$, $B_k\uparrow$ and $B_k\downarrow$ respectively by the linear relations:

$$X_k=\sum_\lambda T_{k\lambda}X_\lambda,\quad X=A\uparrow,\ A\downarrow,\ B\uparrow,\text{ or }B\downarrow,$$
$$X_\lambda=\sum_k T_{\lambda k}^{-1}X_k. \tag{8}$$

Operators x_λ and x_λ^* associated with X_λ are defined by:

$$x_\lambda=\sum_k T_{\lambda k}^{-1}x_k,\qquad x_k=\sum_\lambda T_{k\lambda}x_\lambda,$$
$$x=a\uparrow,\ a\downarrow,\ b\uparrow,\text{ or }b\downarrow, \tag{9}$$
$$x_\lambda^*=\sum_k(T_{\lambda k}^{-1})^*x_k^*,\quad x_k^*=\sum_\lambda T_{k\lambda}^*x_\lambda^*.$$

It will be convenient to take for $T_{k\lambda}$ an orthogonal transformation,[15] so that

$$T_{k\lambda}^*=T_{\lambda k}^{-1}. \tag{10}$$

In fact, under such a transformation, $H'(N)$ retains the simple form that it has in (5).

$$\begin{aligned}H'(N)&=\sigma\sum_k\sum_{\lambda,\rho}T_{k\lambda}T_{k\rho}^*(a_\lambda\uparrow b_\rho\uparrow^*\\&\qquad+b_\lambda\uparrow a_\rho\uparrow^*+a_\lambda\downarrow b_\rho\downarrow^*+b_\lambda\downarrow a_\rho\downarrow^*)\\&=\sigma\sum_{\lambda,\rho}\delta_\lambda{}^\rho(a_\lambda\uparrow b_\rho\uparrow^*\\&\qquad+b_\lambda\uparrow a_\rho\uparrow^*+a_\lambda\downarrow b_\rho\downarrow^*+b_\lambda\downarrow a_\rho\downarrow^*)\\&=\sigma\sum_\lambda O_\lambda,\end{aligned} \tag{11}$$

where $O_\lambda\equiv(a_\lambda\uparrow b_\lambda\uparrow^*+b_\lambda\uparrow a_\lambda\uparrow^*+a_\lambda\downarrow b_\lambda\downarrow^*+b_\lambda\downarrow a_\lambda\downarrow^*)$.

[15] It will be seen that $T_{k\lambda}$ is the transformation which brings the Hermitian matrix $\{\epsilon_{mk}\}$ to principal axes.

On the other hand, if the transformation T is orthogonal it follows that the orthogonal set of functions X_λ cannot be normalized. This is so because, if we assume the set X_λ both orthogonal and normalized, then any orthogonal transformation (8) would yield a set X_k which would be both orthogonal and normalized which is in contradiction to the above statements. We therefore define the scalars c_λ by the relations[16]

$$\int X_\lambda^* X_\mu dv = c_\lambda \delta_\lambda^\mu, \quad X = A\uparrow, A\downarrow, B\uparrow, \text{or } B\downarrow, \tag{12}$$

leading to the commutation relations

$$\begin{aligned} &x_\lambda x_\mu^* + x_\mu^* x_\lambda = \sum_{k,m} T_{k\lambda}^* T_{m\mu} \epsilon_{km} = c_\lambda \delta_\lambda^\mu, \\ &x_\lambda y_\mu^* + y_\mu^* x_\lambda = \text{zero}, \quad x = a\uparrow,\ a\downarrow,\ b\uparrow, \text{ or } b\downarrow \\ &\quad (x \not\equiv y) \qquad\qquad \text{etc.} \end{aligned} \tag{13}$$

The operator O_λ may be again considered as the sum of the commuting operators $O_\lambda\uparrow$ and $O_\lambda\downarrow$:

$$\begin{aligned} &O_\lambda\uparrow \equiv a_\lambda\uparrow b_\lambda\uparrow^* + b_\lambda\uparrow a_\lambda\uparrow^*, \quad O_\lambda = O_\lambda\uparrow + O_\lambda\downarrow, \\ &O_\lambda\downarrow \equiv a_\lambda\downarrow b_\lambda\downarrow^* + b_\lambda\downarrow a_\lambda\downarrow^*, \\ &\qquad\qquad O_\lambda\uparrow O_\lambda\downarrow - O_\lambda\uparrow O_\lambda\downarrow = \text{zero}. \end{aligned} \tag{14}$$

The proper values of O_λ will then be the sums of those for $O_\lambda\uparrow$ and $O_\lambda\downarrow$ and the proper functionals will be product functions of those for $O_\lambda\uparrow$ and $O_\lambda\downarrow$. From (13), iteration of $O_\lambda\uparrow$ shows that

$$\begin{aligned} (O_\lambda\uparrow)^3 &= c_\lambda^2 O_\lambda\uparrow, \\ (O_\lambda\downarrow)^3 &= c_\lambda^2 O_\lambda\downarrow, \end{aligned} \tag{15}$$

so that the lowest proper value of each is $-c_\lambda$ and the lowest proper value of O_λ is $-2c_\lambda$; this value belongs to those functionals in which the states $(A_\lambda\uparrow - B_\lambda\uparrow)/(2c_\lambda)^{\frac{1}{2}}$ and $(A_\lambda\downarrow - B_\lambda\downarrow)/(2c_\lambda)^{\frac{1}{2}}$ are filled and the states $(A_\lambda\uparrow + B_\lambda\uparrow)/(2c_\lambda)^{\frac{1}{2}}$ and $(A_\lambda\downarrow + B_\lambda\downarrow)/(2c_\lambda)^{\frac{1}{2}}$ are empty.

According to the commutation relations (13) the operators O_λ commute and

$$O_\lambda O_\mu - O_\mu O_\lambda = \text{zero}$$

and therefore the proper values of $H'(N)$ will be given by σ times the sums of the proper values of the O_λ. In particular, the lowest proper value will be $-2\sigma\sum_\lambda c_\lambda$ and the corresponding functionals will be those in which all $(A_\lambda\uparrow - B_\lambda\uparrow)/(2c_\lambda)^{\frac{1}{2}}$ and $(A_\lambda\downarrow - B_\lambda\downarrow)/(2c_\lambda)^{\frac{1}{2}}$ are filled and all $(A_\lambda\uparrow + B_\lambda\uparrow)/(2c_\lambda)^{\frac{1}{2}}$ and $(A_\lambda\downarrow + B_\lambda\downarrow)/(2c_\lambda)^{\frac{1}{2}}$ are empty. From (13)

$$\sum_\lambda c_\lambda = \sum_\lambda \sum_{k,m} T_{k\lambda} T_{m\lambda}^* \epsilon_{km} = \sum_k \epsilon_{kk} = N. \tag{16}$$

The lowest proper value of $H'(N)$ is then $-2N\sigma$ and independent of the relative position of the heavy particles.

Part III. Kinetic Energy of Light Particle Field

We now introduce the kinetic energy of the light particles, K, as a perturbation in the calculation of the proper values of

$$H = H' + K. \tag{17}$$

We are interested in the lowest value of H. The lowest level of H' has been seen to be an infinitely degenerate one of energy -2σ. The introduction of K as a perturbation splits these levels and the problem of interest is to find the lowest of the resulting states.

We shall adopt the usual convention of putting the kinetic energy of the state in which no electrons or positrons are present equal to zero. The average value of K in the state ψ is therefore calculated by finding $\int \psi^* K \psi dv$ and subtracting from this value the average value of K in all negative energy levels. The average value for the lowest proper functions of H' is then

$$\begin{aligned} &\tfrac{1}{2}\int (A\uparrow - B\uparrow)^* K (A\uparrow - B\uparrow) dv \\ &\quad + \tfrac{1}{2}\int (A\downarrow - B\downarrow)^* K (A\downarrow - B\downarrow) dv + \bar{\kappa} \\ &\quad - \int B\uparrow^* K B\uparrow dv - \int B\downarrow^* K B\downarrow dv - \bar{\kappa}_0, \end{aligned} \tag{18}$$

where $\bar{\kappa}$ is the average value of K in all states orthogonal to A's and B's and $\bar{\kappa}_0$ is the average value of K in all negative states orthogonal to the B's.

According to the perturbation theory the lowest energy value into which a degenerate state will split is given by the minimum average value of the perturbation for the set of degenerate proper functions under consideration. It is evi-

[16] The numbers c_λ are the proper values of the matrix $\{\epsilon_{mk}\}$.

dent that the matrix of K, calculated in accordance with the preceding paragraph, is positive definite. Also the matrix of $\kappa-\kappa_0$ is positive definite with the minimum value zero for that state in which no positive levels are occupied and all negative levels are full. Therefore the lowest proper value of H will be, in first approximation, the lowest value of H', i.e., -2σ, plus (18) with $\bar{\kappa}=\bar{\kappa}_0$. Since the space dependence of $A\uparrow$, $A\downarrow$, $B\uparrow$, and $B\downarrow$ is taken to be the same

$$\int A\uparrow^* K A\uparrow dv = \int A\downarrow^* K A\downarrow dv$$

$$= -\int B\uparrow^* K B\uparrow dv = -\int B\downarrow^* K B\downarrow dv$$

and the integrals in (18) may be expressed by

$$E_{\text{kin}} = 2\int A\uparrow^* K A\uparrow dv. \tag{19}$$

and we obtain

$$E_{\min} = -2\sigma + E_{\text{kin}}. \tag{20}$$

In a representation including the A's and B's, K also has nondiagonal elements. The order of magnitude of these elements is the same as that of E_{kin}. For example, the element in K coupling the state in which $(A\uparrow-B\uparrow)/\sqrt{2}$, $(A\downarrow-B\downarrow)/\sqrt{2}$ are full and $(A\uparrow+B\uparrow)/\sqrt{2}$, $(A\downarrow+B\downarrow)/\sqrt{2}$ as well as all other positive energy states are empty with the state in which $(A\uparrow-B\uparrow)/\sqrt{2}$, $(A\downarrow+B\downarrow)/\sqrt{2}$ are full and $(A\uparrow+B\uparrow)/\sqrt{2}$, $(A\downarrow-B\downarrow)/\sqrt{2}$ as well as all other positive states are empty is readily calculated to be $\frac{1}{2}E_{\text{kin}}$. However, the diagonal elements for the two states differ by 2σ. According to second order perturbation formulae the correction to the calculation of the minimum energy associated with this transition will be $E^2_{\text{kin}}/8\sigma$. Similar transitions to electron states orthogonal to the A's and B's involve an energy difference approximately equal to σ. We may then say that expression (20) is correct if contributions of the order of $(E^2_{\text{kin}}/\sigma)$ and higher orders may be neglected.

The order of magnitude of the additional energy, E_{kin}, can be estimated if the spatial extent of $A\uparrow$ is known. If the characteristic linear dimension of $A\uparrow$ (its effective radius for example) be "d" then for sufficiently small values of d: $E_{\text{kin}}\sim cp\sim c\hbar/d$. The significance of this energy is seen in considering many heavy particles.

For N heavy particles the total Hamiltonian is

$$H(N) = \sum_i [H_i'] + \sum_i K_i, \tag{21}$$

where K_i is the operator K for the ith heavy particle alone. If contributions of the order E^2_{kin}/σ are neglected the lowest proper value of (21) is, by the same reasoning which led to (20),

$$E_{\min} = -2N\sigma + \int \psi_0^* \sum_i K_i \psi_0 dv$$

$$- \int \chi^* \sum_i K_i \chi dv, \tag{22}$$

where ψ_0 is that functional belonging to $-2N\sigma$ in which all negative levels orthogonal to the B's are filled and all positive levels orthogonal to the A's are empty. χ is the functional of negative states including the B's. The average value of K indicated in (22) cannot be calculated in general without a specific knowledge of the dependence of $A_\lambda\uparrow$, etc., on space coordinates. Since the form of this dependence is not known and since we make no hypothesis regarding it, we are limited to the evaluation of (22) for those special cases which are independent of the shape of the electron functions.

If the N heavy particles are sufficiently widely separated the electron functions ($A_k\uparrow$, etc.) pertaining to each heavy particle may be considered orthogonal. Then the average value of K will be found lowest in that state in which all positive levels orthogonal to the A_k's as well as all $(A_k\uparrow+B_k\uparrow)/\sqrt{2}$, $(A_k\downarrow+B_k\downarrow)$ are empty and all negative levels orthogonal to the B_k's as well as all $(A_k\uparrow-B_k\uparrow)/\sqrt{2}$, $(A_k\downarrow-B_k\downarrow)/\sqrt{2}$ are filled. The average value of $\sum_i K_i$ will be NE_{kin}:

$$E_{\min}(\infty) = -2N\sigma + NE_{\text{kin}}. \tag{23}$$

The other simple case occurs when the N heavy particles may be considered to occupy the same point in space. The proper function of minimum energy in this instance is that in which $(A_1\uparrow-B_1\uparrow)/\sqrt{2}$, $(A_1\downarrow-B_1\downarrow)/\sqrt{2}$ and all negative levels orthogonal to $B_1\uparrow$ and $B_1\downarrow$ are filled and $(A_1\uparrow+B_1\uparrow)/\sqrt{2}$, $(A_1\downarrow+B_1\downarrow)/\sqrt{2}$ and all positive

levels orthogonal to $A_1\uparrow$ and $A_1\downarrow$ are empty. As before these A's and B's are chosen arbitrarily from the N identical possibilities. Then

$$E_{\min}(O) = -2N\sigma + E_{\text{kin}}. \tag{24}$$

Conclusion

The difference between $E_{\min}(\infty)$ in (23) and $E_{\min}(O)$ in (24) is the binding energy obtained if the N particles are brought from infinite distances to the same point. Even if the positions of all heavy particles do not coincide the value of $E_{\min}(O)$ will remain essentially unchanged as long as the mutual distances remain small compared with the linear dimension, d, of the wave functions A and B.

The interaction which we have obtained differs essentially from the ordinary interaction between pairs; if the interaction is the sum of interactions between pairs, then by bringing the heavy particles close together the potential energy will be proportional to the number of pairs, that is, to $\frac{1}{2}N(N-1)$; for the type of nonexchange forces which we have discussed, however, the interaction at close contact will be $E_{\min}(\infty)-E_{\min}(O) = (N-1)E_{\text{kin}}$. Since, for finite separation, no lower potential is to be expected than for coinciding heavy particles, it follows from the discussion given in the introduction that the densities of heavy nuclei will remain essentially constant and that their binding energies will be roughly proportional to the number of heavy particles which they contain. The maximum potential energy per heavy particle will be E_{kin}.

It is evident that the range of the nuclear forces is of the same order of magnitude as the linear dimension, d, of the wave function A or B. From a study of nuclear radii it follows that this range is of the same order of magnitude as the electron radius e^2/mc^2. This means that the wave function A or B will have dimensions comparable to the electron radius and that in the pair emission theory of nuclear binding electron and positron wave-lengths which are small compared with the electron radius do not play an important role. Putting $d=e^2/mc^2$ we obtain $E_{\text{kin}}\sim 137mc^2$. This energy is of the same order of magnitude as the minimum of the potential energy per particle usually assumed in nuclei.

The formalism as given in this paper does not explain the spin dependence of the nuclear forces and does not give the magnetic moments of proton and neutron. An explanation of these phenomena might be forthcoming if it is assumed that the spin of the heavy particle may change during the emission of a pair. A dependence of the spin of the emitted light particles on the spin of the heavy particle has to be introduced. If, moreover, a heavy particle can emit electrons into several orthogonal states simultaneously, sufficient freedom may be gained to describe our empirical knowledge of nuclei.

The form of the wave functions into which emissions can take place remains, in the present state, arbitrary and thus the detailed dependence of the potential on the configuration of heavy particles cannot be calculated. It seems, however, that under rather general assumptions about the functions A and B, the first interaction between two heavy particles approaching each other will be a repulsion. At small distances it has been shown that attraction is obtained. The low binding energies obtained for nuclei like Li^8 or B^{12} in which, owing to the Pauli principle, the average distance between particles will be greater than in Be^8 or C^{12} may be due to this repulsive potential at greater distances.[17]

It is felt that the most serious objection to the theory proposed in this paper is the introduction of the finite distance operator O in Eq. (2). Such an operator may cause creation and annihilation of electrons or positrons at points different from the position of the heavy particle and no way is known for reconciling such processes with the principle of relativity. This means that the present theory will meet with difficulties if one tries to extend it to relativistic velocities of the heavy particles.

In conclusion the authors wish to express their thanks to Professors Bethe, Fermi, Gamow and Oppenheimer for helpful discussions.

[17] The questions mentioned in the two previous paragraphs will be discussed in detail elsewhere.

The Electrical Oscillations of a Prolate Spheroid. Paper I

LEIGH PAGE AND NORMAN I. ADAMS, JR.
Sloane Physics Laboratory, Yale University, New Haven, Connecticut

(Received March 29, 1938)

Differential equation. Solutions in spheroidal coordinates of the differential equation of the electromagnetic field are obtained which are valid all the way from the surface of a prolate spheroid of eccentricity unity to infinity. *Free oscillations.* The wave-length λ and logarithmic decrement δ of the fundamental free oscillations are computed for all eccentricities. *Forced oscillations.* The wave-length λ, current I, and phase ϕ at resonance are computed for six eccentricities near unity for an antenna stimulated by a uniform field varying sinusoidally with the time. Three resonance curves are computed, the radiation resistance at resonance is calculated for six eccentricities and off resonance for two. Expressions for the entire field at all points are given, and reduced to explicit form for the radiation field. An expression is obtained for the mean rate of radiation.

THE problem of the electrical oscillations of a perfectly conducting prolate spheroid is of great interest because, in the case where the eccentricity is nearly equal to unity, it represents to a high degree of precision the problem of the straight wire antenna. The first attack on this problem was made by Abraham,[1] who succeeded in finding the frequencies and decrements of the free oscillations in the limiting case of eccentricity unity, and in obtaining formulas which give rough approximations to the frequencies and decrements for eccentricities a little less than unity. Macdonald[2] also has obtained an expression for the fundamental frequency of the free oscillations of a straight antenna of negligible diameter by treating it as the limiting case of a cone of very small vertical angle. Obviously this is a very poor physical approximation, and therefore it is not surprising that Macdonald's value of the frequency differs from Abraham's by over twenty percent, and from the experimental value by nearly as much. Recently Stratton[3] has investigated the solution of the scalar wave equation in spheroidal coordinates, but his differential equation is not the one to which the problem here considered leads. Apparently no one has made much progress in solving the problem of the forced oscillations of a prolate spheroid, which are, of course, of far more practical importance than the free oscillations in the application to the antenna.

[1] Abraham, Ann. d. Physik **66**, 435 (1898); **2**, 32 (1900).
[2] Macdonald, *Electric Waves* (Cambridge University Press, 1902).
[3] Stratton, Proc. Nat. Acad. Sci. **21**, 51 and 316 (1935).

The object of this paper is to obtain solutions of the differential equation of the electrical oscillations of a prolate spheroid which will describe the electromagnetic field with an accuracy greater than that of experimental measurement all the way from the surface of the most eccentric spheroidal conductor to infinity, and will permit the discussion not only of the free oscillations, but as well of the oscillations forced by a uniform oscillating electric field, such as that of an exciting electromagnetic wave of length long compared with the shorter axis of the spheroid. Although the methods developed are applicable to all the harmonics, we shall limit the analysis in this paper to the fundamental or first harmonic and, to the approximation to which they are needed for the solution of the forced case, to the third and fifth harmonics. The spheroid will be supposed to be perfectly conducting, the only resistance taken into account being that of radiation. Heaviside-Lorentz symmetrical units are used throughout the analysis.

THE DIFFERENTIAL EQUATION

Let x, y, z be a right-handed set of rectangular coordinates with the x axis along the long axis of the prolate spheroid, and put $\rho^2 \equiv y^2+z^2$. We introduce the prolate spheroidal coordinates ξ, η, ϕ by the transformation

$$x = f\xi\eta, \tag{1}$$

$$\rho = f\{(1-\xi^2)(\eta^2-1)\}^{\frac{1}{2}}, \tag{2}$$

$$\tan\phi = z/y, \tag{3}$$

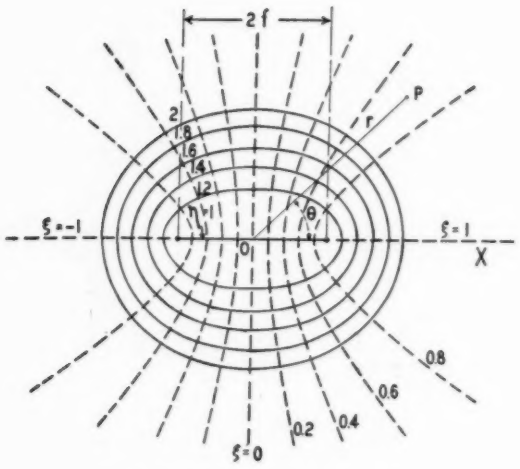

FIG. 1. Spheroidal coordinates.

where $-1\leqslant\xi\leqslant 1$, $1\leqslant\eta<\infty$, $0\leqslant\phi<2\pi$. The coordinate surfaces $\xi=$const. constitute a set of confocal hyperboloids of revolution about the x axis, and the coordinate surfaces $\eta=$const. are a set of confocal prolate spheroids of eccentricity $1/\eta$. The constant f represents the semi-interfocal distance, which is approached by the semi-major axis a of the prolate spheroids as η approaches unity. The unit vectors $\boldsymbol{\xi}_1$, $\mathbf{n}_1$, $\boldsymbol{\phi}_1$, in the directions of increasing ξ, η, ϕ, respectively, constitute a right-handed set in the order named. The radius vector r, whose square is $r^2=f^2(\eta^2+\xi^2-1)$, becomes effectively equal to $f\eta$ at great distances from the origin O, and the cosine of the angle θ which the radius vector makes with the x axis approaches ξ when r becomes very great. A section through the x axis of the coordinate surfaces is shown in Fig. 1.

We are interested in fields whose time dependence is specified by the factor $\exp(-i\omega t)$. Evidently the only nonvanishing field components are E_ξ, E_η, H_ϕ. If we put $A\equiv\rho H_\phi$, it has been shown by Abraham[1] that the field equations give

$$E_\xi=i\left(\frac{\mu}{\kappa}\right)^{\frac{1}{2}}\frac{1}{\epsilon f}\frac{1}{\{(1-\xi^2)(\eta^2-\xi^2)\}^{\frac{1}{2}}}\frac{\partial A}{\partial\eta}, \tag{4}$$

$$E_\eta=-i\left(\frac{\mu}{\kappa}\right)^{\frac{1}{2}}\frac{1}{\epsilon f}\frac{1}{\{(\eta^2-1)(\eta^2-\xi^2)\}^{\frac{1}{2}}}\frac{\partial A}{\partial\xi}, \tag{5}$$

$$H_\phi=\frac{1}{f}\frac{1}{\{(1-\xi^2)(\eta^2-1)\}^{\frac{1}{2}}}A, \tag{6}$$

where A satisfies the differential equation

$$(1-\xi^2)\partial^2A/\partial\xi^2+(\eta^2-1)\partial^2A/\partial\eta^2+\epsilon^2(\eta^2-\xi^2)A=0. \tag{7}$$

Here κ and μ are respectively the permittivity and permeability of the medium surrounding the spheroid, and

$$\epsilon\equiv(\omega/v)f=2\pi f/\lambda, \tag{8}$$

where $v\equiv c/(\kappa\mu)^{\frac{1}{2}}$ is the normal wave velocity in the medium, c represents the velocity of light in vacuum, and λ is the wave-length.

The variables are separable in (7), and if we put $A(\xi,\eta)=X(\xi)Y(\eta)$ we obtain the two ordinary differential equations

$$(1-\xi^2)d^2X/d\xi^2+(\alpha-\epsilon^2\xi^2)X=0, \tag{9}$$

$$(\eta^2-1)d^2Y/d\eta^2+(-\alpha+\epsilon^2\eta^2)Y=0, \tag{10}$$

where α is the constant of separation.

Solution of the Equation in ξ

First we solve (9). Putting

$$X(\xi)=(1-\xi^2)^{\frac{1}{2}}u(\xi), \tag{11}$$

we find

$$\frac{d}{d\xi}\left\{(1-\xi^2)\frac{du}{d\xi}\right\}-\frac{u}{1-\xi^2}+\alpha u=\epsilon^2\xi^2u, \tag{12}$$

from which we infer that the characteristic solutions $u_1, u_2, \cdots u_l, \cdots$ form an orthogonal set of functions. We express the characteristic values and the characteristic functions as power series in ϵ^2, *viz.*

$$\alpha_l=\alpha_{l0}+\alpha_{l1}\epsilon^2+\alpha_{l2}\epsilon^4+\alpha_{l3}\epsilon^6+\alpha_{l4}\epsilon^8+\cdots,$$

and

$$u_l(\xi)=u_{l0}(\xi)+u_{l1}(\xi)\epsilon^2+u_{l2}(\xi)\epsilon^4+u_{l3}(\xi)\epsilon^6+\cdots.$$

Evidently

$$\alpha_{l0}=l(l+1),\quad l=1, 2, 3\cdots,$$

and u_{l0} is the associated Legendrian polynomial

$$u_{l0}=P_{l1}(\xi)=(1-\xi^2)^{\frac{1}{2}}(d/d\xi)P_l(\xi),$$

where $l=1$ represents the fundamental or first

harmonic, $l=2$ the second harmonic, $l=3$ the third harmonic, and so forth.

By the usual perturbation methods we find for the fundamental

$$\alpha_1=2+\frac{1}{5}\epsilon^2-\frac{4}{5^3\cdot 7}\epsilon^4 + \frac{8}{3\cdot 5^5\cdot 7}\epsilon^6-\frac{124}{5^6\cdot 7^3\cdot 11}\epsilon^8+\cdots, \quad (13)$$

$$u_1=P_{11}(\xi)-\frac{1}{3\cdot 5^2}P_{31}(\xi)\epsilon^2 + \left\{\frac{2}{3^2\cdot 5^4}P_{31}(\xi)+\frac{1}{3^2\cdot 5^2\cdot 7^2}P_{51}(\xi)\right\}\epsilon^4 - \left\{\frac{31}{3\cdot 5^5\cdot 7^2\cdot 11}P_{31}(\xi)+\frac{4}{3\cdot 5^4\cdot 7^2\cdot 13}P_{51}(\xi) + \frac{1}{3^4\cdot 5\cdot 7^2\cdot 11\cdot 13}P_{71}(\xi)\right\}\epsilon^6+\cdots. \quad (14)$$

For the third harmonic we get

$$\alpha_3=12+\frac{7}{3\cdot 5}\epsilon^2+\frac{152}{3^4\cdot 5^3\cdot 11}\epsilon^4+\cdots, \quad (15)$$

$$u_3=P_{31}(\xi)+\left\{\frac{6}{5^2\cdot 7}P_{11}(\xi)-\frac{2}{3^3\cdot 7}P_{51}(\xi)\right\}\epsilon^2 - \left\{\frac{4}{5^4\cdot 7}P_{11}(\xi)-\frac{4}{3^6\cdot 5\cdot 7\cdot 13}P_{51}(\xi) - \frac{5}{3^2\cdot 7\cdot 11^2\cdot 13}P_{71}(\xi)\right\}\epsilon^4+\cdots, \quad (16)$$

and for the fifth harmonic

$$\alpha_5=30+\frac{19}{3\cdot 13}\epsilon^2+\cdots, \quad (17)$$

$$u_5=P_{51}(\xi)+\left\{\frac{5}{3^3\cdot 11}P_{31}(\xi) - \frac{15}{11\cdot 13^2}P_{71}(\xi)\right\}\epsilon^2+\cdots. \quad (18)$$

Solution of the Equation in η for Large Values of the Variable

Since we are interested in a diverging wave system the boundary condition at infinity demands a solution of (10) of the form

$$Y(\eta)=v(\eta)e^{i\epsilon\eta}, \quad (19)$$

where $v(\eta)$ is a series in descending powers of η. If we put $z\equiv i/\epsilon\eta$ the differential equation for v becomes

$$z^2\frac{d^2v}{dz^2}+2(z+1)\frac{dv}{dz}-\frac{\alpha-\epsilon^2}{1+\epsilon^2z^2}v=0. \quad (20)$$

We expand the denominator of the last term by the binomial theorem and look for a solution of the form

$$v=1+a_1z+a_2z^2+a_3z^3+\cdots,$$

in which we use the characteristic value α_l already obtained for the particular harmonic under consideration.

After some labor we obtain for the fundamental the two way infinite series

$$Y_1(\eta)=e^{i\epsilon\eta}\Bigg[1 + \frac{i}{\epsilon}\left\{1-\frac{2}{5}\epsilon^2-\frac{2}{5^3\cdot 7}\epsilon^4+\frac{4}{3\cdot 5^5\cdot 7}\epsilon^6-\frac{62}{5^6\cdot 7^3\cdot 11}\epsilon^8+\cdots\right\}\frac{1}{\eta} + \frac{1}{5}\left\{1-\frac{69}{5^2\cdot 7}\epsilon^2-\frac{62}{3\cdot 5^4\cdot 7}\epsilon^4+\frac{3943}{3\cdot 5^5\cdot 7^3\cdot 11}\epsilon^6+\cdots\right\}\frac{1}{\eta^2} + \frac{1}{5}\frac{i}{\epsilon}\left\{1-\frac{94}{5^2\cdot 7}\epsilon^2+\frac{2014}{3^2\cdot 5^4\cdot 7}\epsilon^4+\frac{34{,}588}{3\cdot 5^5\cdot 7^3\cdot 11}\epsilon^6+\cdots\right\}\frac{1}{\eta^3} + \frac{3}{5\cdot 7}\left\{1-\frac{289}{3^3\cdot 5^2}\epsilon^2+\frac{75{,}914}{3^3\cdot 5^4\cdot 7^2\cdot 11}\epsilon^4+\cdots\right\}\frac{1}{\eta^4}$$

(*Formula continued on next page.*)

$$+\frac{3}{5\cdot 7}\frac{i}{\epsilon}\left\{1-\frac{46}{3\cdot 5^2}\epsilon^2+\frac{761{,}914}{3^3\cdot 5^4\cdot 7^2\cdot 11}\epsilon^4+\cdots\right\}\frac{1}{\eta^5}$$

$$+\frac{1}{3\cdot 7}\left\{1-\frac{371}{3\cdot 5^2\cdot 11}\epsilon^2+\cdots\right\}\frac{1}{\eta^6}$$

$$+\frac{1}{3\cdot 7}\frac{i}{\epsilon}\left\{1-\frac{182}{5^2\cdot 11}\epsilon^2+\cdots\right\}\frac{1}{\eta^7}$$

$$+\frac{1}{3\cdot 11}\left\{1+\cdots\right\}\frac{1}{\eta^8}$$

$$+\frac{1}{3\cdot 11}\frac{i}{\epsilon}\left\{1+\cdots\right\}\frac{1}{\eta^9}+\cdots\Big]. \qquad (21)$$

The calculation of this series gives us an absolute check on the correctness of the previously computed characteristic value (13), for the successive terms in the series for α_1 are of just the magnitude necessary to cause each alternate coefficient of z to start with a power of ϵ two greater than the previous coefficient. Shortly we shall obtain an absolute check on the correctness of every coefficient in (21).

Similarly, we obtain for the third harmonic

$$Y_3(\eta)=e^{i\epsilon\eta}\Big[1$$

$$+6\frac{i}{\epsilon}\left\{1-\frac{2}{3^2\cdot 5}\epsilon^2+\frac{38}{3^5\cdot 5^3\cdot 11}\epsilon^4+\cdots\right\}\frac{1}{\eta}$$

$$-15\frac{1}{\epsilon^2}\left\{1-\frac{22}{3^2\cdot 5^2}\epsilon^2+\frac{398}{3^5\cdot 5^4}\epsilon^4+\cdots\right\}\frac{1}{\eta^2}$$

$$-15\frac{i}{\epsilon^3}\left\{1-\frac{8}{5^2}\epsilon^2+\frac{3242}{3^3\cdot 5^4\cdot 11}\epsilon^4+\cdots\right\}\frac{1}{\eta^3}$$

$$-10\frac{1}{\epsilon^2}\left\{1-\frac{1667}{2\cdot 3^3\cdot 5^2\cdot 11}\epsilon^2+\cdots\right\}\frac{1}{\eta^4}$$

$$-10\frac{i}{\epsilon^3}\left\{1-\frac{2521}{3^3\cdot 5^2\cdot 11}\epsilon^2+\cdots\right\}\frac{1}{\eta^5}$$

$$-\frac{75}{11}\frac{1}{\epsilon^2}\left\{1+\cdots\right\}\frac{1}{\eta^6}$$

$$-\frac{75}{11}\frac{i}{\epsilon^3}\left\{1+\cdots\right\}\frac{1}{\eta^7}+\cdots\Big], \qquad (22)$$

and for the fifth harmonic

$$Y_5(\eta)=e^{i\epsilon\eta}\Big[1+15\frac{i}{\epsilon}\{1+\cdots\}\frac{1}{\eta}-105\frac{1}{\epsilon^2}\{1+\cdots\}\frac{1}{\eta^2}$$

$$-420\frac{i}{\epsilon^3}\{1+\cdots\}\frac{1}{\eta^3}+945\frac{1}{\epsilon^4}\{1+\cdots\}\frac{1}{\eta^4}$$

$$+945\frac{i}{\epsilon^5}\{1+\cdots\}\frac{1}{\eta^5}+\cdots\Big]. \qquad (23)$$

to more than the needed degree of approximation.

While (21) serves for the calculaton of the frequency and decrement of the fundamental free oscillation for eccentricities less than 0.8, the series converge altogether too slowly to be useful for the important cases of eccentricities nearly equal to unity. To treat the latter we must obtain solutions of (10) in the neighborhood of the origin ($\eta=1$).

Solution of the Equation in η for Small Values of the Variable

If we put $t\equiv\eta^2-1$ the differential equation (10) becomes

$$4t(1+t)d^2Y/dt^2+2td\,Y/dt$$

$$+\{\epsilon^2(1+t)-\alpha\}\,Y=0. \qquad (24)$$

As this equation is of the second order the complete solution is a linear combination of two independent primitives. We look, therefore, for series solutions in powers of ϵ^2 the coefficients of which are polynomials in positive powers of t.

Denoting the two independent primitives by U and V, we find for the fundamental ($\alpha=\alpha_1$),

$$U_1=t-\frac{1}{2\cdot 5}t^2\epsilon^2-\left(\frac{1}{2\cdot 5^3\cdot 7}t^2-\frac{1}{2^3\cdot 5\cdot 7}t^3\right)\epsilon^4 +\left(\frac{1}{3\cdot 5^5\cdot 7}t^2+\frac{1}{2^2\cdot 3^2\cdot 5^3\cdot 7}t^3 -\frac{1}{2^4\cdot 3^3\cdot 5\cdot 7}t^4\right)\epsilon^6+\cdots, \quad (25)$$

$$V_1=U_1\log\frac{(1+t)^{\frac{1}{2}}-1}{(1+t)^{\frac{1}{2}}+1}+(1+t)^{\frac{1}{2}}\left[2+\left(\frac{4}{5}-\frac{1}{5}t\right)\epsilon^2 +\left(\frac{284}{5^3\cdot 7}-\frac{151}{5^3\cdot 7}t+\frac{1}{2^2\cdot 5\cdot 7}t^2\right)\epsilon^4 +\left(\frac{8632}{3\cdot 5^5\cdot 7}-\frac{115{,}646}{3^4\cdot 5^5\cdot 7}t+\frac{667}{3^4\cdot 5^3\cdot 7}t^2 -\frac{1}{2^3\cdot 3^3\cdot 5\cdot 7}t^3\right)\epsilon^6+\cdots\right]. \quad (26)$$

The most general solution of (10) is, therefore,

$$Y_1=A_1U_1+B_1V_1 \quad (27)$$

in the case of the fundamental, where the constants A_1 and B_1 may be functions of the parameter ϵ. Now, in order to satisfy the boundary condition at infinity, (27) must be identical with (21). Therefore we expand the logarithm in a power series and replace t by η^2-1 in the former, and expand the exponential in a power series in the latter, and compare coefficients. In this way we find that

$$A_1=-\tfrac{1}{3}\epsilon^2a_1, \quad B_1=\tfrac{3}{4}(i/\epsilon)b_1, \quad (28)$$

where

$$a_1\equiv 1-\frac{1}{2\cdot 5^2}\epsilon^2+\frac{187}{2^3\cdot 5^4\cdot 7^2}\epsilon^4-\frac{26{,}021}{2^4\cdot 3^4\cdot 5^6\cdot 7^2}\epsilon^6+\cdots$$
$$=1-0.020{,}000\epsilon^2+0.000{,}763\epsilon^4-0.000{,}026\epsilon^6+\cdots, \quad (29)$$

$$b_1\equiv 1-\frac{19}{2\cdot 5^2}\epsilon^2-\frac{2609}{2^3\cdot 5^4\cdot 7^2}\epsilon^4+\frac{32{,}593}{2^4\cdot 3^4\cdot 5^5\cdot 7^2}\epsilon^6+\cdots$$
$$=1-0.380{,}000\epsilon^2-0.010{,}649\epsilon^4+0.000{,}164\epsilon^6+\cdots. \quad (30)$$

In carrying through this process each term in A_1 and B_1 was calculated by comparing at least *two* different groups of terms in the two solutions, and every term in each solution was used at least once. Therefore the calculation of A_1 and B_1 constituted an absolute check on the accuracy of every numerical coefficient in (21) on the one hand and in (25) and (26) on the other.

Similarly in the case of the third harmonic ($\alpha=\alpha_3$) we find

$$U_3=t+\frac{5}{2^2}t^2-\left(\frac{1}{3\cdot 5}t^2+\frac{5}{2^3\cdot 3^2}t^3\right)\epsilon^2+\cdots, \quad (31)$$

$$V_3=U_3\log\frac{(1+t)^{\frac{1}{2}}-1}{(1+t)^{\frac{1}{2}}+1}+(1+t)^{\frac{1}{2}}\left[\frac{1}{3}+\frac{5}{2}t +\left(\frac{2}{3^3\cdot 5}-\frac{11}{2\cdot 3^3\cdot 5}t-\frac{5}{2^2\cdot 3^2}t^2\right)\epsilon^2+\cdots\right], \quad (32)$$

and the solution satisfying the boundary condition at infinity is

$$Y_3=A_3U_3+B_3V_3, \quad (33)$$

where

$$A_3=\frac{4}{3\cdot 5^2\cdot 7}\epsilon^4a_3, \quad B_3=-\frac{1575}{2^3}\frac{i}{\epsilon^3}b_3, \quad (34)$$

and

$$a_3\equiv 1+\cdots, \quad (35)$$

$$b_3\equiv 1-\frac{37}{2\cdot 3^3\cdot 5^2}\epsilon^2+\cdots. \quad (36)$$

In the case of the fifth harmonic ($\alpha=\alpha_5$)

$$U_5=t+\frac{7}{2}t^2+\frac{21}{2^3}t^3+\cdots, \quad (37)$$

$$V_5=U_5\log\frac{(1+t)^{\frac{1}{2}}-1}{(1+t)^{\frac{1}{2}}+1} +(1+t)^{\frac{1}{2}}\left[\frac{2}{3\cdot 5}+\frac{7}{2}t+\frac{21}{2^2}t^2+\cdots\right], \quad (38)$$

and the solution satisfying the boundary condition at infinity is

$$Y_5=A_5U_5+B_5V_5, \quad (39)$$

where

$$A_5=\text{negligible}, \quad B_5=\frac{3{,}274{,}425}{2^5}\frac{i}{\epsilon^5}b_5, \quad (40)$$

and

$$b_5\equiv 1+\cdots. \quad (41)$$

Fundamental Free Oscillations

The boundary condition at the surface of the conductor for free oscillation is that $E_\xi=0$ for all ξ's. Therefore it follows from (4) that

$$dY/d\eta=0, \qquad \eta=\eta_0, \tag{42}$$

where $1/\eta_0$ is the eccentricity of the conducting surface.

For large values of η_0 we use (21) for the fundamental. Performing the differentiation and solving for $i\omega/v$ by successive approximations we find

$$\begin{aligned}\frac{\omega}{iv}=&\frac{1}{2a}\left\{1-\frac{53}{875}\frac{1}{\eta_0^4}-\frac{3764}{65,625}\frac{1}{\eta_0^6}\right.\\&\left.-\frac{8,242,450}{176,859,375}\frac{1}{\eta_0^8}+\cdots\right\}\\&+i\frac{(3)^{\frac{1}{2}}}{2a}\left\{1+\frac{4}{15}\frac{1}{\eta_0^2}+\frac{971}{7875}\frac{1}{\eta_0^4}\right.\\&\left.+\frac{40,412}{590,625}\frac{1}{\eta_0^6}+\frac{203,351,122}{4,775,203,125}\frac{1}{\eta_0^8}+\cdots\right\}\\=&\frac{1}{2a}\left\{1-0.0606\frac{1}{\eta_0^4}-0.0573\frac{1}{\eta_0^6}\right.\\&\left.-0.0466\frac{1}{\eta_0^8}+\cdots\right\}+i\frac{(3)^{\frac{1}{2}}}{2a}\left\{1+0.2667\frac{1}{\eta_0^2}\right.\\&+0.1233\frac{1}{\eta_0^4}+0.0684\frac{1}{\eta_0^6}\\&\left.+0.0426\frac{1}{\eta_0^8}+\cdots\right\}.\end{aligned} \tag{43}$$

where a is the semi-major axis of the spheroid.

TABLE I. *Wave-lengths and logarithmic decrements for fundamental free oscillation of spheroids of eccentricities between 0 and 0.8.*

$1/\eta_0$	$\lambda/4a$	δ
0.0	1.814	3.628
0.1	1.809	3.618
0.2	1.794	3.588
0.3	1.770	3.537
0.4	1.734	3.461
0.5	1.686	3.356
0.6	1.625	3.214
0.7	1.549	3.024
0.8	1.455	2.772

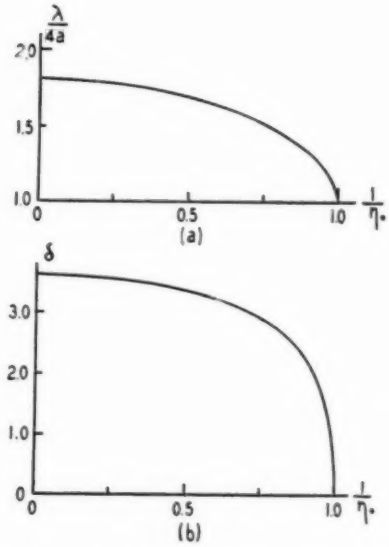

FIG. 2. (a) Wave-length λ and (b) logarithmic decrement δ of fundamental free oscillation of spheroid of eccentricity $1/\eta_0$.

If we write

$$i\omega/v=\chi+i\psi, \tag{44}$$

the ratio of the half-wave-length $\lambda/2$ to the major axis $2a$ of the spheroid is

$$\lambda/4a=\pi/2a\psi \tag{45}$$

and the logarithmic decrement δ is

$$\delta=2\pi\chi/\psi. \tag{46}$$

Unfortunately the series (43) converge too slowly to permit accurate calculations for eccentricities much greater than 0.7. In Table I the quantities $\lambda/4a$ and δ are given for eccentricities from 0 to 0.8. The calculated values are plotted on the graphs of Fig. 2, the portions of the curves corresponding to values of the eccentricity near to unity being plotted from the data in Table II, which will be computed later. We note that both the wave-length and the decrement decrease with increasing eccentricity.

Since (21) does not converge rapidly enough to describe the fundamental free oscillations for eccentricities close to unity, we must resort to the solution (27). We shall consider only eccentricities so close to unity that $t_0=\eta_0^2-1$ and its positive powers are negligible. If then we put

$$l\equiv\left[\log\frac{\eta_0+1}{\eta_0-1}-2\right]^{-1} \tag{47}$$

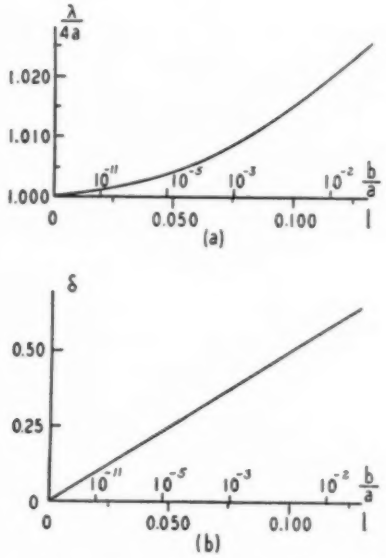

FIG. 3. (a) Wave-length λ and (b) logarithmic decrement δ of fundamental free oscillation of spheroid of major axis a and minor axis b.

and write

$$m_1 \equiv 1-\frac{1}{5}\epsilon^2 l+\frac{9}{5^3\cdot 7}\epsilon^4 l-\frac{886}{3^4\cdot 5^5\cdot 7}\epsilon^6 l+\cdots$$
$$=1-0.200{,}000\epsilon^2 l+0.010{,}286\epsilon^4 l$$
$$-0.000{,}500\epsilon^6 l+\cdots, \quad (48)$$

the boundary condition (42) gives

$$b_1=(4/9)i\epsilon^3 l a_1/m_1. \quad (49)$$

We shall compute the wave-length and decrement for six values of l corresponding to values of ratios of the minor axis $2b$ to the major axis $2a$ of the spheroid extending from 0 to about 1/74.

First consider the limiting case ($l=0$) of eccentricity unity, the ratio of b to a being zero. The boundary condition (49) reduces to $b_1=0$. Therefore ϵ is entirely real and the decrement is zero. This does not mean that no energy is radiated from the spheroid, but rather that the energy stored in the electromagnetic field is infinite compared with the energy radiated during a period of oscillation. Solving for ϵ we find

$$\epsilon=1.5708 \quad (50)$$

correct to five significant figures. This is exactly $\pi/2$. Hence, as $a=f$ in this case, the half-wave-length is exactly equal to the major axis of the spheroid. These values of both wave-length and decrement agree with those obtained by Abraham for the limiting case.

To discuss the remaining cases we multiply (49) by m_1/a_1. Combining the series represented by a_1, b_1 and m_1, we get the formula

$$1-\{0.360{,}000+0.200{,}000l\}\epsilon^2$$
$$-\{0.018{,}612-0.082{,}286l\}\epsilon^4$$
$$+\{0.000{,}093-0.000{,}481l\}\epsilon^6$$
$$=0.444{,}444il\epsilon^3. \quad (51)$$

We know that ϵ cannot differ greatly from $\pi/2$ over the range considered. Hence we put

$$\epsilon=(\pi/2)(1-g-ih). \quad (52)$$

A few trials indicate that an accuracy of one-tenth of one percent or better in the wave-length and better than one percent in the decrement is obtained if we retain terms in g, h, gh, h^2 and neglect all higher powers. Then (51) leads to the simultaneous equations

$$(2.2214-0.9735l)g+(1.5472-2.4039l)h^2$$
$$=5.1677l(h-2gh), \quad (53)$$

$$(2.2214-0.9735l)h-(3.0944-4.8078l)gh$$
$$=1.7226l(1-3g-3h^2), \quad (54)$$

which we may solve for g and h for any given value of l in the range considered. In this range it is unnecessary to distinguish between a and f.

In Table II are entered the results of the computation. The second column contains the ratio of b to a for the assumed value of l. These results are plotted in Fig. 3.

FORCED OSCILLATIONS

We now turn our attention to oscillations forced by an electric field $E=E_0e^{-i\omega t}$ parallel to the x axis. As the assumption of a uniform field

TABLE II. *Wave-lengths and logarithmic decrements for fundamental free oscillation of spheroids of eccentricities near to unity.*

l	b/a	$\lambda/4a$	δ
0.000	0.00	1.000	0.000
0.020	$1.02\ (10)^{-11}$	1.001	0.098
0.050	$3.34\ (10)^{-5}$	1.004	0.247
0.080	$1.42\ (10)^{-3}$	1.009	0.396
0.100	$4.96\ (10)^{-3}$	1.015	0.494
0.125	$1.35\ (10)^{-2}$	1.023	0.613

over the region occupied by the conducting spheroid is a valid approximation only when the wave-length is long compared with the shorter axis of the spheroid, we are limited in our discussion of oscillations in the neighborhood of resonance to eccentricities close to unity. This, however, is the range of most interest.

If γ is the angle which the unit vector ξ_1 (Fig. 1) makes with the x axis, we find

$$\cos\gamma=\eta\left(\frac{1-\xi^2}{\eta^2-\xi^2}\right)^{\frac{1}{2}}. \tag{55}$$

Therefore the boundary condition at the surface of the conductor is

$$E_\xi+E\eta_0\left(\frac{1-\xi^2}{\eta_0^2-\xi^2}\right)^{\frac{1}{2}}=0. \tag{56}$$

With the use of (4) for E_ξ this condition becomes

$$(\partial A/\partial\eta)_0=i(\kappa/\mu)^{\frac{1}{2}}\epsilon a(1-\xi^2)E_0e^{-i\omega t}, \tag{57}$$

where we have replaced $f\eta_0$ by its equal a.

Evidently A must be a linear combination of the solutions representing the odd harmonics, that is,

$$A=\{C_1u_1(\xi)Y_1(\eta)+C_3u_3(\xi)Y_3(\eta)+C_5u_5(\xi)Y_5(\eta)+\cdots\}(1-\xi^2)^{\frac{1}{2}}e^{-i\omega t}, \tag{58}$$

where $u_1(\xi)$, $u_3(\xi)$, $u_5(\xi)$ are given by (14), (16), (18), respectively, and $Y_1(\eta)$, $Y_3(\eta)$, $Y_5(\eta)$ by (27), (33), (39).

Determining the coefficients C_1, C_3, C_5 from the boundary condition (57) we have

$$C_1=i\left(\frac{\kappa}{\mu}\right)^{\frac{1}{2}}\epsilon aE_0\left\{1-\frac{2}{5^4\cdot7}\epsilon^4+\frac{8}{3\cdot5^6\cdot7}\epsilon^6+\cdots\right\}\Big/\left(\frac{dY_1}{d\eta}\right)_0, \tag{59}$$

$$C_3=i\left(\frac{\kappa}{\mu}\right)^{\frac{1}{2}}\epsilon aE_0\left\{\frac{1}{3\cdot5^2}\epsilon^2-\frac{2}{3^2\cdot5^4}\epsilon^4+\cdots\right\}\Big/\left(\frac{dY_3}{d\eta}\right)_0, \tag{60}$$

$$C_5=i\left(\frac{\kappa}{\mu}\right)^{\frac{1}{2}}\epsilon aE_0\left\{\frac{1}{3^4\cdot5\cdot7}\epsilon^4+\cdots\right\}\Big/\left(\frac{dY_5}{d\eta}\right)_0. \tag{61}$$

To save writing we shall put

$$k\equiv2\pi c(\kappa/\mu)^{\frac{1}{2}}aE_0. \tag{62}$$

Then the current I_0 at the center ($\xi=0$) of the antenna is

$$I_0=2\pi c(A)_{\substack{\xi=0,\\ \eta=\eta_0,}}$$

$$=ik\epsilon\Bigg[\left\{1-\frac{2}{5^4\cdot7}\epsilon^4+\frac{8}{3\cdot5^6\cdot7}\epsilon^6+\cdots\right\}u_1(0)\frac{Y_1(\eta_0)}{(dY_1/d\eta)_0}+\frac{1}{3\cdot5^2}\epsilon^2\left\{1-\frac{2}{3\cdot5^2}\epsilon^2+\cdots\right\}u_3(0)\frac{Y_3(\eta_0)}{(dY_3/d\eta)_0}+\frac{1}{3^4\cdot5\cdot7}\epsilon^4\{1+\cdots\}u_5(0)\frac{Y_5(\eta_0)}{(dY_5/d\eta)_0}+\cdots\Bigg]e^{-i\omega t}, \tag{63}$$

where

$$u_1(0)=1+\frac{1}{2\cdot5^2}\epsilon^2-\frac{89}{2^3\cdot5^4\cdot7^2}\epsilon^4+\frac{733}{2^4\cdot3^4\cdot5^5\cdot7^2}\epsilon^6+\cdots, \tag{64}$$

$$u_3(0)=-\frac{3}{2}\left\{1-\frac{13}{2\cdot3^3\cdot5^2}\epsilon^2+\cdots\right\}, \tag{65}$$

$$u_5(0)=\frac{15}{2^3}\{1+\cdots\}, \tag{66}$$

from (14), (16) and (18). We note that $u_1(0)$ is the reciprocal of the series a_1 given by (29).

From (27) we find

$$Y_1(\eta_0)=\frac{3}{2}\frac{i}{\epsilon}-c_1, \tag{67}$$

$$\left(\frac{dY_1}{d\eta}\right)_0=-\frac{3}{2}\frac{i}{\epsilon}-\frac{b_1m_1}{l}-\frac{2}{3}\epsilon^2a_1, \tag{68}$$

to a sufficient degree of approximation for eccentricities so near to unity as those under consideration, where

$$c_1\equiv1+\frac{1}{2\cdot5^2}\epsilon^2-\frac{89}{2^3\cdot5^4\cdot7^2}\epsilon^4+\frac{733}{2^4\cdot3^4\cdot5^5\cdot7^2}\epsilon^6+\cdots$$
$$=u_1(0)=1+0.020{,}000\epsilon^2-0.000{,}363\epsilon^4+0.000{,}004\epsilon^6+\cdots, \tag{69}$$

and from (33)

$$Y_3(\eta_0) = -\frac{525}{2^3}\frac{i}{\epsilon^3}c_3, \tag{70}$$

$$\left(\frac{dY_3}{d\eta}\right)_0 = \frac{1575}{2^2}\frac{i}{\epsilon^3}\frac{b_3 m_3}{l} + \frac{8}{3\cdot 5^2\cdot 7}\epsilon^4, \tag{71}$$

where

$$c_3 \equiv 1 + \frac{23}{2\cdot 3^3\cdot 5^2}\epsilon^2 + \cdots, \tag{72}$$

$$m_3 \equiv 1 - \frac{2}{3}l + \frac{1}{2\cdot 3\cdot 5}\epsilon^2 l + \cdots. \tag{73}$$

As the term in the fifth harmonic is quite negligible we shall not trouble to write it down.

The second term in (71) is negligible compared with the first, and we need retain only the first term in the series for b_3 and c_3 and the first two terms in the series for m_3. Let us put

$$s_1 \equiv 1 - \frac{2}{5^4\cdot 7}\epsilon^4 + \frac{8}{3\cdot 5^6\cdot 7}\epsilon^6 + \cdots$$
$$= 1 - 0.000{,}457\epsilon^4 + 0.000{,}024\epsilon^6 + \cdots, \tag{74}$$

$$s_3 \equiv 1 - \frac{2}{3\cdot 5^2}\epsilon^2 + \cdots. \tag{75}$$

In the series s_3 we need retain only the first term. Thus we obtain for the current I_0 at the center of the antenna

$$I_0 = k\left[\frac{(l\epsilon s_1 c_1^2)(4l\epsilon^3 a_1/9)}{(4l\epsilon^3 a_1/9)^2 + (b_1 m_1)^2} - i\left\{\frac{(l\epsilon s_1 c_1^2)(b_1 m_1)}{(4l\epsilon^3 a_1/9)^2 + (b_1 m_1)^2} - \frac{l\epsilon^3}{300}(1+\tfrac{2}{3}l)\right\}\right]e^{-i\omega t}. \tag{76}$$

The third harmonic contributes only a very small term to the imaginary part of the current.

The series a_1, b_1, m_1 and s_1 are specified by (29), (30), (48) and (74), respectively. The series for c_1^2, obtained by squaring (69), is

$$c_1^2 = 1 + 0.040{,}000\epsilon^2 - 0.000{,}327\epsilon^4 - 0.000{,}007\epsilon^6 + \cdots. \tag{77}$$

The square of the current amplitude I_{00} at the center is

$$I_{00}^2 = k^2\left[\frac{(l\epsilon s_1 c_1^2)^2}{(4l\epsilon^3 a_1/9)^2 + (b_1 m_1)^2}\right] \times\left[1 - \frac{\epsilon^2}{150}b_1(1+\tfrac{2}{3}l)\right] \tag{78}$$

to a sufficient degree of approximation. To find the frequency of resonance we must equate to zero the derivative of this with respect to ϵ, or, more conveniently, with respect to ϵ^2. This leads to the formula

$$b_1 = 0.14750 l^2 \epsilon^6 \frac{1 - 0.00560l}{(1 - 0.43837l)^2}, \tag{79}$$

where, in the very small right-hand member, we have replaced ϵ by $\pi/2$ in the numerator and denominator of the fractional factor. The justification for this lies in the fact that the values of ϵ computed from (79) are found to differ very little from $\pi/2$ in the range under consideration.

We have computed the wave-length λ and the current I_0 at resonance, and also the current amplitude I_{00} and the angle ϕ by which the current leads the electromotive force, for six values of l. These are contained in Table III and are plotted in Fig. 4. In the second column of the table is given the ratio of the minor to the major axis of the spheroid corresponding to the assumed value of l.

It will be noted that the real part of the current is substantially the same for all values of l considered, and that the current leads the electromotive force at resonance for all values of l greater than zero by an angle ϕ which increases with increasing l. For $l=0$ the half-wave-length is exactly equal to the major axis of the spheroid as in the case of free oscillation, but for values of l greater than zero the resonant wave-length is slightly shorter than the wave-length of free oscillation. Experiments on an-

TABLE III. *Wave-lengths and currents at resonance.*

l	b/a	$\lambda/4a$	$I_0/ke^{-i\omega t}$	I_{00}/k	ϕ
0.000	0.00	1.0000	1.045	1.045	0°.0
0.020	1.02 (10)$^{-11}$	1.0004	$1.045-0.028i$	1.045	1°.5
0.050	3.34 (10)$^{-5}$	1.0027	$1.045-0.071i$	1.047	3°.9
0.080	1.42 (10)$^{-3}$	1.007	$1.045-0.113i$	1.050	6°.2
0.100	4.96 (10)$^{-3}$	1.011	$1.045-0.141i$	1.055	7°.7
0.125	1.35 (10)$^{-2}$	1.017	$1.046-0.175i$	1.061	9°.5

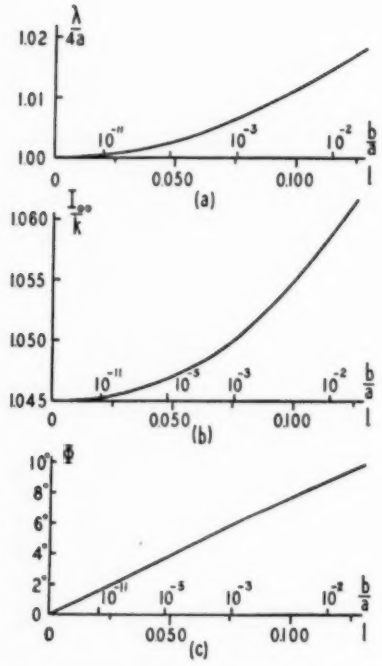

FIG. 4. (a) Wave-length λ, (b) current amplitude I_{00} and (c) lead ϕ of current at resonance.

tennas in the form of right circular cylinders indicate that the half-wave-length at resonance is from five to six percent longer than the antenna.[4] This is in satisfactory qualitative agreement with our calculated ratios of $\lambda/2$ to $2a$ for the prolate spheroid, for the diameter of a prolate spheroid falls to half of its maximum value at a distance $x=0.866a$ from the center whatever the eccentricity may be, and consequently the prolate spheroid which best fits a right circular cylinder is one which is slightly wider at the center and somewhat longer,[5] as illustrated in Fig. 5. We may call this prolate spheroid the *equivalent spheroid* for the given cylinder. Nevertheless it is very desirable that experimental measurements of the ratio $\lambda/4a$ should be made for actual spheroids in order to corroborate the theory.

We have computed resonance curves for $l=0.02$, 0.05 and 0.10. The data for these are given in Tables IV to VI, where ϵ_r represents the value of ϵ at resonance. The current amplitude I_{00} at the center of the antenna and the phase ϕ by which the current leads the electromotive force are depicted in Fig. 6. It will be noted that the resonance is sharper and that the phase shift toward $\pm\pi/2$ as we depart from resonance is more rapid the smaller l.

The distribution of current along the length of a thin antenna at resonance has been measured. Since $\xi=x/f\eta_0=x/a$, the quantity I_ξ/I_0 represents the ratio of the current, at a point whose distance from the center of the antenna is ξa, to the current at the center. The experimental measurements indicate that, at resonance,

$$I_\xi/I_0=\cos\tfrac{1}{2}\pi\xi \tag{80}$$

within the experimental error.

In developing an expression for this ratio from our theory, we obtain sufficient accuracy if we neglect the third and higher harmonics. Then we get the formula

$$\frac{I_\xi}{I_0}=(1-\xi^2)\left[1-\frac{\epsilon^2}{2\cdot5}\left(1-\frac{4}{5^2\cdot7}\epsilon^2+\frac{8}{3\cdot5^4\cdot7}\epsilon^4\right)\xi^2+\frac{\epsilon^4}{2^3\cdot5\cdot7}\left(1-\frac{8}{3^2\cdot5^2}\epsilon^2\right)\xi^4-\frac{\epsilon^6}{2^4\cdot3^3\cdot5\cdot7}\xi^6+\cdots\right]. \tag{81}$$

Let p be the ratio of the frequency for which it is desired to evaluate (81) to the frequency

FIG. 5. Prolate spheroid equivalent to cylinder.

for resonance with $l=0$. Then

$$p=\epsilon/1.5708, \tag{82}$$

and (81) becomes

$$I_\xi/I_0=(1-\xi^2)[1-0.24674p^2\{1-0.05640p^2+0.00371p^4\}\xi^2+0.02174p^4\{1-0.08773p^2\}\xi^4-0.00099p^6\xi^6+\cdots]. \tag{83}$$

TABLE IV. *Current for $l=0.02$, $b/a=1.02\ (10)^{-11}$, $\epsilon_r=1.5701$.*

ϵ/ϵ_r	$I_0/ke^{-i\omega t}$	I_{00}/k	ϕ
0.875	$0.011-0.120i$	0.120	84°.8
0.950	$0.081-0.292i$	0.303	74°.6
0.975	$0.275-0.474i$	0.548	59°.9
0.990	$0.726-0.495i$	0.879	34°.3
1.000	$1.045-0.028i$	1.045	1°.5
1.010	$0.757+0.453i$	0.882	−30°.9
1.025	$0.313+0.464i$	0.560	−56°.0
1.050	$0.107+0.302i$	0.320	−70°.5
1.125	$0.022+0.137i$	0.139	−80°.7

[4] C. R. Englund, Bell System Tech. J. **7**, 404 (1928).
[5] Rayleigh, Phil. Mag. **8**, 105 (1904).

When $p=1$ this reduces to

$$I_\xi/I_0=(1-\xi^2)[1-0.2337\xi^2+0.0198\xi^4 -0.0010\xi^6+\cdots], \quad (84)$$

which is exactly $\cos \pi\xi/2$ to the fourth decimal place. When $l=0$ it should be remembered that the term in the third harmonic disappears from (76) and therefore, in that case, we make no error in neglecting it.

In Table VII are listed the values of I_ξ/I_0 over the range of ξ for various values of p near to resonance.

Next we shall calculate the rate of absorption of energy and the radiation resistance of the antenna. Since the element of distance ds at the surface of the spheroid in the direction of increasing ξ is

$$ds=f\left(\frac{\eta_0^2-\xi^2}{1-\xi^2}\right)^{\frac{1}{2}}d\xi, \quad (85)$$

the electromotive force $d\mathcal{E}$ corresponding to the increment $d\xi$ is

$$d\mathcal{E}=E_0e^{-i\omega t}\cos\gamma ds=E_0e^{-i\omega t}ad\xi \quad (86)$$

from (55).

At any ξ the ratio of the part I_ξ' of the current in phase with the electromotive force to the part I_0' in phase with the electromotive force at the center of the antenna is

$$\frac{I_\xi'}{I_0'}=\frac{(1-\xi^2)^{\frac{1}{2}}u_1(\xi)}{u_1(0)}=\frac{(1-\xi^2)^{\frac{1}{2}}u_1(\xi)}{c_1} \quad (87)$$

from (58).

Hence we obtain from (76) for the mean rate of absorption of energy.

TABLE V. *Current for $l=0.05$, $b/a=3.34\ (10)^{-5}$, $\epsilon_r=1.5666$.*

ϵ/ϵ_r	$I_0/ke^{-i\omega t}$	I_{00}/k	ϕ
0.850	$0.042-0.238i$	0.242	80°.0
0.900	$0.104-0.347i$	0.363	73°.3
0.950	$0.352-0.529i$	0.635	56°.4
0.975	$0.707-0.525i$	0.880	36°.6
1.000	$1.045-0.071i$	1.047	3°.9
1.025	$0.783+0.418i$	0.888	−28°.1
1.050	$0.450+0.482i$	0.660	−46°.9
1.100	$0.182+0.360i$	0.403	−63°.2
1.150	$0.100+0.270i$	0.288	−69°.7

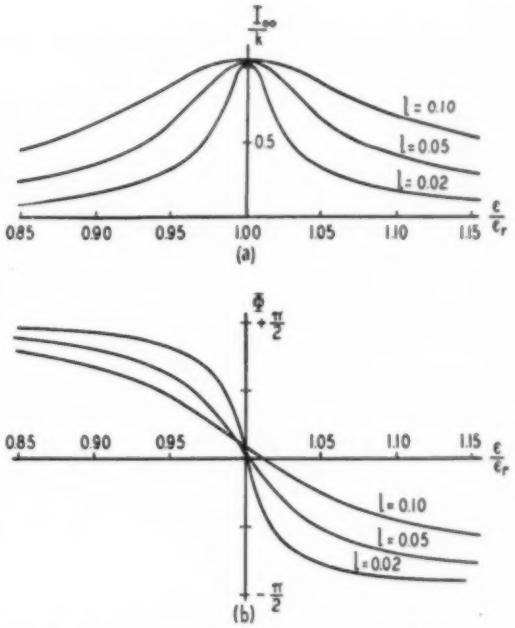

FIG. 6. (a) Current amplitude I_{00} and (b) lead ϕ of current plotted against ratio ϵ/ϵ_r of frequency to frequency at resonance.

$$\left\langle\frac{dU}{dt}\right\rangle_{Av}=\tfrac{1}{2}kE_0\frac{(l\epsilon s_1c_1^2)(4l\epsilon^3a_1/9)}{(4l\epsilon^3a_1/9)^2+(b_1m_1)^2}\cdot\frac{a}{c_1} \times\int_{-1}^{1}(1-\xi^2)^{\frac{1}{2}}u_1(\xi)d\xi. \quad (88)$$

Now

$$\int_{-1}^{1}(1-\xi^2)^{\frac{1}{2}}u_1(\xi)d\xi=\int_{-1}^{1}P_{11}(\xi)u_1(\xi)d\xi=4/3 \quad (89)$$

from (14). Consequently, from the relation $a_1c_1=1$ and from (62),

$$\left\langle\frac{dU}{dt}\right\rangle_{Av}=\frac{64}{27}\pi^3\left(\frac{\kappa}{\mu}\right)^{\frac{1}{2}}cE_0^2\frac{a^2f^2}{\lambda^2}\frac{a_1^4}{s_1} \times\frac{(l\epsilon s_1c_1^2)^2}{(4l\epsilon^3a_1/9)^2+(b_1m_1)^2} \quad (90)$$

TABLE VI. *Current for $l=0.10$, $b/a=4.96\ (10)^{-3}$, $\epsilon_r=1.5539$.*

ϵ/ϵ_r	$I_0/ke^{-i\omega t}$	I_{00}/k	ϕ
0.850	$0.144-0.428i$	0.451	71°.5
0.900	$0.306-0.546i$	0.625	60°.8
0.950	$0.669-0.575i$	0.882	40°.7
1.000	$1.045-0.141i$	1.055	7°.7
1.050	$0.822+0.360i$	0.897	−23°.6
1.100	$0.504+0.450i$	0.676	−41°.8
1.150	$0.326+0.410i$	0.524	−51°.5

in terms of the amplitude E_0 of the exciting field, or

$$\left\langle \frac{dU}{dt} \right\rangle_{Av} = \frac{16}{27}\pi\left(\frac{\mu}{\kappa}\right)^{\frac{1}{2}} \frac{I_{00}^2}{c}\frac{f^2}{\lambda^2}\frac{a_1^4}{s_1} \times\left[1+\frac{\epsilon^2}{150}b_1(1+\tfrac{2}{3}l)\right] \quad (91)$$

in terms of the amplitude I_{00} of the current at the center of the antenna.

The radiation resistance R, defined as the quotient of the mean rate of absorption of energy by $\frac{1}{2}I_{00}^2$, is

$$R=\frac{32}{27}\pi\left(\frac{\mu}{\kappa}\right)^{\frac{1}{2}}\frac{f^2}{c\lambda^2}\frac{a_1^4}{s_1}\left[1+\frac{\epsilon^2}{150}b_1(1+\tfrac{2}{3}l)\right]. \quad (92)$$

In practical units, the radiation resistance R_p in ohms is

$$R_p=87.670\left(\frac{\mu}{\kappa}\right)^{\frac{1}{2}}\left(\frac{4a}{\lambda}\right)^2\frac{a_1^4}{s_1} \times\left[1+\frac{\epsilon^2}{150}b_1(1+\tfrac{2}{3}l)\right], \quad (93)$$

provided we replace f by a. In Table VIII is given the radiation resistance at resonance for the six values of l considered before.

In Table IX we give the quantity $(\kappa/\mu)^{\frac{1}{2}}R_p$ for various fractions ϵ/ϵ_r of the frequency at resonance, both for $l=0.050$ and for $l=0.100$. The results are plotted in Fig. 7.

Finally we turn our attention to the electromagnetic field of the oscillating antenna. The three nonvanishing field components E_ξ, E_η and H_ϕ are given in terms of A and its derivatives by (4), (5) and (6), respectively. Since the coefficient C_3 in (58) may be expressed in terms of C_1 by the relation

$$C_3=-(2b_1/3^2\cdot5^4\cdot7)\epsilon^4C_1 \quad (94)$$

to a quite sufficient degree of accuracy, we find that

$$A=-\frac{ik}{3\pi c}l\epsilon^2 s_1\frac{4l\epsilon^3a_1/9-ib_1m_1}{(4l\epsilon^3a_1/9)^2+(b_1m_1)^2} \left\{u_1(\xi)\,Y_1(\eta)-\frac{2b_1}{3^2\cdot5^4\cdot7}\epsilon^4u_3(\xi)\,Y_3(\eta)\right\}(1-\xi^2)^{\frac{1}{2}}e^{-i\omega t}. \quad (95)$$

At a distance from the nearest point on the antenna not less than the semi-interfocal distance f the field components are specified to better than one percent by using the functions (21) and (22) for $Y_1(\eta)$ and $Y_3(\eta)$, respectively, although very close to the antenna it is necessary to use (27) and (33).

The components of the radiation field are

$$E_\xi=\frac{k}{3\pi c}\left(\frac{\mu}{\kappa}\right)^{\frac{1}{2}}\frac{l\epsilon^2s_1}{f}\frac{1}{(\eta^2-\xi^2)^{\frac{1}{2}}} \times\frac{1}{\{(4l\epsilon^3a_1/9)^2+(b_1m_1)^2\}^{\frac{1}{2}}} \times\left\{u_1(\xi)-\frac{2b_1\epsilon^4}{3^2\cdot5^4\cdot7}u_3(\xi)\right\}e^{i(\epsilon\eta-\omega t+\pi/2-\gamma)}, \quad (96)$$

$$H_\phi=-\frac{k}{3\pi c}\frac{l\epsilon^2s_1}{f}\frac{1}{(\eta^2-1)^{\frac{1}{2}}} \times\frac{1}{\{(4l\epsilon^3a_1/9)^2+(b_1m_1)^2\}^{\frac{1}{2}}} \times\left\{u_1(\xi)-\frac{2b_1\epsilon^4}{3^2\cdot5^4\cdot7}u_3(\xi)\right\}e^{i(\epsilon\eta-\omega t+\pi/2-\gamma)}, \quad (97)$$

where

$$\tan\gamma\equiv\frac{b_1m_1}{4l\epsilon^3a_1/9}. \quad (98)$$

TABLE VII. *Current distribution I_ξ/I_0.*

ξ \ p	0.90	0.95	1.00	1.05	1.10
±0.1	0.988	0.988	0.9877	0.987	0.987
±0.2	0.953	0.952	0.9511	0.950	0.949
±0.3	0.894	0.893	0.8910	0.889	0.887
±0.4	0.815	0.812	0.8090	0.806	0.803
±0.5	0.715	0.711	0.7071	0.703	0.699
±0.6	0.597	0.592	0.5878	0.583	0.578
±0.7	0.464	0.459	0.4540	0.449	0.443
±0.8	0.318	0.313	0.3090	0.304	0.300
±0.9	0.162	0.159	0.1564	0.153	0.150

TABLE VIII. *Radiation resistance at resonance.*

l	$(\kappa/\mu)^{\frac{1}{2}}R_p$(ohms)
0.000	73.1
0.020	73.0
0.050	72.8
0.080	72.3
0.100	71.8
0.125	71.1

For small l it follows that γ is nearly zero at resonance, nearly $\pi/2$ below resonance, and nearly $-\pi/2$ above resonance.

As the Poynting flux is $-cE_\xi H_\phi$ in the direction of increasing η and the element of area of a spheroidal surface is $2\pi f^2\{(\eta^2-\xi^2)(\eta^2-1)\}^{\frac{1}{2}}d\xi$, the mean rate of radiation of energy is

$$\left\langle \frac{dR}{dt} \right\rangle_{\text{Av}} = \frac{16}{9}\pi^3\left(\frac{\kappa}{\mu}\right)^{\frac{1}{2}} cE_0^2 \frac{a^2f^2}{\lambda^2} a_1^4 \times \frac{(l\epsilon s_1 c_1^2)^2}{(4l\epsilon^3 a_1/9)^2+(b_1m_1)^2}\int_{-1}^{1}[u_1(\xi)]^2 d\xi, \quad (99)$$

provided we make use of the relation $a_1c_1=1$ and neglect, as heretofore, the square of the third harmonic. From (14) we find

$$\int_{-1}^{1}[u_1(\xi)]^2 d\xi = \frac{4}{3}\left\{1+\frac{2}{5^4\cdot 7}\epsilon^4-\frac{8}{3\cdot 5^6\cdot 7}\epsilon^6+\cdots\right\}=\frac{4}{3s_1}, \quad (100)$$

TABLE IX. *Radiation resistance* $(\kappa/\mu)^{\frac{1}{2}}R_p$ *in ohms for frequencies near resonance.*

l \ ϵ/ϵ_r	0.850	0.900	0.950	1.000	1.050	1.100	1.150
0.050	55.3	61.0	66.9	72.8	78.7	84.6	90.6
0.100	54.5	60.2	66.0	71.8	77.7	83.6	89.4

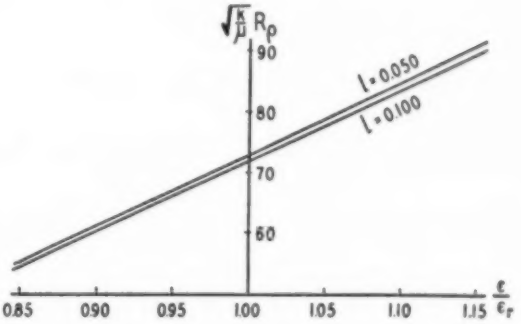

FIG. 7. Radiation resistance R_p in ohms plotted against ratio ϵ/ϵ_r of frequency to frequency at resonance.

where s_1 is the series defined by (74). Therefore

$$\left\langle \frac{dR}{dt} \right\rangle_{\text{Av}} = \frac{64}{27}\pi^3\left(\frac{\kappa}{\mu}\right)^{\frac{1}{2}} cE_0^2 \frac{a^2f^2}{\lambda^2}\frac{a_1^4}{s_1} \times \frac{(l\epsilon s_1 c_1^2)^2}{(4l\epsilon^3 a_1/9)^2+(b_1m_1)^2} \quad (101)$$

in agreement with (90).

In a future communication we hope to discuss the field in more detail.

Note added in proof. Since submitting this article for publication there has come to the attention of the authors a recent paper by L. V. King [Trans. Roy. Soc. London, **236**, 381 (1937)] in which the radiation from a cylindrical antenna is investigated by a very different method from that pursued here.

Statistical Theory of a Scaling Circuit

LEON ALAOGLU AND NICHOLAS M. SMITH, JR.
Department of Mathematics and Ryerson Physical Laboratory, University of Chicago, Chicago, Illinois

(Received February 16, 1938)

The over-all efficiency of a counter circuit embodying a scaling circuit to reduce the rate of recording is investigated. The probability of detecting counts ($G(n, \tau)$) of a scaling circuit and recorder fed with random impulses is shown to be: $1-I(\mu\tau, n)$, where n is the scale of the circuit, τ the resolving time of the recorder, μ the statistical average of incoming counts, and where $I(\mu\tau, n)$ is the ratio of the incomplete gamma-function with upper limit $\mu\tau$ of n to the complete gamma-function of n. Efficiency curves (100 $G(n, \tau)$) are plotted showing that the distribution in time of the impulses leaving the scaling circuit is no longer random, but is a distribution in which the extreme short and long intervals between impulses are averaged out. The average rate of recording counts (μ_n) is $(\mu/n)G(n, \tau)$. The analysis is extended to include the effect of the finite resolving time of the amplifier (σ), yielding when $\tau \geqslant n\sigma$: $\mu_n=(\mu/n)[1/(\mu\sigma+1)][1-I(\mu(\tau-n\sigma), n)]$, and when $\tau \leqslant n\sigma$: $\mu_n=(\mu/n)[1/(\mu\sigma+1)]$, the latter being the response of the amplifier alone. Thus, one need only make $n>\tau/\sigma$ and the scaling circuit and recorder will operate with 100 percent efficiency.

I. INTRODUCTION

A COUNTER-amplifier-recorder circuit is limited in the number of impulses per second it can detect and record mainly by the mechanical recorder which usually has a recovery time much greater than the recovery time of any other part of the circuit. If an impulse to the recorder is preceded by an interval of time t from the last count which is less than the recovery time τ of the recorder, then the latter fails to advance one count.

In order to record counts at a faster rate a scaling circuit is usually introduced which sends only every nth impulse into the recorder. The fact that a scale-of-n counting circuit has an advantage other than simply dividing the counting rate by n has been noted by Stevenson and Getting.[1] They stated that the distribution in regard to time intervals of the impulses leaving the scale-of-n circuit was no longer random, but had a standard deviation less than random counts coming in at the same average rate. This means that there are fewer short intervals, and therefore the mechanical recorder will not miss so many impulses that come to it. It is desired here to derive an expression for the over-all response of a counter-amplifier and scale-of-n recorder set in order that limits of usefulness of the scaling circuit may be evaluated.

[1] E. C. Stevenson and I. A. Getting, Rev. Sci. Inst. **8**, 414 (1937).

II. RESPONSE OF PERFECT SCALING CIRCUIT AND RECORDER FED WITH RANDOM COUNTS

It is of interest to investigate first the response of the scaling circuit and recorder alone. Therefore we assume that the counter, amplifier, and scaling circuits are perfect, and that only the recorder has a resolving time τ not zero. Let $Q(t)dt$ be the probability that the interval of time between a count and its predecessor be greater than t and less than $t+dt$. Let $L(n, t)$, $G(n, t)$ be the probability that the time elapsed when n successive counts follow after an arbitrary count be less (greater) than t. Then always $L(n, t)+G(n, t)=1$.

The probability that $n-1$ counts follow after a first count in time less than $t-x$ is $L(n-1, t-x)$; the probability that the nth count follow after the last of these in time x to $x+dx$ is $Q(x)dx$. Hence the probability that the n counts come together in this fashion is

$$L(n-1, t-x)Q(x)dx. \tag{1}$$

The probability that the combined n-interval be less than t is therefore:[2]

[2] The functions $L(n, t)$ satisfy a simple recursion relation:

$$L(n+m, t)=\int_0^t L'(n, x)L(m, t-x)dx, \tag{2c}$$

where n and m are integers. This relation can be proved by an induction on $n+m$, assuming the formula holds for $L(m, t)$ and $L(m+n-1, t)$ the integral on the right of Eq. (2) can be reduced to that of the definition of $L(n+m, t)$. From this it follows that the output of a scale-of-2^k made up of k stages of scales-of-two in series is that of a scale-of-2^k in one stage. The definition of $L(2, t)$ shows that this is true for a single stage of two. Suppose it is true for the output of

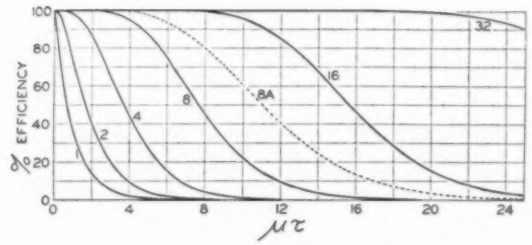

FIG. 1. The efficiency (one hundred times the probability of recording count $=100\,G(n,\tau)$) of a scaling circuit and mechanical recorder as a function of the statistically averaged input frequency (μ) of random counts (solid lines) multiplied by the resolving time (τ) of the recorder. The numbers on the solid lines refer to the scaling ratios. In an actual case the scaling circuit is not fed with random counts from the amplifier, but with a distribution in which the short intervals are removed, increasing the efficiency of the scaling circuit alone. This is shown by the dotted curve ($8A$, for a scale-of-eight), for which τ and σ are taken to be 0.0133 sec. and 0.0005 sec., respectively. If the scale of the circuit were made greater than τ/σ ($=26.6$), the efficiency curve would move off to the right to infinity, and the circuit would detect all counts coming out of the amplifier.

$$L(n,t)=\int_0^t Q(x)L(n-1,t-x)dx, \qquad (2a)$$

when $$L(1,t)=\int_0^t Q(x)dx. \qquad (2b)$$

If now we take $Q(t)$ to be that for random counting,[3] $Q(t)=\mu e^{-\mu t}$, where μ is the average rate of receiving impulses, by an induction on n,

$$L(n,t)=\frac{1}{(n-1)!}\int_0^t \mu e^{-\mu x}(\mu x)^{n-1}dx \qquad (3a)$$

$$=\frac{1}{(n-1)!}\int_0^{\mu t}(\mu x)^{n-1}e^{-\mu x}d(\mu x). \qquad (3b)$$

This is the same expression as that obtained by using a Poisson distribution of intervals. By definition of the Γ-function,

$$L(n,t)=\Gamma(\mu t,n)/\Gamma(n)=I(\mu t,n), \qquad (3c)$$

k stages. Then the probability that an impulse in the output of the kth stage follow its predecessor in time $t-x$ or less is $L(2^k,t-x)$. The probability that the next impulse come in time x to $x+dx$ is $L'(2^k,x)dx$. Hence the probability that these two impulses come as specified is

$$L'(2^k,x)L(2^k,t-x)dx. \qquad (2d)$$

The probability that the two impulses come together in total time less than t is

$$\int_0^t L'(2^k,x)L(2^k,t-x)dx=L(2^{k+1},t) \qquad (2e)$$

by Eq. (2c), and the induction is completed.

[3] For proof of this see Marsden and Barratt, Proc. Phys. Soc. **23**, 367 (1911) and **24**, 50 (1911).

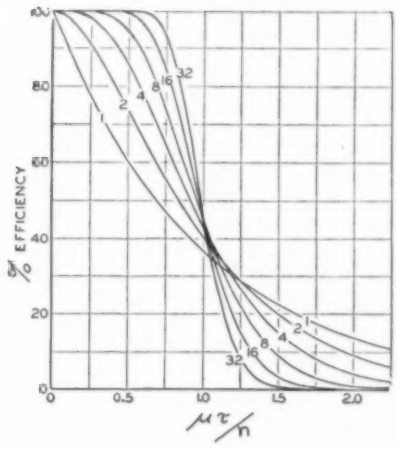

FIG. 2. The same functions (one hundred times probability of recording counts) that are plotted in Fig. 1 are plotted here as functions of $\mu\tau/n$, i.e., as functions of equal average rates of recorder input. For a scale of one the efficiency is that for random counts fed into the recorder; for higher scales the distribution is not random. In these cases, the short intervals are averaged out if $\mu<n/\tau$, increasing the efficiency; for $\mu>n/\tau$ the long intervals are averaged out, decreasing the efficiency in comparison to that for random counts. The curves show that this effect becomes more pronounced as the scale of the circuit increases.

where $\Gamma(\mu t,n)$ is the incomplete Γ-function with upper limit μt of n, $\Gamma(n)$ the complete Γ-function, and $I(\mu t,n)$ this ratio. $I(\mu t,n)$ is given in tables of the incomplete Γ-function.[4] The function $G(n,t)$ has the form

$$G(n,t)=1-L(n,t)=1-I(\mu t,n). \qquad (3d)$$

On carrying out the indicated integration in Eq. (3a) one can obtain by means of a recursion formula:[5]

$$L(n,t)=1-e^{-\mu t}\left(1+\mu t+\frac{(\mu t)^2}{2!}+\cdots+\frac{(\mu t)^{n-1}}{(n-1)!}\right) \qquad (4a)$$

or

$$G(n,t)=e^{-\mu t}\left(1+\mu t+\frac{(\mu t)^2}{2!}+\cdots+\frac{(\mu t)^{n-1}}{(n-1)!}\right). \qquad (4b)$$

$G(n,t)$ is equal to $e^{-\mu t}$ times the first n terms of the expansion of $e^{+\mu t}$ as a power series in t.

If we now consider the impulses being fed into a recorder which will not respond unless the

[4] Karl Pearson, editor, *Tables of the Incomplete Γ-Function* (H. M. Stationery Office, London, 1922).

[5] B. O. Peirce, *A Short Table of Integrals*, No. 403 (Ginn and Company, Boston, 1929).

interval between the count and its predecessor is greater than τ, the fraction of the impulses recorded will be $G(n, \tau)$. The average number, μ_n, recorded per second will then be

$$\mu_n = G(n, \tau)/\hat{\imath}_n, \tag{5a}$$

where $\hat{\imath}_n$ is the average interval between counts in the output of the scale:

$$\hat{\imath}_n = \int_0^\infty tL'(n, t)dt$$

$$= \frac{1}{(n-1)!}\int_0^\infty t\mu e^{-\mu t}(\mu t)^{n-1}dt = n/\mu. \tag{5b}$$

Hence $$\mu_n = (\mu/n)(1 - I(\mu\tau, n)). \tag{5c}$$

Graphs of the efficiency of the scaling circuit ($100\,G(n, \tau)$) against $\mu\tau$ as the argument are shown in Fig. 1 for values of n from one to thirty-two for scales-of-two in series. In order to compare the efficiencies of the various scaling circuits with equal numbers of counts per second going in to the mechanical recorder, $100\,G(n, \tau)$ is also plotted against $\mu\tau/n$ in Fig. 2. The distribution of impulses according to the time interval between counts is the negative derivative of $G(n, t)$ with respect to time, and one can see from an inspection of these graphs that a scaling circuit, in averaging the time intervals n at a time, makes fewer extreme short and long intervals to be passed on to the recorder. Because there are fewer short intervals for a given rate of recorder input when a scaling circuit is used, it is better to increase the efficiency of recording counts by employing a scaling circuit than to attempt to build a mechanical recorder with a smaller time-constant and operate it directly out of the amplifier.

The higher the scale of the circuit, the more the short intervals are averaged out. In Eq. (4b) it can be seen that as n increases, more and more of the terms of the expansion of $e^{+\mu\tau}$ are included so that μ_n approaches the value (for each $\mu\tau$)

$$\mu_n \doteq (\mu/n)e^{-\mu\tau}e^{+\mu\tau} = \mu/n, \quad n \gg \mu\tau. \tag{5d}$$

That is, the scaling circuit and recorder will register all of the incoming counts divided by n. In the next section we shall see that when the effect of the losses in the amplifier is considered, n will not have to increase without bound, but for a finite and practical value of n all the impulses (divided by n) received from the amplifier will be registered.

III. The Effect Due to the Finite Resolving Time of the Amplifier and Counter

In an actual experimental set-up, the scaling circuit is not fed with random impulses, but with a distribution in which the short intervals have been cut out by the counter and amplifier. We assume that the counter and amplifier act together with an effective resolving time, σ.[6] Under such conditions Ruark and Brammer[7] have shown that

$$\mu_1 = \mu e^{-\mu(\tau-\sigma)}/(\mu\sigma+1), \quad \tau \geqslant \sigma \tag{6a}$$

$$\mu_1 = \mu/(\mu\sigma+1), \quad \tau \leqslant \sigma \tag{6b}$$

when no scaling circuit is used.

With a scale-of-n introduced between the amplifier and recorder, we proceed to calculate the probability that an impulse in the output of the scaling circuit shall come within a time t of its predecessor. The probability that an impulse in the amplifier output shall come within time t and $t+dt$ of its predecessor is $Q^*(t)dt$, where

$$Q^*(t) = \mu e^{-\mu(t-\sigma)}, \quad t \geqslant \sigma \tag{7a}$$

$$= 0, \quad t \leqslant \sigma \tag{7b}$$

Eq. (7b) is obvious. The amplifier cuts out all these counts. The probability that a count should come within a time σ or more of its predecessor is $e^{-\mu\sigma}$. This is the fraction of the total counts which makes up the output of the amplifier. The fraction of counts between t and $t+dt$ for $t \geqslant \sigma$ is $e^{-\mu t}dt$. Hence the probability that the output impulse of the amplifier be between t and $t+dt$ of its predecessor is $e^{-\mu(t-\sigma)}dt$, the ratio of the two fractions.

We also assume that if the scaling circuit is one of a single stage, that its recovery time does

[6] This time σ is not necessarily the recovery time of the amplifier. The scaling circuit reacts if a variation of a certain size occurs in the output of the amplifier. If impulses come too closely, this variation is not sufficiently large; it depends on the recovery time of the amplifier, the distortion caused by the amplifier, and the sensitivity (bias control) of the scaling circuit.

[7] These conditions and the following formulae are given by A. E. Ruark and F. E. Brammer, Phys. Rev. **52**, 322 (1937).

not exceed that of the amplifier; if the circuit is a series of scales-of-two, that the recovery time of the kth stage does not exceed $2^{k-1}\sigma$.

Now let $L^*(n, t)$, $(G^*(n, t))$ be the probability that the time elapsed when n successive amplifier impulses follow an arbitrary one be less (greater) than t.

Then, as before,

$$L^*(n, t)=\int_0^t Q^*(x)L^*(n-1, t-x)dx, \quad (8a)$$

where $L^*(1, t)=\int_0^t Q^*(t)dt.$ (8b)

These functions can also be expressed by means of the incomplete Γ-functions:

$$L^*(n, t)=I(\mu(t-n\sigma), n), \quad t\geqslant n\sigma, \quad (9a)$$

$$=0, \quad t\leqslant n\sigma. \quad (9b)$$

This can be shown by induction. For $n=1$, Eq. (9a) and (9b) hold. Let then Eq. (9a) and (9b) hold for n. Then:

$$L^*(n+1, t)=\int_0^t Q^*(x)L^*(n, t-x)dx.$$

By hypothesis, $L^*(n, t-x)$ is zero when $(t-x)\leqslant n\sigma$; i.e. if $x\geqslant(t-n\sigma)$. Also $Q^*(x)=0$ if $x\leqslant\sigma$. Hence $L^*(n+1, t)=0$ if $(t-n\sigma)\leqslant\sigma$, i.e. if $t\leqslant(n+1)\sigma$.

Let $t\geqslant(n+1)\sigma$. Then:

$$L^*(n+1, t)=\int_\sigma^{t-n\sigma}\mu e^{-\mu(x-\sigma)}\times I(\mu(t-n\sigma-x), n)dx. \quad (9c)$$

Substitute $x-\sigma=y$, then

$$L^*(n+1, t)=\int_0^{t-(n+1)\sigma}\mu e^{-\mu y}\times I(\mu(t-\langle n+1\rangle\sigma-y), n)dy \quad (9d)$$

$$=I(\mu(t-\langle n+1\rangle\sigma), n+1) \quad (9e)$$

and the induction is completed.[8]

[8] As before it can be shown that

$$L^*(n+m, t)=\int_0^t L^{*\prime}(n, x)L^*(m, t-x)dx. \quad (9f)$$

If the transformation $y=x-n\sigma$ be made, this is reduced to the same form as that of Eq. (2c) in footnote 2. From this it can be shown that for a scale-of-2^k made up of a series of k scales-of-two, that the recovery time of the lth stage can be made as great as $2^{l-1}\sigma$, and have $L^{*\prime}(2^k, t)$ give the distribution of intervals in the output of the scale-of-2^k.

The function $G^*(n, t)$ has the form:

$$G^*(n, t)=1-I(\mu(t-n\sigma), n), \quad t\geqslant n\sigma \quad (10a)$$

$$=1, \quad t\leqslant n\sigma. \quad (10b)$$

Plots of this function can be obtained by replacing the abscissa of Fig. 1 by $\mu(t-n\sigma)$. It is seen that this probability is increased by the removal of the short intervals by the counter and amplifier.

The dotted line of Fig. 1 has been drawn for a scale-of-eight for which values of $\tau=0.0133$ sec. and $\sigma=0.0005$ sec. are assumed. The abscissae are as indicated in the figure.

As before, the rate of recording is

$$\mu_n^*=G^*(n, \tau)/\bar{t}_n^*, \quad (11a)$$

where

$$\bar{t}_n^*=-\int_0^\infty tG^{*\prime}(n, t)dt \quad (11b)$$

$$=\frac{1}{(n-1)!}\int_{n\sigma}^\infty t\mu e^{-\mu(t-n\sigma)}[\mu(t-n\sigma)]^{n-1}dt \quad (11c)$$

$$=(n/\mu)(1+\mu\sigma). \quad (11d)$$

Hence[9]

$$\mu_n^*=(\mu/n)[1-I(\mu(\tau-n\sigma), n)]/(1+\mu\sigma), \quad \tau\geqslant n\sigma \quad (12a)$$

$$=\frac{\mu}{n}\frac{1}{1+\mu\sigma}, \quad \tau\leqslant n\sigma. \quad (12b)$$

For $n=1$ these are the formulae of Ruark and Brammer, for the function $G^*(n, \tau)$ when not unity is $e^{-\mu(\tau-n\sigma)}$ multiplied by the first n terms of the expansion of $e^{+\mu(\tau-n\sigma)}$.

IV. Conclusions

For a scale-of-2^k, the probability that an impulse in the output of the lth stage comes before a time t from its predecessors is $L^*(2^l, t)$. This vanishes if $t\leqslant 2^l\sigma$. Hence the resolving time of the $(l+1)$st stage can be made as great as $2^l\sigma$. If for any stage the resolving time exceeds this figure, the formulae given do not hold, and some rather complicated expressions will enter into the formula for $L^*(2^k, t)$.

[9] *Note added in proof.* For amplifiers not of the Neher-Harper type, $\mu_n=(\mu/n)P(\sigma)G^*(n, \tau)$, where $P(\sigma)$ is the amplifier's probability of counting.

We do not attempt to draw response curves for various values of τ and σ, for these are best drawn for a particular apparatus. Instead we wish to point out a practical limitation to the scale of the circuit. In Eqs. (12) the term expressing the losses of the scaling circuit and recorder alone drops out if $\tau \leqslant n\sigma$. In this case the recorder counts the full output of the amplifier; i.e., if the scale $n \geqslant \tau/\sigma$. Thus for $\tau = 0.0133$ sec. and $\sigma = 0.0005$ sec., $\tau/\sigma = 26.6$, and a scale-of-32 would be sufficient; a higher scale would not increase the efficiency, for the losses due to the amplifier are independent of the scale.

This analysis shows that a determination of the amplifier's resolving time[7] would be necessary no matter what the scale; for small values of $\mu\sigma$ the error is equal to $\mu\sigma$, for large $\mu\sigma$ it becomes quite appreciable, being about 1 percent for $\sigma = 0.0005$ sec. and $\mu = 20$ impulses per second and about 9 percent when $\mu = 200$ impulses per second.

V. Acknowledgments

The problems which this paper attempts to solve arose in connection with a scaling circuit constructed as part of the work in nuclear physics at this laboratory under the direction of Professor S. K. Allison. Grateful acknowledgment is made to Professor Carl Eckart who suggested to the authors the use of the incomplete gamma-functions, and who made many helpful criticisms of the manuscript.

MAY 15, 1938 PHYSICAL REVIEW VOLUME 53

Electromagnetic and Gravitational Radiation

L. Infeld
Institute for Advanced Study, Princeton, N. J.
(Received February 24, 1938)

Guided by the analogy of the electromagnetic field we consider here the influence of gravitational radiation on the gravitational field and on the equations of motion in the case of a two-body problem. This leads to a generalization of the previously developed methods of solving the gravitational equations and finding the equations of motion.

THE "new approximation method" applied to the gravitational equations[1] leads to the formulation of the equations of motion of mass points represented by singularities of the gravitational field. In I it was claimed that this new approximation method in which no direction of time flow is distinguished differs from the old one, based on the linearized equations and on the use of retarded potentials. There seems to be no place for radiation in the new approximation method as developed in I. It is just this point which could arouse suspicion as to whether the new method of solving the field equations and formulating the equations of motion leads to results corresponding to reality. The purpose of this note is to discuss the point and to investigate the connection between the new and the old approximation methods.

[1] Einstein, Infeld and Hoffmann. "The Gravitational Equations and the Problem of Motion," Ann. Math. **39**, 65 (1938) quoted here as I.

§1. The New Approximation Method and the Equations of Electrodynamics

The equations of electrodynamics are well suited to show the essential features of the new approximation method. We write them in the following form:

$$\gamma_{0|ss} - \gamma_{0|00} = -\rho, \tag{1.1a}$$

$$\gamma_{m|ss} - \gamma_{m|00} = \rho\dot{\xi}^m, \tag{1.1b}$$

$$\gamma_{m|m} = \gamma_{0|0}. \tag{1.1c}$$

Here γ_0 is the electric, γ_m $(m = 1, 2, 3)$ the magnetic potential, ρ the charge density and $\dot{\xi}^m$ the velocity vector. (Latin indices run from 1 to 3 and their repetition implies summation.) Finally: $\gamma_{|m} = \partial\gamma/\partial x^m$; $\gamma_{|0} = \partial\gamma/\partial x^0$; $(x^0 = t;\ c = 1)$.

The advanced and retarded potentials are solutions of (1.1). The usual procedure is to regard the advanced potential as physically meaningless and to distinguish the direction of the flow of time by taking solutions corresponding only to the retarded potential. We shall show that in the new approximation method we are not faced with the choice between "past and future," not, at any rate, in the old form in which the choice between advanced and retarded potential had to be made.

Let us assume that the velocity of a particle having the charge e is small compared with "1" that is, with the velocity of light. Then, if γ_0 is of the order "2" (by convention), γ_m is of the order $|\gamma_0 \xi^m|$, that is, small compared with γ_0; we shall regard γ_m as of the order "3." Therefore:

$$|\gamma_0| \sim \lambda^2; \quad |\gamma_m| \sim \lambda^3. \tag{1.2}$$

We can devise a method of solving the Eqs. (1.1) a method particularly well suited to the quasi static case. The first step is to express explicitly that the time derivative of γ_0, γ_m is small compared with γ_0, γ_m and with its spatial derivatives. To do this we introduce an auxiliary time coordinate

$$\tau = \lambda x^0 \tag{1.3}$$

and assume that every field quantity is a function of (τ, x^1, x^2, x^3) rather than (x^0, x^1, x^2, x^3). If γ's are such quantities then γ, $\gamma_{|m}$, $\partial y/\partial \tau$ are of the same order of magnitude, so that $\gamma_{|0}$ is of the order of $\lambda\gamma$. Denoting now

$$\begin{aligned} \gamma_{|m} &= \gamma_{,m} = \partial\gamma/\partial x^m; \\ \gamma_{|0} &= \partial\gamma/\partial x^0 = \lambda\partial\gamma/\partial\tau = \lambda\gamma_{,0}, \end{aligned} \tag{1.4}$$

we may write (1.1):

$$\gamma_{0,ss} = -\rho + \lambda^2\gamma_{0,00}, \tag{1.5a}$$

$$\gamma_{m,ss} = \rho\dot{\xi}^m + \lambda^2\gamma_{m,00}, \tag{1.5b}$$

$$\gamma_{m,m} = \lambda\gamma_{0,0}. \tag{1.5c}$$

Furthermore we shall assume that charges are represented not by given charge densities but by singularities with spherical symmetry, so that the set of equations written above takes, outside of the singularities, the form:

$$\gamma_{0,ss} = \lambda^2\gamma_{0,00}, \tag{1.6a}$$

$$\gamma_{m,ss} = \lambda^2\gamma_{m,00}, \tag{1.6b}$$

$$\gamma_{m,m} = \lambda\gamma_{0,0}. \tag{1.6c}$$

We now expand the γ's in power series of λ taking the lowest powers of the expansion to be of the order determined by (1.2). From the fact that only second derivatives of the γ's with respect to the time enter the equations (1.6a, b) it follows that the powers of λ in successive terms of the expansion of the γ's *may* differ by "two." Thus we are led to the simple assumption that:

$$\gamma_0 = \lambda^2{}_2\gamma_0 + \lambda^4{}_4\gamma_0 + \lambda^6{}_6\gamma_0 + \cdots, \tag{1.7a}$$

$$\gamma_m = \lambda^3{}_3\gamma_m + \lambda^5{}_5\gamma_m + \cdots. \tag{1.7b}$$

and the equations (1.6) split into:

$${}_{2l}\gamma_{0,ss} = {}_{2l-2}\gamma_{0,00}, \tag{1.8a}$$

$${}_{2l+1}\gamma_{m,ss} = {}_{2l-1}\gamma_{m,00}, \tag{1.8b}$$

$${}_{2l+1}\gamma_{m,m} = {}_{2l}\gamma_{0,0}; \quad l = 1, 2\cdots. \tag{1.8c}$$

The numbers before the γ's denote their order. It should be noted that "zeros" after a comma change the order; thus, for example, ${}_2\gamma_{0,0}$ is of the order "3," ${}_2\gamma_{0,00}$ is of the order "4" etc.

Let us consider the case of one point singularity with its motion represented by $\xi^s(\tau)$. The equations (1.8) in the lowest order ($l=1$) take the form:

$${}_2\gamma_{0,ss} = 0; \quad {}_3\gamma_{m,ss} = 0; \quad {}_3\gamma_{m,m} = {}_2\gamma_{0,0}. \tag{1.9}$$

The solution of these equations corresponding for $\dot{\xi}^m = 0$ to the static solution is:

$$\begin{aligned} {}_2\gamma_0 &= e/r; \quad {}_3\gamma_m = -e/r\dot{\xi}^m; \\ r^2 &= (x^s - \xi^s)(x^s - \xi^s). \end{aligned} \tag{1.10}$$

Indeed, ${}_2\gamma_0$, ${}_3\gamma_m$ are harmonic functions and

$${}_2\gamma_{0,0} = -e(\partial/\partial x^s)(1/r)\dot{\xi}^s = {}_3\gamma_{m,m}, \tag{1.11}$$

so that the equations (1.9) are satisfied.

The nature of the solution is determined by this initial choice of the harmonic functions for ${}_2\gamma_0$ and ${}_3\gamma_m$ if we agree to add no arbitrary harmonic functions in the further approximation steps. We obtain:

$${}_{2l}\gamma_0 = \frac{e}{(2l-2)!}\frac{d^{2l-2}}{d\tau^{2l-2}}(r^{2l-3}), \tag{1.12a}$$

$${}_{2l+1}\gamma_m = -\frac{e}{(2l-2)!}\frac{d^{2l-2}}{d\tau^{2l-2}}(r^{2l-3}\dot{\xi}^m), \tag{1.12b}$$

and the power series,

$$\gamma_0 = e\sum_{l=1}^{\infty}\lambda^{2l}\frac{1}{(2l-2)!}\frac{d^{2l-2}}{d\tau^{2l-2}}(r^{2l-3}), \tag{1.13a}$$

$$\gamma_m = -e\sum_{l=1}^{\infty}\lambda^{2l+1}\frac{1}{(2l-2)!}\frac{d^{2l-2}}{d\tau^{2l-2}}(r^{2l-3}\dot{\xi}^m), \tag{1.13b}$$

if they are convergent, satisfy the electrodynamic equations. These power series for γ_0 and γ_m are well known.[2] They correspond to a standing wave, that is, to the sum

$$\tfrac{1}{2}\text{ advanced} + \tfrac{1}{2}\text{ retarded potential},$$

whenever the series are convergent.

The possibility of this solution of the electrodynamic equations was frequently discussed at the time of Bohr's theory. It was intended to show that there is no contradiction between Bohr's theory of stationary electron paths without radiation and classical electrodynamics. Here we have tried only to show that the familiar solution can be gained by applying our approximation method which, in its simplest form, leads to the standing and not to the outgoing wave.

Is it possible to obtain only the outgoing or only the incoming wave by the use of our approximation method? The existence of such a possibility can be shown although, from the formal point of view, it seems to be more artificial and less simple than the above solution.

Instead of the power series (1.7) we can take a more general expansion,

$$\gamma_0 = \lambda^2{}_2\gamma_0 + \lambda^3{}_3\gamma_0 + \lambda^4{}_4\gamma_0 + \lambda^5{}_5\gamma_0 + \cdots, \tag{1.14a}$$

$$\gamma_m = \lambda^3{}_3\gamma_m + {}^4{}_4\gamma_m + \lambda^5{}_5\gamma_m + \cdots, \tag{1.14b}$$

and apply the approximation method as before. The odd and even powers of λ do not mix since the electrodynamic equations are linear and of the second order. The final solution in this more general case is characterized not only by the choice of ${}_2\gamma_0$, ${}_3\gamma_m$ but also by the choice of the harmonic functions ${}_3\gamma_0$, ${}_4\gamma_m$. We now have besides (1.8), the equations:

$${}_{2l+1}\gamma_{0,ss} = {}_{2l-1}\gamma_{0,00}, \tag{1.15a}$$

$${}_{2l+2}\gamma_{m,ss} = {}_{2l}\gamma_{m,00}, \tag{1.15b}$$

$${}_{2l+2}\gamma_{m,m} = {}_{2l+1}\gamma_{0,0}; \quad l = 1, 2\cdots. \tag{1.15c}$$

Let us take for ${}_3\gamma_0$, ${}_4\gamma_m$ the simple harmonic functions, satisfying (1.15) for $l=1$:

$${}_3\gamma_0 = 0; \quad {}_4\gamma_m = e(d^2\xi/d\tau^2). \tag{1.16}$$

Then in the further approximations we find:

$${}_{2l+1}\gamma_0 = -\frac{e}{(2l-1)!}\frac{d^{2l-1}}{d\tau^{2l-1}}(r^{2l-2}), \tag{1.17a}$$

$${}_{2l+2}\gamma_m = \frac{e}{(2l-1)!}\frac{d^{2l-1}}{d\tau^{2l-1}}(r^{2l-2}\dot{\xi}^m). \tag{1.17b}$$

The general power series in (1.14) if (1.12) and (1.17) are inserted, correspond exactly whenever they are convergent, to Lenard-Weichert's solution, that is, to the retarded potential. By taking only even powers in the expansion for γ_0 (and odd in γ_m) we obtain the ($\frac{1}{2}$ advanced $+\frac{1}{2}$ retarded) potential. Similarly, taking only odd powers in the expansion for γ_0 (and even in γ_m) and starting with (1.16) we obtain a solution representing the ($\frac{1}{2}$ retarded $-\frac{1}{2}$ advanced) potential. By taking both the solutions, that is, by inserting (1.12) and (1.17) in (1.14) we obtain the retarded potential developed into a power series.

It follows from our argument that for two charges e_1 and e_2 moving with velocities $\dot{\eta}^s$, $\dot{\zeta}^s$ we should have for ${}_2\gamma_0$, ${}_3\gamma_m$, ${}_3\gamma_0$, ${}_4\gamma_m$

$$\begin{aligned} {}_2\gamma_0 &= e_1/r_1 + e_2/r_2; \\ {}_3\gamma_m &= -e_1/r_1\dot{\eta}^m - e_2/r_2\dot{\zeta}^m; \end{aligned} \tag{1.18}$$

$${}_3\gamma_0 = 0; \quad {}_4\gamma_m = e_1\frac{d^2\eta^m}{d\tau^2} + e_2\frac{d^2\zeta^m}{d\tau^2}; \tag{1.19}$$

$$r_1^2 = (x^s-\eta^s)(x^s-\dot{\eta}^s); \quad r_2^2 = (x^s-\zeta^s)(x^s-\dot{\zeta}^s).$$

§2. Generalization of the Gravitational Case

The method of approximation used in I is essentially that presented here in §1. The difference consists, however, not only in the fact that the calculations are, in the gravitational case, incomparably more complicated owing to the nonlinear character of the gravitational equations. There is another, much more fundamental,

[2] Nordstrom, Proc. Acad. Amsterdam **22**, 145 (1920); Page, Phys. Rev. **24**, 296 (1924); comp. also Wentzel, Zeits. f. Physik **86**, 479, 635; **87**, 726 (1933).

difference. The motion of the singularities is quite arbitrary in the case of the electrodynamic field and determined on appropriate choice of coordinate conditions in the case of a gravitational field. We shall quote here, very briefly, the results obtained in I with respect to the problem of motion of the field singularities.

In the gravitational case we had 10 gravitational[3] potentials $\gamma_{\mu\nu}$. (The Greek indices run from 0 to 3.) The power development used for $\gamma_{\mu\nu}$ in I was:

$$\gamma_{00}=\lambda^2{}_2\gamma_{00}+\lambda^4{}_4\gamma_{00}+\lambda^6{}_6\gamma_{00}+\cdots, \quad (2.1a)$$

$$\gamma_{0m}=\quad \lambda^3{}_3\gamma_{0m}+\lambda^5{}_5\gamma_{0m}+\cdots, \quad (2.1b)$$

$$\gamma_{mn}=\quad \lambda^4{}_4\gamma_{mn}+\lambda^6{}_6\gamma_{mn}+\cdots. \quad (2.1c)$$

In I only odd powers in λ for γ_{0m} and only even for γ_{00}, γ_{mn} were taken. The whole treatment corresponds, therefore, to that in the electrodynamic case for which the solution is a standing wave, that is, the sum of the advanced and retarded potentials.

The following set of split equations was investigated in I:

$$_{2l}\gamma_{00,ss}=2_{2l}\Lambda_{00}, \quad (2.2a)$$

$$_{2l+1}\gamma_{0m,ss}=2_{2l+1}\Lambda_{0m}, \quad (2.2b)$$

$$_{2l+1}\gamma_{0m,m}=_{2l}\gamma_{00,0}, \quad (2.2c)$$

$$_{2l+2}\gamma_{mn,ss}=2_{2l+2}\Lambda_{mn}, \quad (2.3a)$$

$$_{2l+2}\Lambda_{mn,n}=0; \quad l=1, 2\cdots. \quad (2.3b)$$

The similarity between the equations (2.2) and the electrodynamic equations (1.8) is evident. The only difference in the left-hand side of these two sets of equations is the additional index "0" in (2.2). In both cases the right-hand side is known and determined by the previous approximation steps. The Λ's in (2.2) and (2.3) are functions of γ's calculated in the previous approximations.[4] (The definition of Λ's given fully in I is repeated in the footnote.) The main idea in the solution of the gravitational equations is, as in the electrodynamic case, to bring them, by the use of our approximation method and by application of the coordinate conditions into the form

$$\Delta\gamma=\Lambda,$$

where γ are the unknown and Λ the known functions. The equations (2.2) (2.3) have been derived from the gravitational equations for empty space ($R\mu\nu=0$) together with the coordinate conditions and their relation to the gravitational equations has been investigated. The equations (2.2) (2.3) are *more general* than the gravitational equations. They enable us to determine the field in every approximation step, provided the motion of the singularities is *given*. In (2.2) (2.3) the motion of the singularities can be prescribed in an arbitrary way and is not restricted by these equations. It turned out to be convenient to investigate the equations (2.2) (2.3) which represent a more general case than that of the gravitational equations, and then to ask: what additional conditions must be imposed upon the equations (2.2) (2.3) so that their solution becomes a solution of the gravitational equations for empty space?

Let us assume, for the sake of definiteness, that only *two* singularities are present, their motion being described by the functions $\eta^s(\tau)$, $\zeta^s(\tau)$. Let us form, in each approximation step, the integrals

$$\frac{1}{4\pi}\int^1 2_{2l+2}\Lambda_{mn}\cos(\mathbf{n}\cdot\mathbf{N})dS=_{2l+2}c_m;$$
$$\frac{1}{4\pi}\int^2 2_{2l+2}\Lambda_{mn}\cos(\mathbf{n}\cdot\mathbf{N})dS=_{2l+2}d_m. \quad (2.4)$$

Here the integrals are taken over an arbitrary surface enclosing only the first and the second singularity respectively, as indicated by the number on the top of the integral. Furthermore $(\mathbf{n}\cdot\mathbf{N})$ denotes the "angle" between the direction of x^n and the "normal" to S, and the summation convention applies to the n. These integrals do not depend on the shape of the surface enclosing the singularity, because of (2.3b). Both $_{2l+2}c_m$ and $_{2l+2}d_m$ will be functions of τ only. We can now state the additional condition which must be fulfilled in order that the solution of (2.2) (2.3)

[3] The $\gamma\mu\nu$ are not the usual gravitational potentials but their linear combinations: $\gamma\mu\nu=h\mu\nu-\frac{1}{2}\eta\mu\nu\eta^{\sigma\rho}h\sigma\rho$, where $h\mu\nu=g\mu\nu-\delta\mu\nu$ and: $\eta_{mn}=\delta_{mn}$; $\eta_{m0}=0$; $\eta_{00}=-1$.

[4] The linear terms are only present in $2_{2l+2}\Lambda_{mn}$. They are:

$$-_{2l+1}\gamma_{0m,\,0n}-_{2l+1}\gamma_{0n,\,0m}+\delta_{mn}{}_{2l}\gamma_{00,\,00}+{}_{2l}\gamma_{mn,\,00}.$$

The nonlinear terms are the result of the development of

$$2\Lambda\mu\nu=2L\mu\nu-\eta\mu\nu\eta^{\sigma\rho}L\sigma\rho,$$

where $L\sigma\rho$ is equal to the nonlinear part of $R\sigma\rho$.

should also be a solution of the gravitational equations for empty space. It is:

$$\lambda^4{}_4c_m+\lambda^6{}_6c_m+\lambda^8{}_8c_m+\cdots=0, \quad (2.5a)$$

$$\lambda^4{}_4d_m+\lambda^6{}_6d_m+\lambda^8{}_8d_m+\cdots=0. \quad (2.5b)$$

There are 6 differential equations for η^s, ζ^s and their solution gives the possible motions of the particles represented by the singularities of the field. In this essential point the gravitational equations differ from the electrodynamic one, because they together with the coordinate condition determine the motion of the field singularities.

By carrying the calculation of Λ_{mn} up to, say, the *sixth* approximation (as in I), approximate equations of motion can be obtained. They are:

$$\lambda^4{}_4c_m+\lambda^6{}_6c_m=0, \quad (2.6a)$$

$$\lambda^4{}_4d_m+\lambda^6{}_6d_m=0. \quad (2.6b)$$

In the first approximation step the equations for ${}_2\gamma_{00}$ and ${}_3\gamma_{0m}$ are

$$\begin{gathered}{}_2\gamma_{00,ss}=0; \quad {}_3\gamma_{0m,ss}=0; \\ {}_3\gamma_{0m,m}={}_2\gamma_{00,0},\end{gathered} \quad (2.7)$$

which are exactly the equations (1.9). The solution from which we started in I corresponding to the existence of *two* point singularities with central symmetry was

$$\begin{gathered}{}_2\gamma_{00}=2{}_2\varphi; \quad {}_2\varphi=-2m_1/r_1-2m_2/r_2, \\ {}_3\gamma_{0m}=4m_1/r_1\dot\eta^m-4m_2/r_2\dot\zeta^m, \\ r_1{}^2=(x^s-\eta^s)(x^s-\eta^s); \quad r_2{}^2=(x^s-\xi^s)(x^s-\xi^s).\end{gathered} \quad (2.8)$$

The constant and positive coefficients m_1 and m_2 are the masses of the point singularities. Their sign is determined by the fact that two masses attract each other. Again we see a similarity between (2.8) and (1.18a) (1.18b), the only difference being in the constant coefficients. The next step was to calculate ${}_4\Lambda_{mn}$ and the integrals ${}_4c_m$, ${}_4d_m$. As was to be expected, the equations of motion up to this approximation, that is the equations

$${}_4c_m=0; \quad {}_4d_m=0 \quad (2.9)$$

proved to be the Newtonian equations of motion. We may note for future use that in the same approximation we had

$${}_4c_m+{}_4d_m\leqq m_1\frac{d^2\eta^m}{d\tau^2}+m_2\frac{d^2\zeta^m}{d\tau^2}={}_40; \quad (2.10)$$

therefore, $m_1(d^2\eta/d\tau^2)+m_2(d^2\zeta/d\tau^2)$ is, at least, of the *sixth* order.

So far we have tried to repeat briefly those results obtained in I which we shall use later.

Our problem now is to investigate for the gravitational case a more general solution in which the powers of λ in the development for γ's do not change by "2" but only by "1." As in the electromagnetic case, we shall seek here a solution corresponding not to a standing wave, but to an outgoing one. It is indeed possible to generalize our procedure by introducing for γ's instead of (2.1) the more general development

$$\gamma_{00}=\lambda^2{}_2\gamma_{00}+\lambda^3{}_3\gamma_{00}+\lambda^4{}_4\gamma_{.0}+\lambda^5{}_5\gamma_{00}+\cdots, \quad (2.11a)$$

$$\gamma_{0m}=\lambda^3{}_3\gamma_{0m}+\lambda^4{}_4\gamma_{0m}+\lambda^5{}_5\gamma_{0m}+\cdots, \quad (2.11b)$$

$$\gamma_{mn}=\lambda^4{}_4\gamma_{mn}+\lambda^5{}_5\gamma_{mn}+\cdots. \quad (2.11c)$$

We shall add the new arbitrary expressions in such a way that the arbitrary harmonic functions by which we start our calculations are the beginning of series representing the retarded gravitational potentials and not, as in I, the standing wave. It is of some interest to investigate the influence of such a more general procedure upon the equations of motion, or in other words, the part which can be played by the radiation in the gravitational case, brought in through this generalization. In this more general case the equations (2.2) (2.3) would have to be supplemented by the equations

$${}_{2l+1}\gamma_{00,ss}=2{}_{2l+1}\Lambda_{00}, \quad (2.12a)$$

$${}_{2l+2}\gamma_{0m,ss}=2{}_{2l+2}\Lambda_{0m}, \quad (2.12b)$$

$${}_{2l+2}\gamma_{0m,m}={}_{2l+1}\gamma_{00,0}, \quad (2.12c)$$

$${}_{2l+3}\gamma_{mn,ss}=2{}_{2l+3}\Lambda_{mn}, \quad (2.13a)$$

$${}_{2l+3}\Lambda_{mn,n}=0; \quad l=1, 2\cdots, \quad (2.13b)$$

and instead of (2.5) we should have:

$$\lambda^4{}_4c_m+\lambda^5{}_5c_m+\lambda^6{}_6c_m+\lambda^7{}_7c_m+\cdots=0, \quad (2.14a)$$

$$\lambda^4{}_4d_m+\lambda^5{}_5d_m+\lambda^6{}_6d_m+\lambda^7{}_7d_m+\cdots=0, \quad (2.14b)$$

where

$$ {}_{2l+3}C_m = \frac{1}{4\pi}\int {}^1 2_{l+3}\Lambda_{mr} \cos(\mathbf{n}\cdot\mathbf{N})dS; $$
$$ {}_{2l+3}d_m = \frac{1}{4\pi}\int {}^2 2_{l+3}\Lambda_{mn} \cos(\mathbf{n}\cdot\mathbf{N})dS. \tag{2.15} $$

For $l=1$ the equations (2.12) take the form

$$ {}_3\gamma_{00,ss}=0; \quad {}_4\gamma_{0m,ss}=0; $$
$$ {}_4\gamma_{0m,m}={}_3\gamma_{00,0}. \tag{2.16} $$

For their solution we take, as in (1.19)

$$ {}_3\gamma_{00}=0; \quad {}_4\gamma_{0m}=-4m_1\frac{d^2\eta^m}{d\tau^2}-4m_2\frac{d^2\zeta^m}{d\tau^2}. \tag{2.17} $$

But in this case we have

$$ {}_5\Lambda_{mn}=0, \tag{2.18} $$

and therefore

$$ {}_5C_m=0; \quad {}_5d_m=0. \tag{2.19} $$

This shows that the radiation terms do not influence the equations of motion up to the *sixth* order and that the right hand side of ${}_4\gamma_{0m}$ in (2.17) is of the *sixth* order at least. We can, however, go one step further and calculate the equations of motion up to the *seventh* order. For $l=2$ the equations (2.12) again take the form

$$ {}_5\gamma_{00,ss}=0; \quad {}_6\gamma_{0m,ss}=0; $$
$$ {}_6\gamma_{0m,m}={}_5\gamma_{00,0}. \tag{2.20} $$

We take as a solution of these equations:

$$ {}_5\gamma_{00}=-\frac{4}{6}\frac{d^3}{d\tau^3}(m_1r_1^2+m_2r_2^2), \tag{2.21a} $$

$$ {}_6\gamma_{0m}=-4\frac{d}{d\tau}(m_1\dot\eta^m+m_2\dot\zeta^m) $$
$$ -\frac{4}{6}\frac{d^3}{d\tau^3}(m_1r_1^2\dot\eta^m+m_2r_2^2\dot\zeta^m). \tag{2.21b} $$

This solution can be deduced from (1.17) if we take into account the different constant coefficients for the gravitational problem and the fact that we are now dealing with a two-particle problem. Both functions in (2.21) are harmonic and of the desired order because of the equations of motion. We can now calculate in turn ${}_7\Lambda_{mn}$ and ${}_7C_m$, ${}_7d_m$. The result is:

$$ 2_7\Lambda_{mn} = -{}_6\gamma_{0m,n0}-{}_6\gamma_{0n,m0}+\delta_{mn}({}_5\gamma_{00,00}) $$
$$ -({}_2\varphi)({}_5\gamma_{00,mn})-({}_5\gamma_{00})({}_2\varphi_{,mn})-(\tfrac{1}{2})({}_5\gamma_{00,m})({}_2\varphi_{,n}) $$
$$ -(\tfrac{1}{2})({}_5\gamma_{00,n})({}_2\varphi_{,m})+\tfrac{3}{2}\delta_{mn}({}_5\gamma_{00,l})({}_2\varphi_{,l}) \tag{2.22} $$

The calculation of the surface integrals gives:

$$ {}_7C_m=-\frac{4}{3}m_1\left(m_1\frac{d^3\eta^m}{d\tau^3}+m_2\frac{d^3\zeta^m}{d\tau^3}\right), \tag{2.23a} $$

$$ {}_7d_m=-\frac{4}{3}m_2\left(m_1\frac{d^3\eta^m}{d\tau^3}+m_2\frac{d^3\zeta^m}{d\tau^3}\right). \tag{2.23b} $$

But again, because of the equations of motion, the right-hand side is not of the *seventh*, but at least of the *ninth* order. From Robertson's calculation it follows[5] that the time mean value of (2.23) is at least of the eleventh order. The result shows the astonishingly small role played by the gravitational radiation in the motion of double stars.

I wish to thank Professors Einstein and Robertson for their interest in this problem and for much stimulating discussion.

[5] Robertson, Ann. Math. **39**, 101 (1938).

LETTERS TO THE EDITOR

Prompt publication of brief reports of important discoveries in physics may be secured by addressing them to this department. Closing dates for this department are, for the first issue of the month, the eighteenth of the preceding month, for the second issue, the third of the month. Because of the late closing dates for the section no proof can be shown to authors. The Board of Editors does not hold itself responsible for the opinions expressed by the correspondents.

Communications should not in general exceed 600 words in length.

Magnetic Moment of Li^7 in the α-Particle Model

The new method of Rabi[1] yields values of the nuclear magnetic moments of unprecedented accuracy. For Li^7, a moment of 3.265 ± 0.016 nuclear magnetons has been found[1] while preliminary measurements[2] of the proton moment gave 2.78 with an accuracy of about one percent. This gives a difference between the Li^7 and H^1 moments of 0.48, with a probable error of about ten percent. In contrast to this, existing theories based on the one-particle (Hartree) model[3, 4] give only 0.28 to 0.32 for this difference, a discrepancy of about 50 percent. It seems therefore worth while to re-examine the theoretical situation.

It seems almost certain that the total angular momentum of the Li^7 nucleus ($\frac{3}{2}$) is composed of a spin $\frac{1}{2}$ and an orbital momentum 1, and that the spin is due to the odd proton in the nucleus. These conclusions follow from the fact that pairs of like particles have a strong tendency to have resultant spin zero. There is considerable direct evidence for this tendency in that all nuclei with even numbers of neutrons and protons have zero spin. The tendency is also understandable theoretically because a strong repulsive force between like particles with parallel spins is required in order to give saturation of the nuclear forces, *i.e.*, to balance the attraction of like particles with opposite spin. Direct evidence for the repulsion of like particles in the triplet state may be found in the high mass of light nuclei of high isotopic number[5] such as Li^8 and B^{12}. In the particular case of Li^7, the four neutrons and two of the protons will give resultant spin zero, leaving only the spin of the third proton. Inglis[4] has shown by explicit calculation that there is only an extremely small probability for a state of affairs in which the two neutrons outside the alpha-particle have their spins parallel to the total spin and the proton opposite. Therefore, in first approximation, the magnetic moment of Li^7 should be equal to the proton moment plus the moment due to the orbital motion.

The calculation of the orbital magnetic moment requires a much more extensive use of a model than does the magnetic moment due to the spin. In the single particle model, it is assumed essentially that Li^7 consists of an α-particle core around which the three other particles are moving in a symmetric fashion. Thus the orbital momentum 1 will be shared about equally between the three particles, giving a momentum $\frac{1}{3}$ for the proton. Since the neutron orbital momentum contributes nothing to the magnetic moment, the orbital magnetic moment will be $\frac{1}{3}$, as pointed out by Inglis.[4] Only very small corrections have to be added to this figure which reduce it to about 0.30.

It may seem more satisfactory to consider the Li^7 nucleus as made up of an α-particle and a triton (H^3). This model seems more appropriate in our case than in many others because the binding energy of Li^7, as compared with He^4+H^3, is only 2.76 mMU (milli-mass-units) whereas the internal binding energies of H^3 and He^4 (as compared with free neutrons and protons) are 8.94 and 30.23 mMU, respectively. According to Teller,[6] it is plausible that the system of α-particle and triton must have an orbital momentum unity around its center of mass, in agreement with the experimental spin of Li^7 (see above).

With this model, the magnetic moment of Li^7 becomes equal to the intrinsic moment of the triton plus the orbital moment. The triton moment is certainly very close to the proton moment because the two neutrons in H^3 will have zero resultant spin (see above). The orbital angular momentum is shared between triton and α-particle in the inverse mass ratio. Since H^3 has a specific charge of $\frac{1}{3}$, He^4 one of $\frac{2}{4}$ times the proton specific charge, we find for the contribution of the orbital motion to the magnetic moment of Li^7

$$\mu_0 = \tfrac{4}{7} \cdot \tfrac{1}{3} + \tfrac{3}{7} \cdot \tfrac{2}{4} = \tfrac{17}{42} = 0.40_5.$$

This is in much better agreement with the observed value of 0.48 than the result of the single particle model, the difference being just within the experimental error. The reason for the improvement is that now the α-particle receives a share of the orbital momentum, and since its specific charge is greater than that of the triton, it gives a larger contribution to the magnetic moment. This may be considered as some evidence in favor of the α-particle model for lightly bound nuclei. For Li^6 which also falls in this class the model would predict exactly the deuteron moment.

H. A. BETHE

Cornell University,
Ithaca, New York,
April 27, 1938.

[1] Rabi, Zacharias, Millman and Kusch; Phys. Rev. **53**, 318, 495 (1938).
[2] Private communication from Professor Rabi.
[3] Rose and Bethe, Phys. Rev. **51**, 205, 993 (1937).
[4] Inglis, Phys. Rev., to appear shortly.
[5] Feenberg and Wigner, Phys. Rev. **51**, 95 (1937).
[6] Teller and Hafstad, Phys. Rev., to appear shortly.

Radial Lines in Laue Spot Photographs

When taking Laue spot photographs with a simple type of Laue spot camera which is described elsewhere,[1] radial lines were noticed apparently emanating from the edge of the shadow cast by the lead button which was used to prevent halation around the central spot. As the size of the button was reduced these radial lines became more definite and with a button of 5 mm diameter the result obtained with a 7-hour exposure is shown in Fig. 1 which was taken at approximately perpendicular incidence to a 100 plane of a natural sodium chloride crystal. The film was 5 cm from the crystal and the x-ray tube a Coolidge water-cooled type with tungsten target operated at about 40 kv peak and 15 ma. The same pattern was obtained with a natural potassium chloride crystal but not with Iceland spar, mica, zinc blend, fluorite, or gypsum, each perpendicular to a natural cleavage face. If the crystal is not as nearly perpendicular to a 100 plane for sodium chloride the same 8 radial lines show up but they begin on a rectangle rather than a square.

The result of a much longer exposure, 15 hours, is shown in Fig. 2 for the same crystal as for Fig. 1 but after it had been re-mounted some weeks later. The longer exposure was undertaken after the negatives had been shown to several men at the New York meeting in February and one of them had suggested that it might be due to a sort of crossed lattice effect, much as a similar pattern is obtained in the visible region with crossed gratings. Another observation on this plate which does not show up in the print, is the peculiar "structure" of those spots which appear exactly round. Instead of being of uniform intensity they have the appearance shown in Fig. 3, the rectangular portion being much darker and having its long side perpendicular to a radius from the center. Crystals from several sources far removed geographically were supplied by our geology department but no change in pattern was observed, i.e., no radial lines were exhibited except for sodium chloride and potassium chloride crystals, but invariably for these.

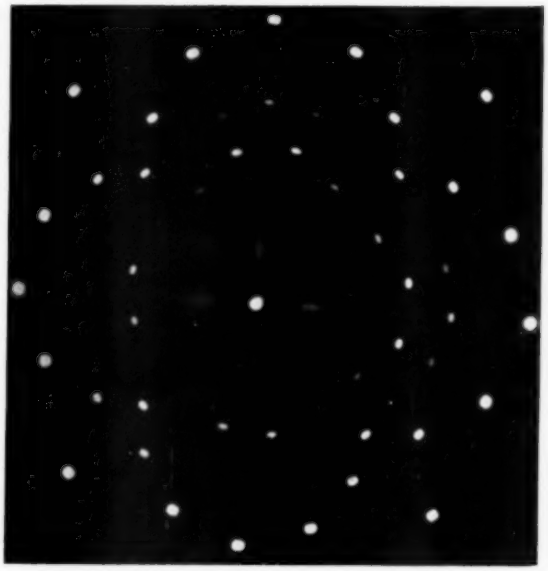

FIG. 1. Laue spot photograph taken at approximately perpendicular incidence to a 100 plane of a natural sodium chloride crystal.

FIG. 2. Result of a 15-hour exposure with the same crystal as in Fig. 1.

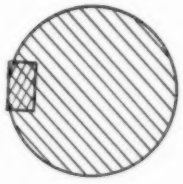

FIG. 3.

In order to obtain comparison photographs sodium chloride and potassium chloride crystals were grown from a saturated solution of the respective salts. Chemically pure salts were first allowed to crystalize and these crystals then used to form a second saturated solution from which the crystals finally used were obtained. These crystals were not clear although apparently well formed. Nevertheless the potassium chloride crystals used showed a pattern exactly like that shown in Fig. 1. To date the author has had no explanation of these lines nor is he prepared to offer one at present. If they are due to strain why should they appear only with the two crystals mentioned and not with the others examined.

A. P. R. WADLUND

Jarvis Physical Laboratory,
Trinity College,
Hartford, Connecticut,
April 2, 1938.

[1] A. P. R. Wadlund, "A Portable Laue Spot Camera," Am. Phys. Teacher, 6, 103 (1938).

Comments on the Article by A. P. R. Wadlund: Radial Lines in Laue Spot Photographs

It is well known that the diffraction spots in a Laue photograph of a strained crystal are drawn out into radial streaks and that new streaks appear as well. The Laue photographs reproduced in the article by Mr. Wadlund show well-defined spots, indicating that the bulk of the crystal is subjected to little or no strain. It seems unreasonable therefore that the streaks are due to strain.

Indeed, it proves possible to interpret the radial streaks as due to two-dimensional lattice effects. The directions of the diffraction maxima from a two-dimensional lattice are given by: $\mathbf{u}-\mathbf{u}_0=\lambda[H_1\mathbf{b}_1+H_2\mathbf{b}_2]+p\mathbf{k}$. Here $\mathbf{u}_0$ and $\mathbf{u}$ designate the directions of incident and scattered beams, $\mathbf{a}_1$ and $\mathbf{a}_2$ are the lattice vectors, $\mathbf{b}_1$ and $\mathbf{b}_2$ their reciprocals, while $\mathbf{k}$ is a unit vector normal to the lattice plane. λ is the wave-length, H_1 and H_2 two integers. The quantity p has to be fixed so that the right-hand side of the equation equals $|\mathbf{u}-\mathbf{u}_0|$.

If a surface layer of a sodium chloride cube is normal to the incident beam, the equation becomes:

$$\mathbf{u}=\frac{\lambda}{a^2}[H_1\mathbf{a}_1+H_2\mathbf{a}_2]\pm\left[1-\frac{\lambda^2}{a^2}(H_1^2+H_2^2)\right]^{\frac{1}{2}}\mathbf{k}$$

with $\mathbf{a}_1\cdot\mathbf{a}_2=0$ and $\mathbf{a}_1=\mathbf{a}_2=5.63$A. The two-dimensional structure factor is: $F_{H_1H_2}=2[fna+(-1)^{H_1}fcl]$ with H_1+H_2 even. Thus the intensity of the diffration effects will be very small unless H_1 and H_2 are both even integers.

It is readily seen from the second equation that the eight reflections with H_1H_2 assuming the values $(\pm2,0)$ $(0,\pm2)$ $(\pm2,\pm2)$ will give rise to eight spots (λ constant) on the photographic plate. The eight spots will lie at the corners of a square ($H_1H_2=\pm2,\pm2$) and at the midpoints of the edges of the square ($H_1H_2=\pm2,0$ and $0,\pm2$).[1] As the wave-length increases the eight spots move radially away from the central spot and thus produce the group of eight inner streaks. (See Fig. 1 of Wadlund's article.) The edge of the square formed by the lower wave-length limits of the eight streaks is 1.1 cm. This gives a value of 0.31A for the minimum wave-length present in the incident beam. This value agrees remarkably well with $\lambda_{min}=0.30$A obtained by interpretation of the regular Laue pattern. (Mr. Wadlund states that a peak voltage of 40 kv was used. This corresponds to $\lambda_{min}=0.31$A, which is slightly too high.)

The much weaker streaks lying in the region of the photographic plate where the regular Laue spots occur, are not sufficiently well defined in the reproductions to permit quantitative measurements. It is clear, however, that the six surface layers of a NaCl cube will give rise to a distribution of radial streaks of the type observed.

It may be stated with confidence that an exact treatment of the x-ray diffraction from a finite crystal must give rise to boundary solutions corresponding to diffraction from the boundary layer. Usually these effects are too weak to be observed. The reason for their occurrence in the case of NaCl and KCl may be sought in the pronounced mosaic character of these crystals. It is well known that these crystals may be considered as consisting of a huge number of independently scattering crystal blocks in nearly parallel orientation. The great number of discontinuities naturally means a corresponding enhancement of the surface effects.

University of Chicago, Chicago, Illinois, April 18, 1938. W. H. ZACHARIASEN

[1] The edges of the square are actually hyperbolae, as a simple consideration shows.

Gamma-Radiation from Proton Bombardment of Carbon

The resonance capture of protons by carbon has recently been investigated by Dee, Curran and Petrzilka.[1] Of the two resonances observed, the one at 480 Kev is to be associated with the capture of protons by C^{12} with the subsequent emission of 2.6 Mev γ-radiation and the other at about 560 Kev to the capture by the less abundant isotope C^{13} with the formation of N^{14}. The assignment of the first resonance can be made unambiguously since the positron emission from the residual nucleus N^{13} can be observed.[2] Moreover the γ-ray energy agrees fairly well with the expected energy release (binding energy of proton in $N^{13}=1.9$ Mev). The measurement of the γ-ray energy was carried out by the absorption method of Bothe and Becker.[3] A similar analysis of the 2.6 Mev γ-radiation from Th C'' showed practical coincidence between this absorption curve and that from the radiation which is to be attributed to $C^{12}+H^1\rightarrow N^{13}+h\nu$. This radiation is very probably monochromatic or composed of two lines of almost the same energy (cf. reference 2).

The assignment of the 560 Kev resonance to the proton capture by C^{13} is based essentially on the fact that the γ-ray energy in this case is much greater than the energy release (including proton energy) in the C^{12} capture. From the fact that with 11 mm of Al the absorption curve merges with the continuous background, Dee and his collaborators deduce a γ-ray energy of 7.4 Mev, whereas the energy release in the reaction

$$C^{13}+H^1+560\text{ Kev}\rightarrow N^{14}+h\nu$$

is 8.2 Mev. However the use of the end of the absorption curve for the determination of the γ-ray energy is decidedly questionable since the absorption should approach zero intensity asymptotically. Moreover the half-value thickness (thickness required to reduce the intensity to 50 percent) is only 2 mm Al and from an analysis[3] of the transmission of the electrons through the absorber an absorption curve with this half-value thickness should correspond to a γ-ray energy of only 4.6 Mev, cf. Fig. 1, assuming that the radiation is monochromatic.

It is almost certain, however, that the radiation is not monochromatic. The absorption curves for monochromatic radiation consist of an almost straight portion arising from energy loss with negligible scattering for small absorber thickness, and then a "tailing off" due to diffusion of the electrons at larger thicknesses. With increasing γ-ray energy the straight portion of the absorption curve will be relatively longer. An examination of the observed absorption curve shows that it is composed essentially of two straight portions indicating the presence of at least two γ-rays.

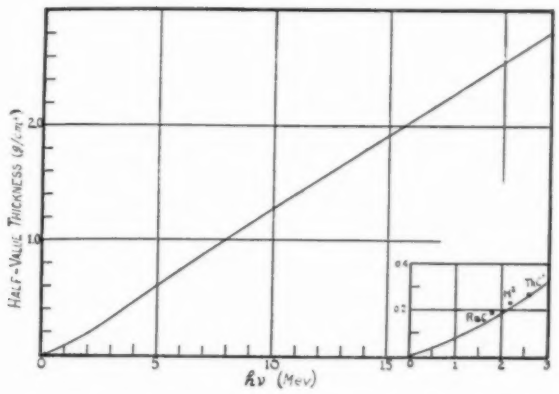

FIG. 1. Half-value thickness in aluminum for the absoprtion of Compton and pair electrons generated by monochromatic γ-rays of energy $h\nu$. The inset gives the curve for small energy in greater detail. The experimental data for Th C'' (2.6 Mev) and H^2 (2.2 Mev) were obtained by Fleischmann (reference 3) and for Ra C (1.8 Mev) by Mitchell and Langer (reference 7).

Further support of this interpretation is obtained from the observation of γ-rays in the bombardment of carbon by deuterons which is to be ascribed to the reaction[5]

$$C^{13}+H^2 \rightarrow N^{14}+n^1.$$

This furnishes evidence for the existence of an excitation level of N^{14} at about 4 Mev. We may then expect three γ-rays, one of 8.2 Mev corresponding to the transition to the ground state and two γ-rays of about 4 Mev corresponding to the cascade process involving the 4 Mev excitation level.[6] We shall make the plausible assumption that no other γ-rays are present with appreciable intensity.

The observed absorption curve should then be a superposition of the three individual absorption curves weighted according to the intensities of the γ-rays. Inasmuch as the energies of the γ-rays differ sufficiently so that the individual absorption curves do not interfere strongly, the relative intensities of the components of the radiation may be found by extrapolating to zero thickness the straight line portion corresponding to the hard component. In this way we find the relative intensity 2 : 1 of soft to hard component.

In conclusion it may be pointed out that while the half-value thickness *versus* γ-ray energy curve given in Fig. 1 is limited in its application to monochromatic radiation, in some cases it may be used as above in conjunction with disintegration data as a rough indication of the number of lines and relative intensities involved in the γ-ray spectrum.

Cornell University,
Ithaca, New York,
April 26, 1938.

M. E. ROSE

[1] P. I. Dee, S. C. Curran and V. Petrzilka, Nature **141**, 642 (1938).
[2] Such activity associated with a resonance peak at 480 Kev has also been observed by Hafstad and Tuve, Phys. Rev. **48**, 306 (1935) who observed in addition a resonance peak at 400 Kev proton energy.
[3] Bothe and Becker, Zeits. f. Physik **76**, 421 (1932); see also Fleischmann, Zeits. f. Physik **103**, 113 (1936).
[4] H. A. Bethe, M. E. Rose and L. P. Smith, Proc. Am. Phil. Soc. **78**, 573 (1938).
[5] Tuve and Hafstad, Phys. Rev. **48**, 106 (1935); Bonner and Brubaker, Phys. Rev. **50**, 308 (1936); cf. also Livingston and Bethe, Rev. Mod. Phys. **9**, 245 (1937), §101, *B* and *C*.
[6] We assume that selection rules do not forbid these transitions.
[7] Mitchell and Langer, Phys. Rev. **52**, 137 (1937).

A Low Temperature Thermal Source of Li Ions

It was found by Blewett and Jones[1] that the β-eucryptite ($Li_2O \cdot Al_2O_3 \cdot 2SiO_2$) they had prepared had an emissivity of Li ions about twice as large as that of spodumene, the well-known Li^+ source. Rumbaugh and others[2, 3] working with Kunsman catalysts were also able to get a much larger Li^+ current than with spodumene. Another type of complex compound, which occurs in natural minerals, known under the name amblygonite ($LiAl(F, OH)PO_4$) was tried in a mass spectrometer equipped with an electrometer tube amplifier. It was finely powdered and, with water as the binder, was mounted on a thin platinum cup welded to a tantalum strip filament. Li ions were emitted at a temperature as low as about 700°C with a total current of about 10^{-6} ampere per cm^2. The Li^7 current obtained at this temperature was more than 10 times larger than that obtained from spodumene at about 1000°C. It is believed that this natural compound will be suitable as a low temperature Li^+ source for large scale separation of the isotopes.

Since the two isotopes were completely resolved, it was possible to observe simultaneously the time change of the emission of each individual ion. In a continuous 12-hour run, it was observed that while the total current remained fairly steady, the Li emission (peak value) of either kind increased slowly with time for the first four hours and then more rapidly to a maximum. After that the emission decreased gradually with time and apparently attained a final constant value. The curves in log-scale are shown in Fig. 1. One can only speculate on what causes the initial rising emission. The latter decay part of the curve is probably due to the gradual withdrawal of moisture from the interior of the salt. In another run without water binding the highest emission was reduced by about ¼ and reached the final value earlier. That moisture enhances emission has been found by Birkenberg.[4]

The variation with time of the abundance ratio of the two isotopes of Li is of interest. These time change curves show that the ratio Li^7/Li^6 increased rapidly with time in

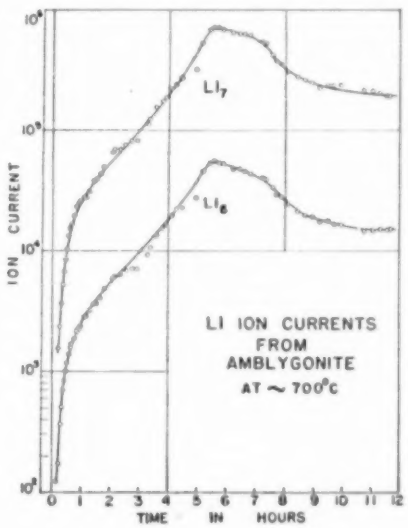

FIG. 1.

the first hour, but then attained a fairly constant value for several hours, and then gradually increased again. The latter part is, therefore, in agreement with that observed by Brewer[5] from an impregnated filament. The ratio of the areas under the time change curves is 12.29 for Li^7/Li^6.

HOFF LU

Department of Physics,
University of Minnesota,
Minneapolis, Minnesota,
April 26, 1938.

[1] Blewett and Jones, Phys. Rev. **50**, 464 (1936).
[2] Rumbaugh, Phys. Rev. **49**, 882 (1936).
[3] Smythe, Rumbaugh, and West, Phys. Rev. **45**, 724 (1934).
[4] Birkenberg, Ann. d. Physik **1**, 157 (1929).
[5] Brewer, J. Chem. Phys. **4**, 350 (1936).

Note on the Range of Occurrence of Stable Isotopes

If we arrange the known stable (nonradioactive) isotopes of the elements in an $A-2Z$, Z (Harkins) diagram, we notice that for each value of the isotopic number $A-2Z$, the isotopes extend in almost unbroken sequence from the lowest to the highest atomic number Z for which stable isotopes have been found.

For odd values of $A-2Z$ the sequence of atomic numbers is continuous, for even values of $A-2Z$ only, even values of Z are found for elements $Z>7$, in accord with the known rule that for elements beyond nitrogen no isotope of odd atomic number has even atomic weight. There are in all only 19 gaps in the sequences, corresponding to isotopes which have not yet been observed. In view of the large number (about 275) of stable isotopes already known, we may predict with considerable certainty that if isotopes corresponding to the 23 gaps are discovered, they would also be found to be nonradioactive, defining the limit of "radioactivity" to correspond to half-lives less than about 10^{12} years. It is evident that nonradioactivity does not necessarily imply abundance, although the converse (rarity of short lived elements) is necessarily true. On the above basis the following elements should be stable: $_{18}A^{37}$, $_{18}A^{39}$, $_{23}V^{49}$, $_{24}Cr^{51}$, $_{22}Ti^{52}$, $_{24}Cr^{56}$, $_{25}Mn^{53}$, $_{26}Fe^{55}$, $_{26}Fe^{60}$, $_{28}Ni^{64}$, $_{38}Sr^{90}$, $_{40}Zr^{88}$, $_{43}Ma^{97}$, $_{43}Ma^{99}$, $_{52}Te^{120}$, $_{56}Ba^{140}$, $_{57}La^{137}$, $_{58}Ce^{139}$, $_{58}Ce^{141}$, $_{58}Ce^{144}$, $_{59}Pr^{143}$, $_{61}Il^{145}$, $_{61}Il^{147}$. The isotope $_{19}K^{40}$ is known to be radioactive as might have been expected since it has odd Z and even A. For $_{37}Rb^{87}$ the odd even rule is obeyed, but because of its radioactivity we need not expect stable isotopes between it and $_{42}Mo^{97}$ in the $A-2Z=13$ sequence.

HARRISON BROWN

Department of Chemistry,
University of California,
Berkeley, California,
March 29, 1938.

A Relation Between Atomic Number and Isotopic Number for Stable Isotopes

In Fig. 1 the isotopic numbers $A-2Z$ of all stable isotopes are plotted against the atomic number Z. Known isotopes are represented by dashes, and the gaps for which stable isotopes are expected in the preceding letter by circles. In Fig. 2 the value of $A-2Z$ at the midpoint of each sequence is plotted against the corresponding atomic number Z, for all even values, and in Fig. 3 for all odd values of $A-2Z$. Between cusps which lie at values of $A-2Z$ fourteen units apart, with an additional cusp at $A-2Z=8$, the points in Fig. 2 lie on remarkably smooth curves. In Fig. 3 the spacing of 14 units between cusps is also evident, and in addition the ranges of 14 units are broken up into 8 and 6, respectively. In no case do the points deviate from the smooth curve more than could be accounted for by the lack of a single isotope at the extremity of a sequence, with the exception of the two points marked by crosses. The point at $A-2Z=20$ in Fig. 2 falls on the curve if we exclude $_{62}Sm^{144}$. The single cross in Fig. 3 corresponds to $_{37}Rb^{87}$, which has already been proved to be radioactive. Possibly $_{62}Sm^{144}$ is α-radioactive, if not it is the only one besides $_4Be^8$ which appreciably disturbs the smoothness of the curves.

G. E. GIBSON
HARRISON BROWN

Department of Chemistry,
University of California,
Berkeley, California,
March 29, 1938.

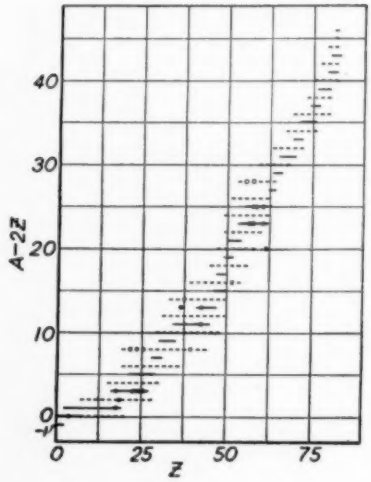

FIG. 1.

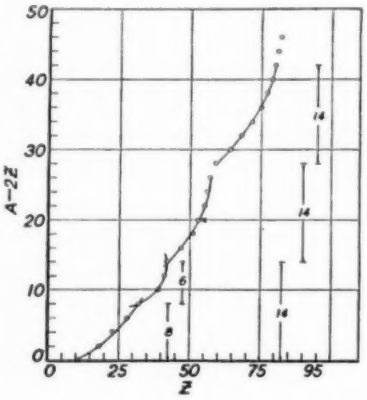

FIG. 2.

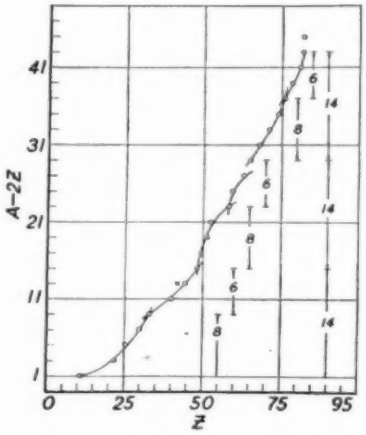

FIG. 3.

Long-Lived Radio Cobalt Isotopes

We have already reported[1] confirmation of a long-lived radio-cobalt produced by irradiating cobalt with neutrons. This effect was first observed by Sampson, Ridenour and Bleakney,[2] who gave the half-life as over a year. Recently Risser[3] has quoted the figure as 2.0±0.5 years, after observing the decay for six weeks.

We have been following chemically separated radio-cobalt samples, obtained from neutron and from deuteron bombardment of C.P. cobalt oxide, for about a year and find the decay curves not to be simple exponentials. For the first 100 days the rate of decay does indeed suggest a 2-year period, but for the remaining interval the half-life is much longer, appearing to be about 10 years or more. When this is well established, subtraction will show the initial decay to be due to a much weaker activity of the order of several months half-life. A somewhat older deuteron-activated sample of cobalt oxide, but without chemical analysis, bears out these observations, as may be seen in Fig. 1.

Absorption curves in Al and in Pb of the 10-year cobalt (chemically separated from a Co+D bombardment) are shown in Fig. 2. No appreciable difference is found in such curves taken a year apart, indicating that the shorter period is in fact very weak. The gamma-ray is reduced to half-value by 12 grams per cm² Pb, indicating an energy of about 1.3 Mev. The range of the electrons is not well defined and may indicate two electron groups with ranges of 0.03 to 0.06 and perhaps 0.3 gram per cm² Al, respectively. These absorption measurements are in substantial agreement with those of Risser.[3]

It is not yet certain that the shorter-lived and low intensity radio-cobalt is actually formed from cobalt; slight traces of iron or nickel in the cobalt oxide could yield radio-cobalt with a period of this magnitude, as we have shown from bombardments of iron with deuterons[1] and of nickel with neutrons and deuterons.[4]

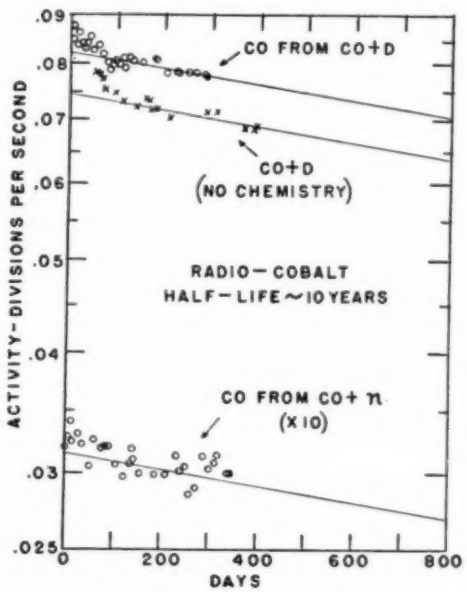

FIG. 1. Activity of cobalt.

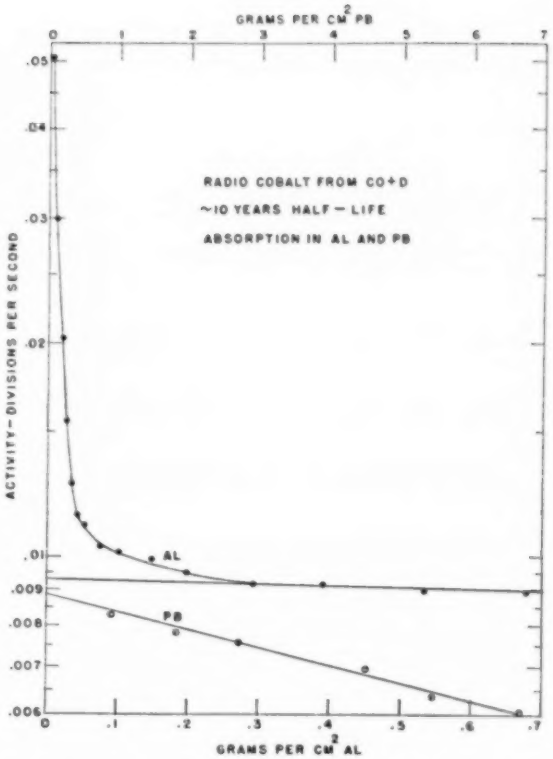

FIG. 2. Absorption in lead and aluminum of radiation from cobalt.

Perrier, Santangelo and Segrè[5] have reported radio-cobalts of half-lives about 1 month and about 215 days obtained from copper filings from the deflector plate of the Berkeley cyclotron, the decay having been followed for about a year. Since cobalt should not be formed from copper by deuterons, they suggest that stray neutrons on copper have produced Co^{60} and Co^{62} by the (n, α) reaction. However, they were unable to confirm this, after irradiating copper for several weeks with the neutrons from 500 mC of Rn+Be. We have looked for such an activity by examining borings taken from beneath the surface of the copper utility target holder of the cyclotron after it had received the neutrons from at least 1000 microampere hours of 4 to 6 Mev deuterons on Be, and must also report negative results. We would like to suggest that iron sputters onto the deflecting plate from the iron lid and base plate of the cyclotron vacuum tank (marks of this are always evident) and hence that Perrier *et al.* are really observing the two cobalt periods that are known[1] to be produced from the deuteron bombardment of iron. In fact, their curve is identical with ours (for Co from Fe+D) for about a year; beyond that, our half-life has lengthened somewhat and there is no assurance that it will not continue to increase even more, with consequent lengthening of the period of the shorter lived component.

The bombardment of iron for 1 hour with 100 microamperes of 3.2 Mev protons yields a long-lived activity

(as well as the 18-hour Co^{55}) and a slow decay is also found after activating manganese for 1 hour with 0.1 microampere of alpha-particles at 16 Mev. The present apparent half-lives of these samples are about 180 days and 80 days, respectively. But since these activities, as well as those of the above-mentioned radio-cobalts from the activated nickel[4] and iron, apparently have not yet settled down to a single rate of decay, it seems premature to attempt to analyze them into component periods which might be identified with each other or to speculate on their isotopic origin.

We gratefully acknowledge the support of the Chemical Foundation, the Research Corporation and the Josiah Macy, Jr. Foundation.

J. J. LIVINGOOD
G. T. SEABORG

Radiation Laboratory, Dept. of Physics (J.J.L.),
Department of Chemistry (G.T.S.),
University of California,
Berkeley, California,
April 29, 1938.

[1] Livingood, Seaborg and Fairbrother, Phys. Rev. **52**, 135 (1937).
[2] Sampson, Ridenour and Bleakney, Phys. Rev. **50**, 382 (1936).
[3] Risser, Phys. Rev. **52**, 768 (1937).
[4] Livingood and Seaborg, Phys. Rev. **53**, 765 (1938).
[5] Perrier, Santangelo and Segrè, Phys. Rev. **53**, 104 (1938).

Erratum: Ferromagnetic Anisotropy of Nickel-Iron Crystals at Various Temperatures

I wish to take this opportunity to point out and correct a mistake in the discussion of "Results" in my paper in the *Physical Review*.[1]

The fourth sentence in this section of the paper which now reads "The most unexpected result is that the direction for easiest magnetization changes not from <111> to <100> as iron increases beyond a critical amount, but from <111> to <110>," should read "The most unexpected result is that the direction for most difficult magnetization changes not from <100> to <111> as iron increases beyond a critical amount, but from <100> to <110.>"

J. D. KLEIS

Research Laboratory,
Fansteel Metallurgical Corporation,
North Chicago, Illinois,
April 20, 1938.

[1] Phys. Rev. **50**, 1178–1181 (1936).

On the Penetrating Component of the Cosmic Radiation

In a previous work[1] we have pointed out, that at a great depth (about 800 meters water equivalent) the ionizing part of the cosmic radiation consisted only of shower particles produced by a nonionizing radiation. We emphasized also our view, that these penetrating nonionizing rays are neutrinos, created somewhere in the atmosphere or in the earth, in multiple shower processes (as described by Heisenberg[2]). In a recent article V. C. Wilson[3] comes in consequence of his measurements to the same conclusion, but he even believes that at great depth successively two kinds of radiation are perceivable "heavy electrons" and "neutrinos." In Fig. 1 we can see the intensity variation of cosmic-ray showers from 4000 m above sea level down to 1000 m water equivalent depth. The points represent experimental data of different authors.[1, 3, 4] We may notice bends on the curve 2: at about 10–20 m and a second somewhere near 250 m water equivalent, but the place of the second bend cannot be located with great accuracy. The first bend may perhaps signify that from this depth onward the majority of the observed showers are produced by heavy electrons and from 250 m on by neutrinos. This interpretation is also in best agreement with the results arrived at by V. C. Wilson.

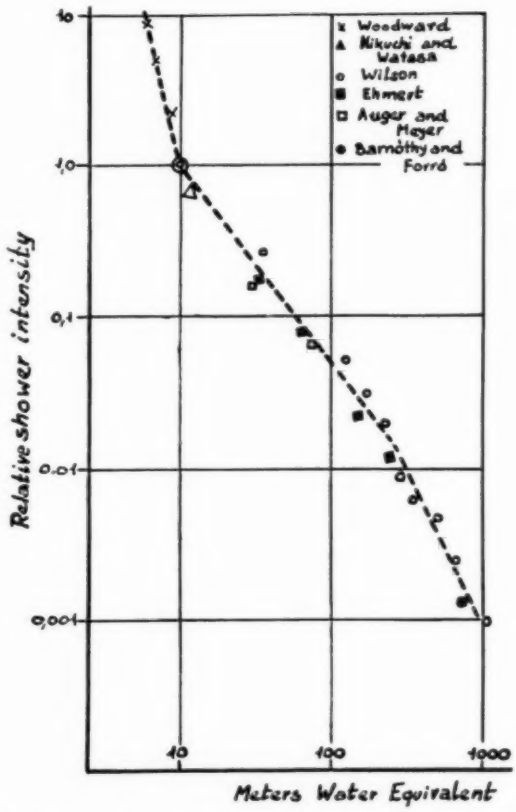

FIG. 1. Relative intensity of shower *versus* depth from the top of the atmosphere plotted on a logarithmic scale. All intensities, observed by different authors, were put equal to 1 at sea level.

J. BARNÓTHY
M. FORRÓ

Institute for Experimental Physics,
University of Budapest,
Budapest, Hungary,
April 13, 1938.

[1] J. Barnóthy and M. Forró, Zeits. f. Physik **104**, 741 (1937).
[2] W. Heisenberg, Zeits. f. Physik **101**, 533 (1936).
[3] V. C. Wilson, Phys. Rev. **53**, 337 (1938).
[4] R. H. Woodward, Phys. Rev. **49**, 711 (1936); S. Kikuchi and J. Watasa, Proc. Phys. Math. Soc. Japan **18**, 210 (1936); P. Auger and G. Meyer, Comptes rendus **204**, 572 (1937); A. Ehmert, Zeits. f. Physik **106**, 751 (1937).

Program of Research Papers at the Annual Meeting of the Southeastern Section of the American Physical Society

UNIVERSITY OF ALABAMA, TUSCALOOSA, ALABAMA

April 1 and 2, 1938

Newly elected officers of the Southeastern Section of the American Physical Society are:

OTTO STUHLMAN, JR.—*Chairman*
B. A. WOOTEN —*Vice Chairman*
PHILIP RUDNICK —*Secretary*
W. S. NELMS —*Treasurer*

INVITED PAPERS

1. Radioactivity. KARL K. DARROW, *Bell Telephone Laboratories.*

2. Thermodynamical Viewpoints in the Study of Nuclear Reactions. L. W. NORDHEIM, *Duke University.*

3. Twenty-Five Years of Wilson Cloud Chamber Research; an Illustrated Survey of the More Important Discoveries Made with the Cloud Chamber. ARTHUR E. RUARK, *University of North Carolina.*

ABSTRACTS OF CONTRIBUTED PAPERS

1. Measurement at High Frequencies of the Diamagnetic Faraday Effect in Liquids. G. C. COMSTOCK, *The Citadel.*—Direct measurements of the Verdet constants of four diamagnetic liquids: carbon disulfide, glycerine, isopropyl and amyl alcohols, for optical frequencies far removed from their absorption regions, have been made in the comparatively high radiofrequency range from 1 to 1.7×10^7 c.p.s. by the modification of a method due to Bretscher,[1] in which a photo-cell coupled to a tuned radiofrequency amplifier was used as the detector of the rotations of the plane of polarization. The variations of the plate current in the output circuit were calibrated in terms of the peak Faraday rotations. The radiofrequency values of the Verdet constants were compared with those obtained by measurement at 60 cycles and with direct current using a.f. and d.c. photoelectric amplifiers. The Verdet constants were found to be independent of the frequency of the field up to 1.7×10^7 c.p.s. within the experimental accuracy of about 5 percent. These measurements are in agreement with the theoretical predictions of Persico[2] of the constancy of the Faraday rotation with variable magnetic field frequency for optical frequencies far removed from the absorption frequencies of the liquids. No anomalous effects were found at radiofrequencies for which these liquids show strong absorption of the radio waves.

[1] E. Bretscher, Helv. Phys. Acta **9**, 42 (1936).
[2] E. Persico, Rend. Linc. **3**, 561, 603 (1926).

2. Optical Activity of Nickel Sulfate, α-Hexahydrate. EDWARD B. NELSON, *Vanderbilt University.*—Nickel sulfate crystals of the α-hexahydrate form have been examined to determine the relative number of laevo- and dextrorotatory crystals, the activity of their solutions, and the rotatory dispersion of the crystals. The relative abundance of the laevo- and dextrorotatory crystals is a one to one ratio. The crystals are found to be mirror-image crystals, since sections of equal thickness give numerically equal rotations for any particular wave-length. Aqueous solutions of only laevo- and of only dextrorotatory crystals were separately examined throughout the visible spectrum, but no optical activity was observed. Visual observations with a Lippich half-shade polarimeter and photographic observations with an adaptation of the method of Fizeau and Foucault were made of the rotatory dispersion of the crystals which was found to be of an anomalous nature. The rotation is zero for light of wave-length 5030A. Above

this point the rotation increases gradually in magnitude to about 6200A where it begins to increase rapidly. Below 5030A the rotation increases gradually in magnitude to about 4600A where it begins to increase rapidly. The sign of the rotation of each crystal changes on passing the zero point. The rotation for the D line of sodium is approximately 1.55° per mm.

3. The Effect of Humidity and Irradiation on the 2.0 cm Sphere Gap. ARTHUR B. LEWIS, *University of Mississippi.*—Quantitative data are presented showing the effects of humidity and irradiation on the 2.0 cm sphere-gap voltmeter in the lower voltage ranges. Preliminary work has been confined to a single gap setting, 4.0 mm (about 10 kv peak). Irradiating this gap with a 500-watt cored-carbon arc lowers the sparking voltage by 2.0 percent from the value obtained when the gap is completely dark, and decreases the probable error of a single observation from about ±0.7 percent with the gap dark to about ±0.1–0.2 percent with the gap irradiated. A sixfold increase in the intensity of this irradiation causes no further significant decrease in either the sparking voltage or the scattering of individual observations. The presence of water vapor in the gap causes a roughly linear increase in the sparking voltage of +0.1 percent in voltage per mm (of Hg) increase in vapor pressure. The control of these two variables permits the reproduction of the sparking voltage of this particular gap to ±0.3 percent. This increased accuracy of indication, however, reveals the presence of other variables which affect the indications of the sphere-gap voltmeter and which must be isolated and controlled if the full accuracy of the instrument is to be realized. These are being investigated.

4. A Sensitive Differential Barometer. WILLIAM HURST, *Duke University.* (*Introduced by W. M. Nielsen.*)—A sensitive differential barometer has been designed and constructed for application in clinical medicine. Its sensitivity, small cost, and other characteristics suggest that it may have a wider range of usefulness. In place of the more conventional metal bellows, a drum with light weight rubber stretched over it is used. Motion of the rubber due to differential pressure is applied through a train of gears from a small jeweled wrist watch to an indicating arm attached to the last gear. The device is sensitive to pressure changes equivalent to 0.002 cm of mercury and is capable of indicating pressure changes as rapidly as 10 pulses per second. Because of the design and character of the component parts, the instrument is quite stable. It should be of particular usefulness in the measurement of pressure variations in systems of small volume.

5. Separation of Solutions by the Tubular Centrifuge.* J. W. BEAMS, *University of Virginia.*—The tubular vacuum type air-driven centrifuge[1] has been modified and applied to the separation of solutions. The centrifuge "bowl" consists of an alloy steel tube which is spun in a vacuum chamber. The solution enters the spinning tube at the top continuously through a stainless steel tube, gauge 14. The ighter and heavier fractions are collected at the axis and periphery respectively by channels in the bottom of the spinning tube. These fractions are led to the outside through coaxial tubes, gauges 15 and 12, which support the rotor. Vacuum tight oil glands seal the vacuum chamber and separate the chambers in which the two fractions are collected. The ratio of the quantities of light to heavy fractions collected can be varied over wide ranges. The oil glands or bearings are maintained at approximately the same temperature as the rotor by circulating water or oil. Possible stirring where the solution enters the centrifuge and where the fractions are drawn off is prevented by baffles. Experiments also show that the remixing caused by comparatively wide variations in rotational speed could be prevented by a coil of screen wire which filled the centrifuge. The observed separation was in rough accord with the calculations of Archibald.[2]

* Supported by a grant from the Division of Natural Sciences of the Rockefeller Foundation.

[1] Beams, Linke and Skarstrom, Science **86**, 293 (1937).

[2] In press.

6. Practical Applications of Electronic Control Principles to the Operation of a Wilson Cloud Chamber. I. I. HOPKINS, R. T. DICKERSON AND W. M. NIELSEN, *Duke University.*—A circuit for the complete electronic control of a Wilson cloud chamber has been designed by one of us (R.T.D.), constructed, and put into operation. The general idea is based on the maximum possible use of gaseous discharge valves and typical resistance capacitance time circuits. Tracks are illuminated by two capillary helium-mercury discharge lamps, each operating from a five microfarad condenser charged to about five thousand volts.

7. Probable Errors in Counts from Geiger-Müller Counters. ERIC RODGERS, *University of Alabama.*—When a large number N of random events are counted with a Geiger-Müller counter, the result is usually written as $N\pm(N)^{\frac{1}{2}}$. This is based on the assumption that the events being counted follow a Poisson distribution, in which case the standard deviation equals the square root of the average. If x is assumed to represent the "true" average count for a given time interval, the probability that a single trial does not deviate from x by more than $(x)^{\frac{1}{2}}$ lies between $(2/\pi e)^{\frac{1}{2}}$ and $(2/\pi)^{\frac{1}{2}}$ if x is sufficiently large. Thus $(x)^{\frac{1}{2}}$ is perhaps not a bad approximation to the probable error, which is that deviation from x for which the chances are equal that a single trial yield a result within or without the range. However, when a single observation is made, the result may differ widely from the "true" average for that interval. It therefore seems that not much faith can be put in the practice of taking the square root of the number of counts obtained in an interval and calling it the probable error even if the interval is of such length that many counts are obtained.

8. Construction and Use of Lissajous Figures. F. H. MITCHELL, *University of Alabama.*—Beginning with space models of Lissajous figures, their equations may be deduced and the component sine waves analyzed without their being in phase. The results are checked by the actual figures as produced by the oscillograph.

9. Hysteresis Testing with Cathode Rays. C. T. RAZOR, *The Citadel.*—Application of the conventional type of cathode-ray oscillograph with electrostatic deflection plates to draw hysteresis loops of magnetic specimens. No modification of the instrument is needed. Hysteresis tests may also be made on the cores of completed machines without damage or dismantling. The method is applicable either to quantitative measurements or to quick and easy demonstration. The necessary accessories are found in most laboratories.

10. A Device for Controlling the Temperature of Absorption Cells. DUDLEY WILLIAMS AND RICHARD TASCHEK, *University of Florida.*—A device for controlling the temperature of small absorption cells is described. The arrangement involves a thermocouple, a galvanometer, a photronic cell, and a miniature relay. A light beam reflected from the galvanometer mirror falls upon the photronic cell when the temperature of the absorption cell increases to a certain value. The photronic cell operates a miniature relay which serves to increase the resistance in series with the heating coil, thus reducing the heater current. By proper adjustment of resistances the temperature of the absorption cell can be kept within a certain range. In the arrangement used at present it is possible to control the temperature of the absorption cell to 0.1 degree C at any point between 25 degrees C and 160 degrees C. By the use of a more sensitive galvanometer it should be possible to reduce the range of variation. This arrangement may prove useful in other experimental work where the geometry of the apparatus precludes the possibility of using ordinary forms of thermostatic controls.

11. A Spectroscopic Study of Deuterium Bonds. WALTER GORDY, *Mary Hardin-Baylor College.*—Mixtures of deuterium oxide with dioxane and with acetone have been studied in the region 3 μ to 12 μ. The effect of dioxane and of acetone on the spectrum of the deuterium oxide was to shift the intense 4 μ band to the shorter wave-lengths by about 0.2 μ. In the most dilute solutions, however, the position of the band appeared at wave-lengths appreciably longer than that of the corresponding band of deuterium oxide vapor. In the change from the liquid to the solution state, the shift to the shorter wave-lengths probably indicates the breaking of deuterium bonds between the deuterium oxide molecules. The appearance of the band at longer wave-lengths in the solution than in the vapor state may be a result of the formation of deuterium bonds between the solute and the solvent; variation of certain bands of the solvent provide additional evidence for this interpretation.

12. Calibration Wave-Lengths for Infra-Red Spectrometers. P. E. SHEARIN AND E. K. PLYLER, *University of North Carolina.*—About 20 wave-lengths which have been measured on grating spectrometers have been given for the calibration of prism spectrometers in region from about 2 μ to 24 μ. A number of lines due to H_2O and CO_2 can be normally observed due to atmospheric absorption. Since not many sharp bands have been measured on grating spectrometers from 7 μ to 13 μ, several sharp bands in ethyl alcohol and amyl alcohol in the liquid state have been measured in this region. The values found in the present work check well with those previously found by Weniger except those in the 9 μ and 10 μ region. Here some of the bands differ by about 0.2 μ from those found in this work. This difference is probably due to the fact that Weniger did not have the more accurate values of the index of refraction of rocksalt due to Paschen at his disposal.

13. A Portable Eagle Mounting for a 3 m Grating.* HERTHA SPONER AND WILLIAM HURST, *Duke University.*—Confronted with the necessity of building a grating spectrograph which would take little room and could be easily moved, we have tried the following construction of an Eagle mounting of relatively light weight. The instrument consists of two independent parts. One is the actual spectrograph having an I beam chassis, supporting an optical bench for movement of the grating, and the plate holder. This mechanism is surrounded by a double wall insulating box. The second part is a steel carrier on which the instrument rests on three points, at a convenient height above the floor. The carrier has three rubber tired wheels which may be removed and easily replaced for moving the instrument around the building. Mr. F. B. Key adjusted the instrument. Results have proven so far to be satisfactory with no broadening of the lines even when the instrument was subjected to light blows in short exposure experiments. It should be added that the floor of the room where the instrument is now set up is floated. Another important feature of this apparatus is that the construction was relatively inexpensive.

* Read by title.

14. X-Ray Crystal Structure Study of Tetramethyl Ammonium Tri-Iodide. R. C. L. MOONEY, *Newcomb College, Tulane University.*—Tetramethyl ammonium tri-iodide was prepared by a method analogous to that used for ammonium tri-iodide; crystals of suitable size and perfection were obtained from slow cooling of an alcoholic solution. They were definitely identified as the tri-iodide by quantitative chemical analysis. X-ray diffraction data were obtained by means of the single crystal oscillation method. The complete set consisted of six overlapping fifteen degree oscillations about each axis. The Patterson modification of the Fourier series method was used to locate atomic positions. The cell size of the crystal is 10.43A, 8.60A, 14.62A along the a, b, and c directions, respectively. The class is orthorhombic bypyramidal, with the space group symmetry of D_{2h}^{12} ($Pnmn$). All of the iodines are in special positions, lying in the reflection plane perpendicular to the y axis. The six parameters necessary to locate them in the plane were found by consideration of observed diffraction intensities. Some assumptions of reasonable interatomic distances were required to decide the positions of the cations. Three iodines are associated to form a monovalent complex anion group. The group is linear, with an iodine to iodine distance of 2.75A. A comparison of the details of this structure

with those of ammonium tri-iodide previously examined demonstrates the effects of the relative sizes of anion and cation.

15. Infra-Red Absorption Spectrum of a Liquid Crystal. RICHARD TASCHEK AND DUDLEY WILLIAMS, *University of Florida.*—The infra-red spectrum of the anisotropic liquid peri- (peri-ethoxy-benzalamino) cinnamate has been studied at temperatures from 20°C to 160°C, in the region between 2μ and 12μ. Intense characteristic absorption is found at 3.3μ, 5.85μ, 6.25μ, 7.7μ, 8.0μ, 8.6μ, 9.7μ, and 11.6μ. All but the 8.0μ and 8.6μ bands can be assigned to known inner vibrations of the groups occurring in the molecule. In the anisotropic liquid phase the 3.3μ and 7.7μ bands are found to be shifted to slightly longer wave-lengths than in the solid or isotropic liquid. At constant wave-length, the transmission as a function of temperature remains constant while the compound is solid. Between the melting point and clearing point the transmission increases, the rate and continuity of increase depending upon the wave-length. The transmission remains constant beyond the clearing point and shows a marked hysteresis on cooling the compound. For most wave-lengths one or more "arrests" are observed at definite temperatures in the temperature-transmission curves. The increase in transmission with temperature is attributed to lessened scattering from the constituent "swarms" of the anisotropic phase as it passes to the clear liquid.

16. The Infra-Red Spectra of Nitrate Solutions. DUDLEY WILLIAMS AND LORAINE DECHERD, *University of Florida.*—The absorption of several nitrate solutions has been measured in the region between 2μ and 16μ. The results are compared with earlier measurements of nitrate absorption. In the solutions the nitrate bands near 7.5μ and 15.5μ are intense, while the bands near 3μ, 4.8μ, and 12μ, are comparatively weak. It is found that the characteristic frequencies of the NO_3 group in solution are slightly lower than those of the NO_3 group in crystals, a result in accord with Pfund's early reflection measurements.

17. Design and Calibration of an Infra-Red Spectrometer with a Fluorite Prism. E. S. BARR, *Tulane University.*—An infra-red spectrometer of the Wadsworth type, with an aperture of 0.218, has been built for use with a 60° fluorite prism (sides 45 by 75 mm.). Arrangements have been made for observing prism settings by means of a calibrated dial, or directly to 10″ from a circle. There is provision for interchanging prisms to vary the range of the instrument. Using the index of refraction values of fluorite given by Coblentz,[1] tables have been prepared for circle readings of angles of incidence and for effective slit widths as functions of the wave-length and are shown in the form of curves. By the use of a secondary prism, the fluorite prism is set at minimum deviation for sodium light. The Wadsworth mirror was set visually for sodium light from a sodium arc lamp. For finer adjustment of the mirror and for calibration, atmospheric absorption bands due to CO_2 and H_2O were used. Other well-established points from spectra measured by grating instruments serve as a check on the correctness of the calibration.

[1] W. W. Coblentz, J. Opt. Soc. Am. **4**, 432 (1910).

18. The Refractive Index of Air in the Visible and Photographic Infra-Red. DAVID BENDER, *California Institute of Technology.*—The refractive index of dry CO_2-free air has been measured from 5300A to 11,200A by means of a Fabry-Perot interferometer with invar separating posts. The following dispersion curve was obtained for standard conditions (0°C and 760 mm):

$$(n_0-1)10^7 = 2885.59 + \frac{15.77}{\lambda^2} + \frac{0.421}{\lambda^4}$$

where λ is expressed in μ. A comparison of the present result with those of other observers shows that this curve lies above the others by about 10 parts in 10^7, and that all curves are nearly parallel. This suggests that the discrepancies are due to systematic errors, providing, as seems to be the case, that the constitution of air remains sufficiently constant. In the present experiments systematic errors due to phase change at reflection, methods of purification of the air, and bulk modulus of the invar posts were considered. A calculation concerning the oxygen absorption band at 7600A indicates that this band has no measurable effect on the dispersion of air.

* Now at Louisiana State University.

19. The Polar Moment of Cellosolves. W. H. BYERS AND A. A. BLESS, *University of Florida.*—The polar moment of 2-methoxy ethanol and of 2-ethoxy ethanol was determined using the heterodyne beat method for finding the dielectric constant. With benzene as a solvent the moment is 2.05×10^{-18} e.s.u. for the first compound and 2.13×10^{-18} e.s.u. for the second. The relation between these values and the values of the moment of the related alcohols is discussed. Work is now in progress on the other members of the series.

20. A Sensitive Method of Detecting Magnetic Impurities. F. W. CONSTANT AND J. M. FORMWALT, *Duke University.*—The presence of ferromagnetic impurities in any small solid specimen may be detected and magnetic moments per cc as small as 10^{-7} (compared with 10^3 for pure iron), measured by the following method. The specimen is first placed in a strong magnetic field which serves to magnetize all the magnetic impurities in the same direction. Their residual magnetism is then measured by suspending the specimen by a delicate quartz fiber at right angles to a weak field supplied by Helmholtz coils. By noting the deflection and calibrating the fiber the residual magnetic moment is determined. It was found to range from 7×10^{-2} per cc for brass, to 3×10^{-7} per cc for Pyrex, all materials tested showing some ferromagnetic impurity. It is of interest that such small impurities are still ferromagnetic; further study of their magnetic properties is being made.

21. A Displacement Polarimeter. NEWTON UNDERWOOD, *Vanderbilt University.*—The device is based on a deformation of the fringe system seen when a uniaxial crystal cut with its faces perpendicular to its optic axis is observed in convergent elliptically polarized light. The polarimeter is constructed using Polaroid, quartz and Cellophane, arranged in the following order; the polarizer, the specimen, the wave plate which covers one-half of the field, the converging lens, the quartz, and finally the analyzer Polaroid. The field of the instrument consists of the rings due to the quartz and is bisected by the edge of the Cellophane wave plate. The rings form continuous smooth curves when the axis of the wave plate is parallel to either the analyzer or polarizer. A rotation of the plane of polarization produced by inserting a specimen immediately in front of the polarizer causes a break to appear in the curves at the edge of the wave plate. Rotation of the polarizer or analyzer to compensate for the rotation introduced by the specimen causes the curves to line up again and thus affords a measurement of the rotation due to the specimen. The measurements are accurate to 0.1°.

22. Collision Relations. ARTHUR E. RUARK AND CREIGHTON JONES, *University of North Carolina.*—Braunbek[1] has published formulas dealing with energy and momentum relations in the collision of two unequal relativistic particles. His results cover both radiative and nonradiative collisions. We have worked out more formulas, with a view to cloud-chamber applications, and will present a systematic summary of those which appear most useful.

[1] Zeits. f. Physik **96**, 600 and **104**, 619.

Organization Meeting of the New York State Section of the American Physical Society

UNION COLLEGE, SCHENECTADY

April 2, 1938

FINAL steps were taken in the organization of the New York State Section of the American Physical Society at a meeting held at Union College, Schenectady on Saturday, April 2. One hundred seventy-five persons attended, representing institutions in all parts of the state (exclusive of the metropolitan area) and including a large group of High School physics teachers as well as physicists in college and industrial work. After the constitution and by-laws were adopted 83 persons enrolled as charter members and paid their annual dues.

The following officers were elected for a two year term:

Chairman, P. I. WOLD, Union College
Vice Chairman, W. B. RAYTON, Bausch & Lomb Optical Co.
Secretary, P. R. GLEASON, Colgate University
Treasurer, G. H. CAMERON, Hamilton College
Members of Executive Committee:
Terms expiring in 1942:
MRS. ANNA W. PEARSALL, Hamilton High School
R. E. BURROUGHS, Eastman Kodak Co.
Terms expiring in 1940:
R. C. GIBBS, Cornell University
C. A. MOOSE, Milne High School, Albany

At the dinner meeting Professor Gibbs brought official greetings to the new organization as President of the Optical Society of America; Dr. Irving Langmuir brought similar greetings from the American Chemical Society.

The program of invited papers was as follows:

Morning Session

Address of Welcome. D. R. Fox, *President, Union College.*
Television Transmission. E. H. B. Bartelink, *General Electric Co.*
Biological Effects of Cathode Ray Irradiations. C. P. Haskins, *Union College.*

Afternoon Session

Recent Developments in Glass Manufacture. H. P. Gage, *Corning Glass Works.*
Physics in Aeronautical Science. P. E. Hemke, *Rensselaer Polytechnic Institute.*
Electron Optics. R. P. Johnson, *General Electric Co.*

Paul R. Gleason
Secretary